

MCR-79-560  
Contract NAS9-15302

NASA CR-  
160244  
May 1979

Interim  
Report

Volume I

Technical Discussion

# Analysis and Test for Space Shuttle Propellant Dynamics (1/10<sup>th</sup> Scale Model Test Results)

(NASA-CR-160244) ANALYSIS AND TEST FOR  
SPACE SHUTTLE PROPELLANT DYNAMICS (1/10TH  
SCALE MODEL TEST RESULTS). VOLUME 1:  
TECHNICAL DISCUSSION Interim Report, May  
1978 - May 1979 (Martin Marietta Corp.)

N79-25240

HC A05/MF A01

Unclas  
G3/28 23409



**MARTIN MARIETTA**

MCR-79-560  
Contract NAS9-15302

Volume I

Interim  
Report

May 1979

---

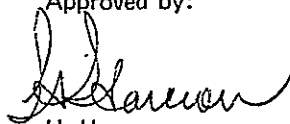
Technical Discussion

**ANALYSIS AND TEST FOR SPACE  
SHUTTLE PROPELLANT DYNAMICS  
(1/10th SCALE MODEL TEST  
RESULTS)**

Authors:

Robert L. Berry  
James R. Tegart  
Leonard J. Demchak

Approved by:



H. Harcrow  
Program Manager

Prepared for:

National Aeronautics and Space Administration  
Lyndon B. Johnson Space Center  
Houston, Texas 77058

Prepared by:

**MARTIN MARIETTA CORPORATION**  
**DENVER DIVISION**  
P. O. Box 179  
Denver, Colorado 80201

## FOREWORD

---

This report, prepared by the Martin Marietta Corporation, Denver Division, under contract NAS9-15302, presents the results of an analytical and experimental study of Space Shuttle propellant dynamics during ET/Orbiter separation in the RTLS (return to launch site) mission abort sequence. The study employed a 1/10<sup>th</sup> scale model of the ET LOX tank. The study was performed from May 1978 to May 1979 and was administered by the National Aeronautics and Space Administration, Lyndon B. Johnson Space Center, Houston, Texas, under the direction of Mr. Mark Craig.

This report is published in two volumes:

- Volume I Technical Discussion
- Volume II 1/10 Scale Model Test Data

In addition to this report, a high-speed 16 mm movie has been produced which documents the test results.

## ABSTRACT

---

This report presents the results of Phase II of an experimental investigation of Space Shuttle propellant dynamics during ET/Orbiter separation in the RTLS (return to launch site) mission abort sequence. This phase (II) of the study employed a 1/10th scale model of the ET LOX Tank. Phase I employed a 1/60th scale model and the results are summarized in Reference 1. During the RTLS abort sequence, the ET and orbiter separate under aerodynamic loading, with propellant remaining in the ET. The separation event includes a seven-second decelerating coast period during which the residual propellant accelerates relative to the ET/orbiter. At separation, ET clearance is primarily provided by aerodynamics acting on the ET to move it away. The motion of the propellant, primarily LOX, significantly influences the resulting ET motion and could cause the ET to recontact the orbiter. A test program was conducted in the NASA KC-135 "Zero G" aircraft using a 1/10th-scale model of the ET LOX Tank. Low-g parabolas were flown from which thirty tests were selected for evaluation. The objective was to acquire data on the nature of low-g propellant reorientation, in the ET LOX Tank, and to measure the forces exerted on the tank by the moving propellant. The data will provide a basis for correlation with an analytical model of the slosh phenomenon in Phase III of this contract.

## ACKNOWLEDGEMENTS

---

The authors would like to express their appreciation to all the NASA, JSC and Martin Marietta Corporation personnel who contributed to the successful completion of this study. We would like to express our special appreciation to the following individuals: Mr. Mark Craig, NASA JSC, assisted in formulation of the test program and provided guidance for the entire study, Mr. Don Griggs and Mr. Bob Williams, NASA JSC, who coordinated the NASA KC-135 aircraft test operations, and Mr. Duane Brown, Martin Marietta Corporation, whose technical expertise provided us with the test fixture, modified-1/10 scale task model and in addition Mr. Brown was the Martin Marietta instrumentation technician for the flight test program. Mr. Roger Guinn, Martin Marietta Corporation analytical mechanics, provided invaluable assistance in data reduction and computer programming.

CONTENTS

	<u>Page</u>
I. INTRODUCTION . . . . .	I-1
II. EXPERIMENTAL INVESTIGATION . . . . .	II-1
A. Scaling Analysis . . . . .	II-1
B. Test System Description . . . . .	II- 6
1. Test Fixtures . . . . .	II- 6
2. KG-135 Zero-g Aircraft . . . . .	II-12
3. Instrumentation . . . . .	II-15
C. Test Conditions . . . . .	II-17
D. Data Reduction . . . . .	II-19
1. Digitization . . . . .	II-19
2. Transformation of Forces to Tank Coordinates . . . . .	II-25
E. Tank Geometry and Test Constants . . . . .	II-41
III. OBSERVATION ON LIQUID MOTION . . . . .	III- 1
A. Liquid Motion in Bare Tank . . . . .	III- 1
B. Liquid Motion in the Baffled Tank . . . . .	III- 9
C. Test Comparisons . . . . .	III-10
1. Comparison of Aircraft and Drop Tower Tests . . . . .	III-12
2. Comparison Between Aircraft Tests . . . . .	III-14
D. Summary . . . . .	III-17
IV. OFT 1 EVALUATION . . . . .	IV-1
V. CONCLUSIONS . . . . .	V-1
VI. REFERENCES . . . . .	VI-1

## I. INTRODUCTION

---

Space shuttle has been designated as America's prime space launch vehicle for the eighties and beyond. As such, it encompasses numerous missions for variable payloads and flight objectives. The shuttle system is a manned flight system requiring extensive mission planning and contingency operations. A prime mission planning event is the contingency abort mission sequence prior to orbital insertion. Space shuttle has an intact abort mode in which the mated orbiter/external tank "flies" back to a landing site at an altitude of over 200,000 ft using the main orbiter engines. This RTLS (return to launch site) abort mission sequence requires the orbiter and external tank (ET) to separate under aerodynamic loads when a significant amount of propellant remains in the ET. The typical separation sequence is as follows:

- 1) Begin pitchdown, from angle of attack  $\geq 40^\circ$ , at MECO -10 s;
- 2) using the thrust vector control and aft reaction control system, achieve an angle of attack of  $-4^\circ$ ;
- 3) MECO, main orbiter engine cutoff;
- 4) coast for approximately 7 s using the reaction control system (RCS) to maintain attitude; and
- 5) separation of orbiter/ET using all downfiring orbiter RCS thrusters to move the orbiter away from the ET.

During the separation sequence, the ET nominally contains a 1% volume of liquid oxygen (LOX)\*. This is approximately 195 cubic ft (13,376 lb). Additionally the LOX line is full. The liquid hydrogen (LH<sub>2</sub>) tank in the ET also contains a residual volume but its impact due to liquid motion is small in comparison to the LOX tank.

During the 7 s coast period between main engine shutdown and separation, the propellant develops a velocity relative to the orbiter-ET. At separation, the ET clearance is provided somewhat by orbiter reaction control jets moving the orbiter away, but more significantly by aerodynamics on the ET moving it away. The motion of the propellant, mainly LOX, in the ET significantly affects the ET motion and could cause the ET to recontact the orbiter. It is not possible to lower the dynamic pressure at separation sufficiently to avoid this phenomena, nor can initial conditions be obtained to avoid it. JSC's simulation of this phenomena

---

\*1% is the OFT 1 baseline volume, future missions may baseline separation volumes much higher (e.g., 25%)..

shows a severe collision problem, but it is felt that this simulation, (not based on empirical data) is inaccurate and that collision would not occur. However, to assure that there is no collision, empirical data must be obtained. Furthermore, the test data must be obtained in a low-g environment with a model of the LOX tank internal geometry.

A three-phase study has been undertaken to develop an experimental data bank on which to base a mechanical analog that simulates large amplitude propellant reorientation during the RTLS abort separation and to develop a technique to analytically simulate the interaction forces between the ET and reorienting propellant in full-scale simulations.

Phase I of this study was a drop tower test program designed to simulate the ET LOX motion during RTLS. Thirty-two tests were conducted in Martin Marietta's Drop Tower Test Facility using two 1/60th scale models of the LOX tank; one with internal baffles, and one without. During the tests, small biaxial accelerations were applied to the tanks simulating aerodynamic deceleration of the ET during RTLS separation sequence. The resulting propellant reorientation forces exerted on the tank were measured by crystal load cells. The tests were conducted both with and without LOX tank baffles in order to facilitate analytical model development and to assess the effect of baffles on reorientation. In addition, a limited number of tests were performed simulating inflow from the LOX feedline. The test data was reduced to engineering units and analyzed to determine scaling validity and applicability of JSC's mechanical analog. Three test liquids were employed in the testing: FC114B2, FC43, and Hexane. The results of this study (Reference 1) included observations on the liquid motion and scaling, effects of the baffles, and analytical correlations using a model similar to JSC's SVDS simulation computer code.

The Phase I study indicated the importance that Bond and Reynolds number scaling had on the character of propellant orientation. The tests demonstrated that the motion of the bulk liquid did not change even though the Reynolds number was varied by a factor of 10 by changing test liquids; however, both the Bond and Reynolds numbers were much smaller than the values for the full-size LOX tank. Closer simulation of Bond number and Reynolds number was not possible due to the restrictions in model size imposed by the drop tower geometry.

To further investigate the effects of Bond and Reynolds number and to validate the scaling concepts, it was desirable to conduct a test program with a larger LOX tank model. Hence, Phase II of the study was initiated. In this phase, an available 1/10th scale LOX tank model was modified for use in NASA's KC-135 zero-g test aircraft. The aircraft could be flown at greater levels of



acceleration than could be applied in the drop tower tests, allowing a closer simulation of full-scale Reynolds and Bond numbers as indicated in Table I-1.

*Table I-1  
Comparison of Test and Full Scale  
Parameters for Propellant Reorientation Tests*

<u>Parameter</u>	<u>Full Scale LOX</u>	<u>1/10th Scale Freon 113</u>	<u>1/60th Scale Freon 114B2</u>
Bond number	$2.19 \times 10^5$	$2.70 \times 10^4$	$4.49 \times 10^2$
Reynolds number	$5.16 \times 10^7$	$2.39 \times 10^6$	$1.35 \times 10^5$

The results of the Phase II test program are summarized in this report. In this Phase II study, eighty-nine low-g parabolas were flown with an average test time of 20 s. The tests were conducted with and without baffles. Two test liquids were used: FC113 and a water-methocel solution. Each test was photographed with a high-speed movie camera (60 frames/s) and the liquid reorientation forces were recorded on magnetic tape. The liquid force data was digitized and transformed to engineering units for use in analytical comparisons. Details of this experimental investigation are discussed in Chapter II.

Chapter III presents observations on liquid motion. These observations are based on film data comparison of the various test conditions as well as comparisons of aircraft and drop tower tests. The influence of baffles, acceleration magnitude, tank orientation, and liquid viscosity on propellant reorientation are discussed. Additionally, an evaluation of the validity of the test scaling approach is presented. The results of this evaluation indicate that geometric scaling with the use of Froude number is valid for the ET LOX tank propellant reorientation.

Chapter IV of this report discusses the conservatism of NASA's OFTI slosh analysis. The ability of the single-point mass model to accurately simulate propellant reorientation is investigated by comparisons of the test data to analytical model results. Parameters of generalized ET pitch rate and rotation resulting from the applied angular impulse of the liquid are used to evaluate the conservatism of the model.

The conclusions of the Phase II study along with the recommendations for the Phase III analytical model development are presented in Chapter V.

## II. EXPERIMENTAL INVESTIGATION

Propellant motion like that which would occur in the LOX tank as the external tank separates from the space shuttle orbiter during an RTLS abort, was simulated during the experimental investigation. The full-scale conditions were scaled so that representative liquid motion could be produced in a subscale tank, using the NASA KC-135 zero-g aircraft to produce the necessary acceleration environment. These tests continue the investigation that began with tests in Martin Marietta's drop tower test facility. The aircraft tests permitted a much larger scale model compared to the drop tower (1/10 versus 1/60).

The primary objective of both the aircraft and drop tower test programs was to acquire data on the characteristics of propellant re-orientation in the LOX tank and the dynamic interaction forces applied to the tank by the moving propellant. The tests also demonstrated the influence of various parameters such as the internal baffles and liquid properties, on the motion of the liquid. Comparison of the data from the aircraft and the drop tower permitted the scaling approach to be evaluated. This chapter details the aircraft experimental investigation.

### A. SCALING ANALYSIS

During the RTLS separation maneuver, the external tank experiences axial and lateral accelerations due to aerodynamic forces. The accelerations are indicated as  $A_x$  and  $A_z$  in Figure II-1, with respect to the X and Z axes of the orbiter. The initial position of the residual liquid oxygen is established by the direction of the main engine thrust vector, which is oriented at an angle to the X axis. Following shutdown of the main engines, deceleration of the tank causes motion of the residual propellant toward the top of the tank. The following values for each of these variables defined the full-scale conditions that were considered in the test program.

$$A_x = 0.015g \text{ to } 0.030g$$

$$A_z = 0.005g \text{ to } 0.030g$$

$$\gamma = 0^\circ, 13^\circ \text{ and } 30^\circ$$

Residual propellant volume = 1%, 2%, 5%, 10%, 15% and 25%.

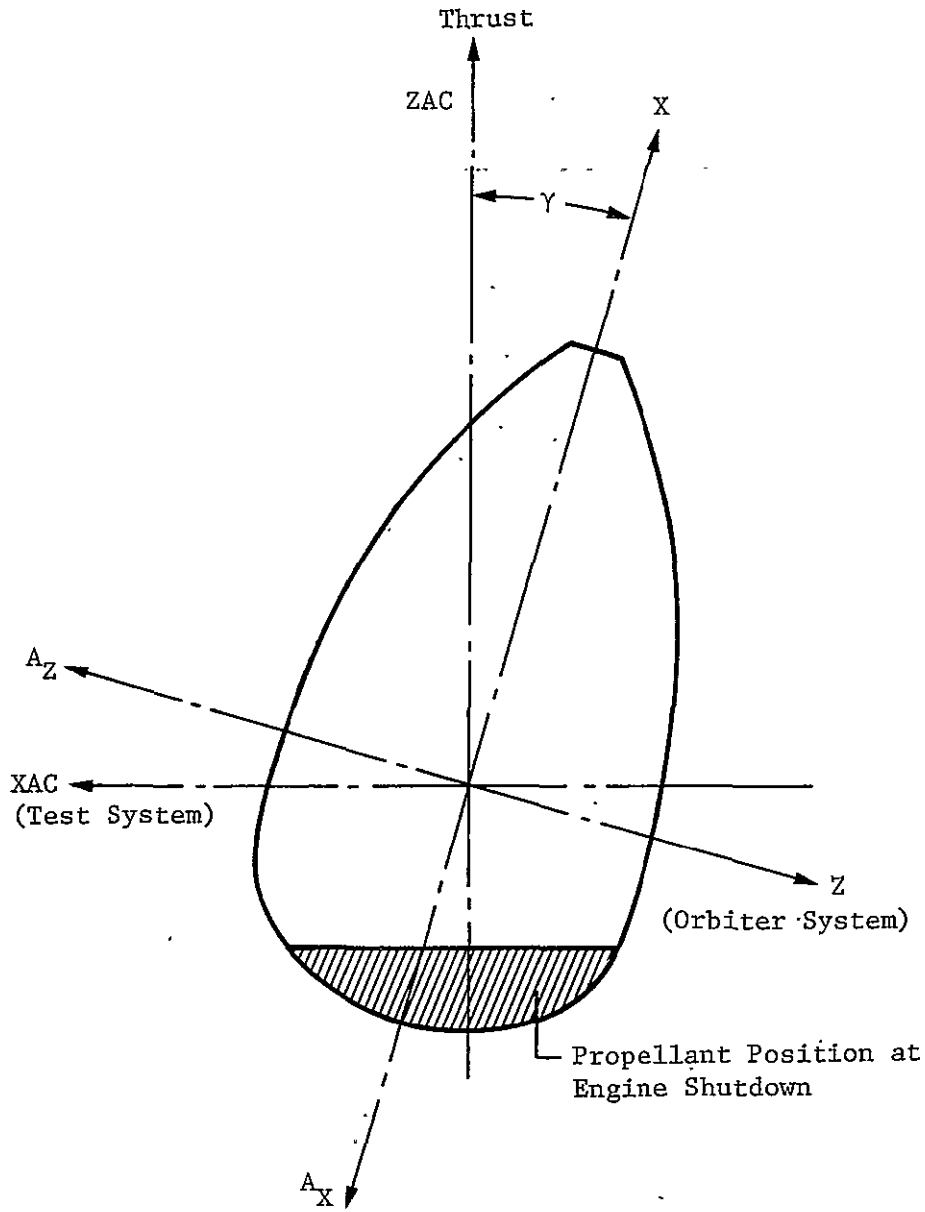


Figure II-1 Orientation of Tank Axes

The scaling analysis performed for the drop tower tests and presented in Reference 1 is equally applicable to the aircraft tests. That analysis established three dimensionless parameters that characterize propellant motion:

$$Fr = \frac{V}{\sqrt{Ar}} \quad (\text{Froude number}); \text{ ratio of inertia to acceleration force.}$$

$$Bo = \frac{\rho Ar^2}{\sigma} \quad (\text{Bond number}); \text{ ratio of acceleration to surface tension force.}$$

$$Re = \frac{\rho Vr}{\mu} \quad (\text{Reynolds number}); \text{ ratio of inertia to viscous force.}$$

For any propellant reorientation having a Bond number greater than 10 and a Reynolds number greater than 50, scaling can be based on Froude number alone. Equating the Froude number of the prototype or full-scale tank (subscript p) to the Froude number for the model tank (subscript m) yields the following equation for the scaling of time, based on dimensional scaling and the applied accelerations.

$$\frac{t_p}{t_m} = \sqrt{\frac{A_m}{A_p} \frac{r_p}{r_m}}$$

The propellant motion was simulated using NASA's zero-g aircraft, a KC-135 especially equipped to perform the required maneuvers. During the maneuver, the aircraft vertical acceleration (ZAC in Figure II-1) changes from a positive (tank accelerating upward) high-g to a negative low-g acceleration that can be sustained for a period of about 20 seconds. A lateral acceleration component (XAC) can also be applied during the maneuver, so the aircraft can simulate the characteristics of the actual acceleration environment the external tank experiences during the RTLS separation.

The aircraft capabilities imposed limits on the values of  $t_m$ ,  $A_m$ , and  $r_m$  in establishing the time scaling of the tests. Increasing the value of  $A_m$  increases the time period that is being simulated ( $t_p$ ). A large value of  $A_m$  increases the forces applied to the liquid, improving the resolution and measurement of the resulting dynamic forces. Large values for the Bond and Reynolds numbers, which are directly proportional to  $A_m$ , are also desired. A limit of  $-0.2g$  for  $A_m$  was established, based on the aircraft operational requirements, so values of  $-0.1g$  and  $0.2g$  were selected for the tests.

A number of factors influenced the selection of the value of  $r_m$ , which determines the dimensional scaling of the model. A large value of  $r_m$ , improves the force resolution since the liquid volume is increased. The value of  $Re$  is directly proportional to  $r_m$  and  $Bo$  is proportional to  $r_m^2$ , so increasing  $r_m$  helps to make both numbers larger. However, increasing  $r_m$  will decrease the simulated time period ( $t_p$ ), but this was not a problem with the aircraft tests because the test time ( $t_m$ ) was sufficiently long. Since the LOX tank is so large and force resolution was important, a large value for  $r_m$  was desired. An available 1/10 scale tank model was selected for the test program. This tank was close to the maximum model size that could be physically accommodated by the aircraft.

Based on the selected values of  $r_m$  and  $A_m$ , the test time period of approximately 20 s was more than adequate to obtain the desired liquid motion. During the first 10 s of the test, the most significant liquid motion occurred and during the remaining 10 s, the liquid was essentially at its final equilibrium position.

The liquid properties enter into the scaling in assuring that the Bond and Reynolds number are sufficiently large. A very dense liquid helps to make both  $Re$  and  $Bo$  large, and also assures that the forces due to a given volume of liquid will be large. Low surface tension and viscosity are also desirable.

The selection of the test liquids had to consider safety, compatibility with a plastic tank, and the above discussed property requirements. The primary test liquid was Freon 113 (also known as Freon TF). It has a high density, low surface tension and viscosity, and does not pose any hazards. This Freon has a vapor pressure of 3.7 N/cm<sup>2</sup> (5.3 psia) at 20°C, which is usually not a problem at normal temperatures. Problems of rapid vaporization were encountered when the Freon and the model tank were at temperatures around 30°C.

In order to evaluate the influence of viscous effects, a second test liquid with a higher viscosity was desired. This was achieved by using water to which a thickening agent had been added. Methocel, a methyl cellulose thickener made by Dow Chemical, was used to increase the viscosity of the water. Type F4M Methocel was used in the proportion of 2.1 grams per liter of water to increase the viscosity from its normal 1.0 cp to 5.1 cp. This gave a factor of 10 increase in the kinematic viscosity over that of the Freon. An antifoam emulsion (SWS-211 made by SWS Silicones Corp.) was added to the water to reduce foaming of the mixture. Some foam was created during a test but the bubbles coalesced within approximately one minute preventing any accumulation of foam in the test tank.

The properties of the two test liquids, measured using samples of the actual liquids, are listed in Table II-1. Also listed in the table are the properties of liquid oxygen, the propellant which was simulated by the test liquids.

*Table II-1 Liquid Properties*

Liquid	Density (grams/cm <sup>3</sup> )	Surface Tension (dynes/cm)	Viscosity (cp)
Oxygen (-183°C)	1.14	13.5	0.195
Freon 113 (25°C)	1.57	20.1	0.67
Water-Methocel Mixture (25°C)	0.998	47.9	5.05

Having selected the test system parameters, the premise that Bo and Re be sufficiently large to permit Fr scaling can now be verified. It is also desirable to have the values of Bo and Re of the test be as close to the values for the full-scale conditions as possible. Listed in Table II-2 are the calculated values for these numbers for the full-scale tank and for both of the test liquids in the model tank. In order to calculate Re, the value to be used for the liquid velocity must be defined. A representative velocity is the free-fall velocity based on the tank length, which would approximate the maximum velocity achieved by the liquid as it first moves to the other end of the tank.

*Table II-2 Dimensionless Parameters*

Conditions	Bond Number	Reynolds Number
<u>Full-Size Tank, Oxygen</u>		
A <sub>p</sub> = 0.015g	2.19 x 10 <sup>5</sup>	5.16 x 10 <sup>7</sup>
A <sub>p</sub> = 0.030g	4.38 x 10 <sup>5</sup>	7.30 x 10 <sup>7</sup>
<u>Model Tank, Freon 113</u>		
A <sub>m</sub> = 0.1g	1.35 x 10 <sup>4</sup>	1.69 x 10 <sup>6</sup>
A <sub>m</sub> = 0.2g	2.70 x 10 <sup>4</sup>	2.39 x 10 <sup>6</sup>
<u>Model Tank, Water-Methocel Mixture</u>		
A <sub>m</sub> = 0.1g	3.60 x 10 <sup>3</sup>	1.42 x 10 <sup>5</sup>
A <sub>m</sub> = 0.2g	7.20 x 10 <sup>3</sup>	2.01 x 10 <sup>5</sup>

As shown by the values in Table II-2, the basic requirement that  $Bo$  be greater than 10 and  $Re$  greater than 50, has been satisfied by a wide margin. In addition, the numbers for Freon are within an order of magnitude of the values for the full-size system. The values of  $Re$  for the water mixture were intentionally made to be an order of magnitude less than those for Freon. Due to its lower density and higher surface tension the water had a lower  $Bo$ , but the viscous influence was of primary interest. The very large values for  $Bo$  and  $Re$  indicate that the denominator of the ratios is insignificant compared to the numerator, i.e. surface tension and viscous forces are insignificant compared to the acceleration and inertial forces.

The dimensionless parameters for the aircraft tests were significantly greater than the parameters for the drop tower tests. The value of  $Re$  was between  $10^4$  and  $10^5$  for the drop tower tests, so it has been increased by an order of magnitude. Evaluation of the influence of viscous effects on the liquid motion observed during the drop tower tests concluded that viscous effects were negligible under those test conditions. The maximum  $Bo$  was 500 for the drop tower tests and was two orders of magnitude larger for the aircraft tests. This was enough of a change in  $Bo$  to note some difference in the effects of surface tension on the liquid motion, as discussed in Chapter III.

## B. TEST SYSTEM DESCRIPTION

The NASA zero-g aircraft was used to produce the required sub-scale model test conditions. This aircraft is operated by NASA as a facility to provide a reduced gravity environment for test and training purposes. The test fixture, associated apparatus, and instrumentation for this test program was mounted in the aircraft to perform these tests.

### 1. Test Fixture

The test fixture consists of the model tank, box frame support, and base. This fixture is shown along with the test instrumentation rack in Figure II-2.

Figure II-2

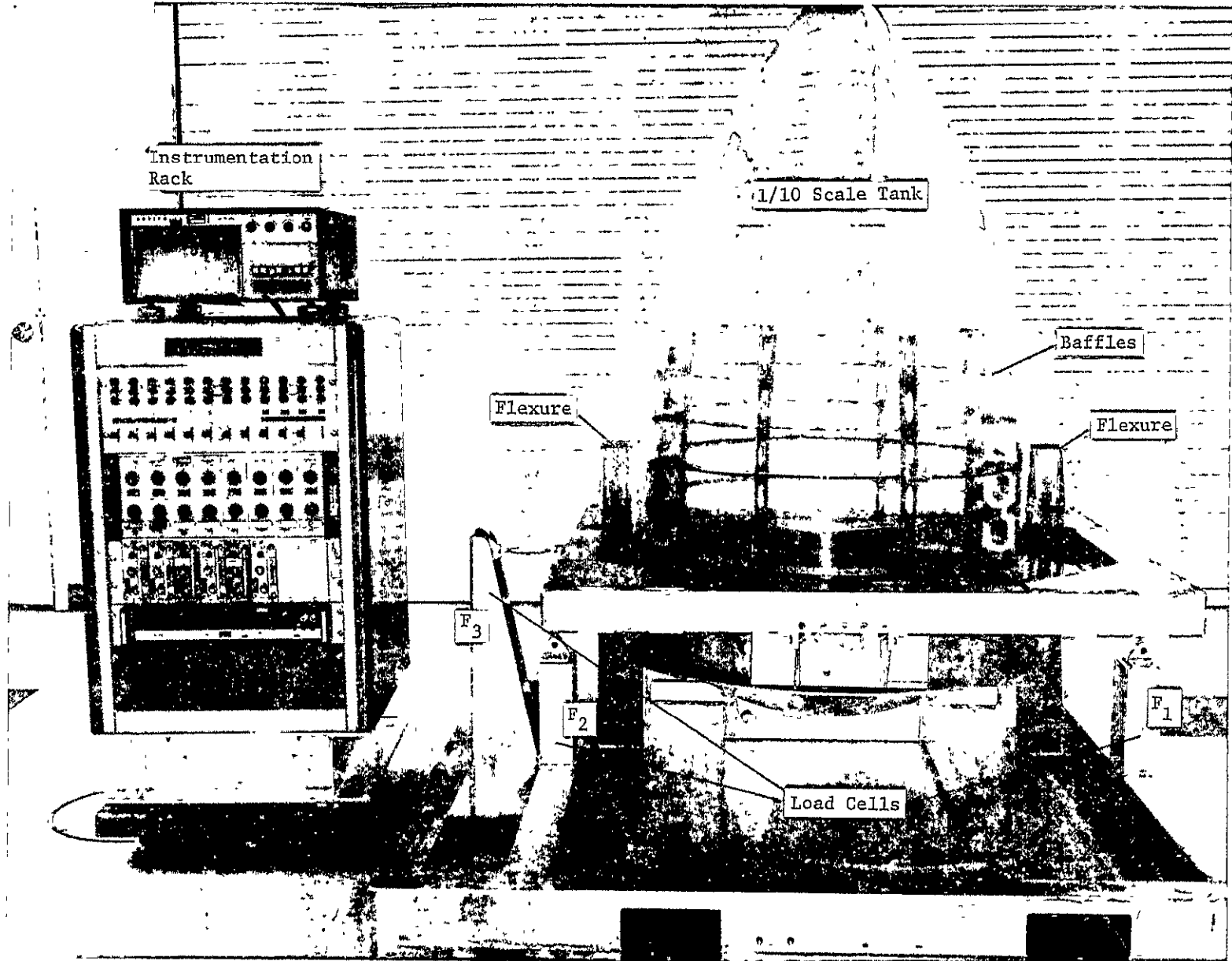


Figure II-2 1/10 Scale LOX Tank, Test Fixture and Instrumentation Rack

II-7

ORIGINAL PAGE IS  
OF POOR QUALITY



The model tank was a 1/10 scale model of the ET LOX tank. Its overall length was 151 cm and the barrel section diameter was 84 cm. The tank was made of transparent acrylic plastic. It was made in two sections joined with bolted flanges at the junction of the lower dome. Following a structural failure of the tank during testing, (discussed later in this section), the flange on the upper portion of the tank was replaced with an aluminum ring that was glued and bolted to the original plastic tank section.

An antivortex baffle made from transparent acrylic plastic is positioned where the actual tank outlet would be located. The ET LOX tank has its outlet positioned off center, while this model has the outlet on the tank center line.

The ring baffles are representative of the actual LOX tank baffles. They have the same size and spacing to the tank wall, but lack the details of the supports between the baffles. These baffles were made of aluminum and were built as an integral unit. Both the antivortex baffle and the ring baffles could be removed from the tank, after it was separated at its flanges, to perform tests with a bare tank.

The tank was mounted to the box frame through two pivot joints. By rotating the tank about the pivot axis and locking it into place, tank orientations of  $0^\circ$ ,  $13^\circ$  and  $30^\circ$  were obtained. The  $13^\circ$  and  $30^\circ$  orientations are shown in Figures II-3 and II-4 respectively.

The box frame was supported from the base by the three load cells. The load cells measured the forces in the plane of the tank; parallel with the aircraft longitudinal axis. This is the plane in which the accelerations act, as defined by Figure II-1. Two load cells are mounted vertically on each side of the box frame, and one is mounted laterally. Rod end bearings were used on each end of the load cells to attach them to the fixture.

Four flexure rods prevented movement of the tank and box frame in any direction other than the plane of the load cells. The stiffness of the flexures when acted upon by forces in the plane of the load cells was much less than the stiffness of the load cells so the flexures had no influence on the measurement of forces in that plane.

The other ends of the load cells and flexures were attached to the test fixture base. A hole pattern in the base was compatible with the aircraft mounting points and fork-lift pick-up holes were provided. Other system components, such as the pump and valves, were mounted on the base.

ORIGINAL PAGE IS  
OF POOR QUALITY

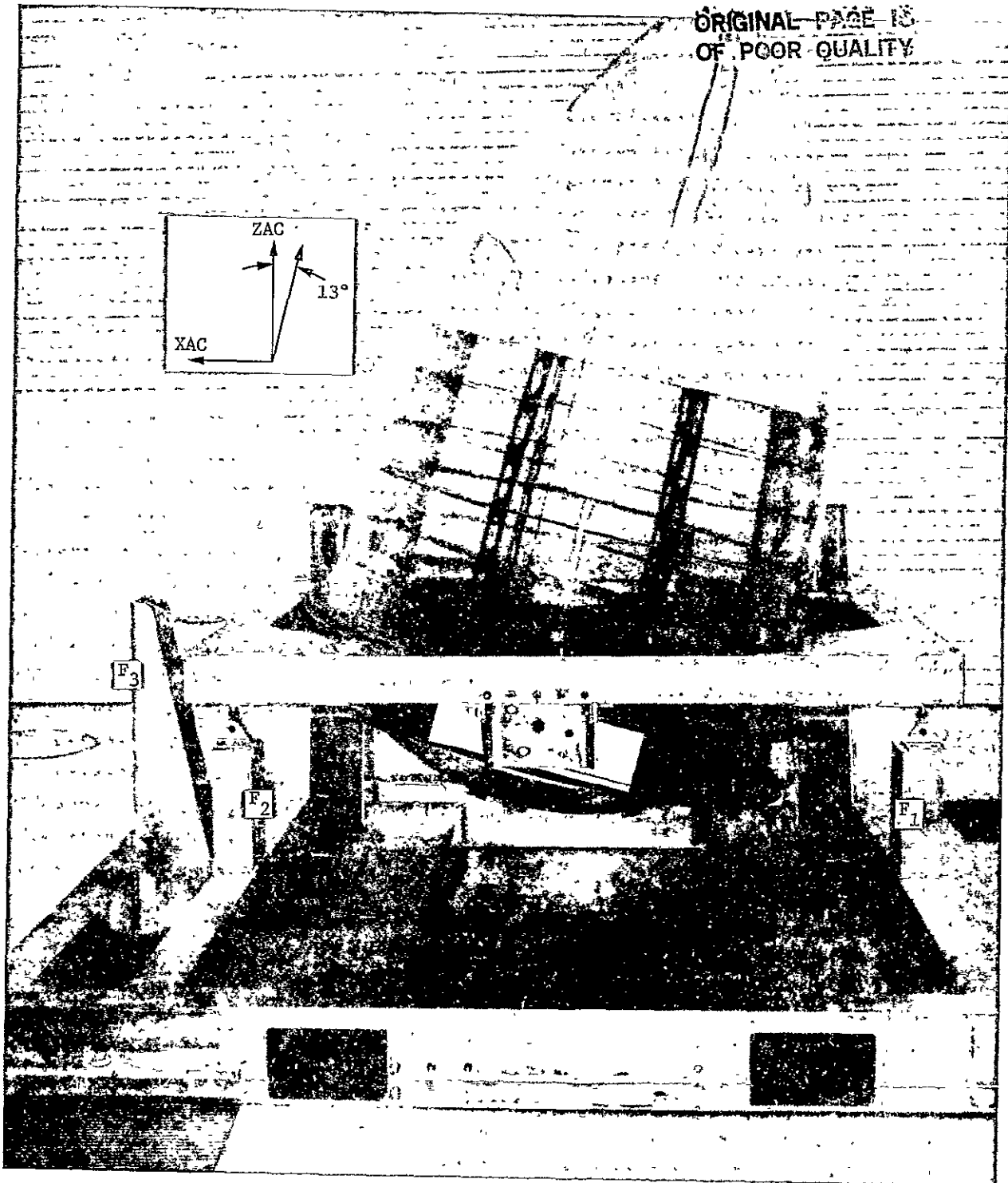


Figure II-3 1/10 Scale Model 13° Orientation

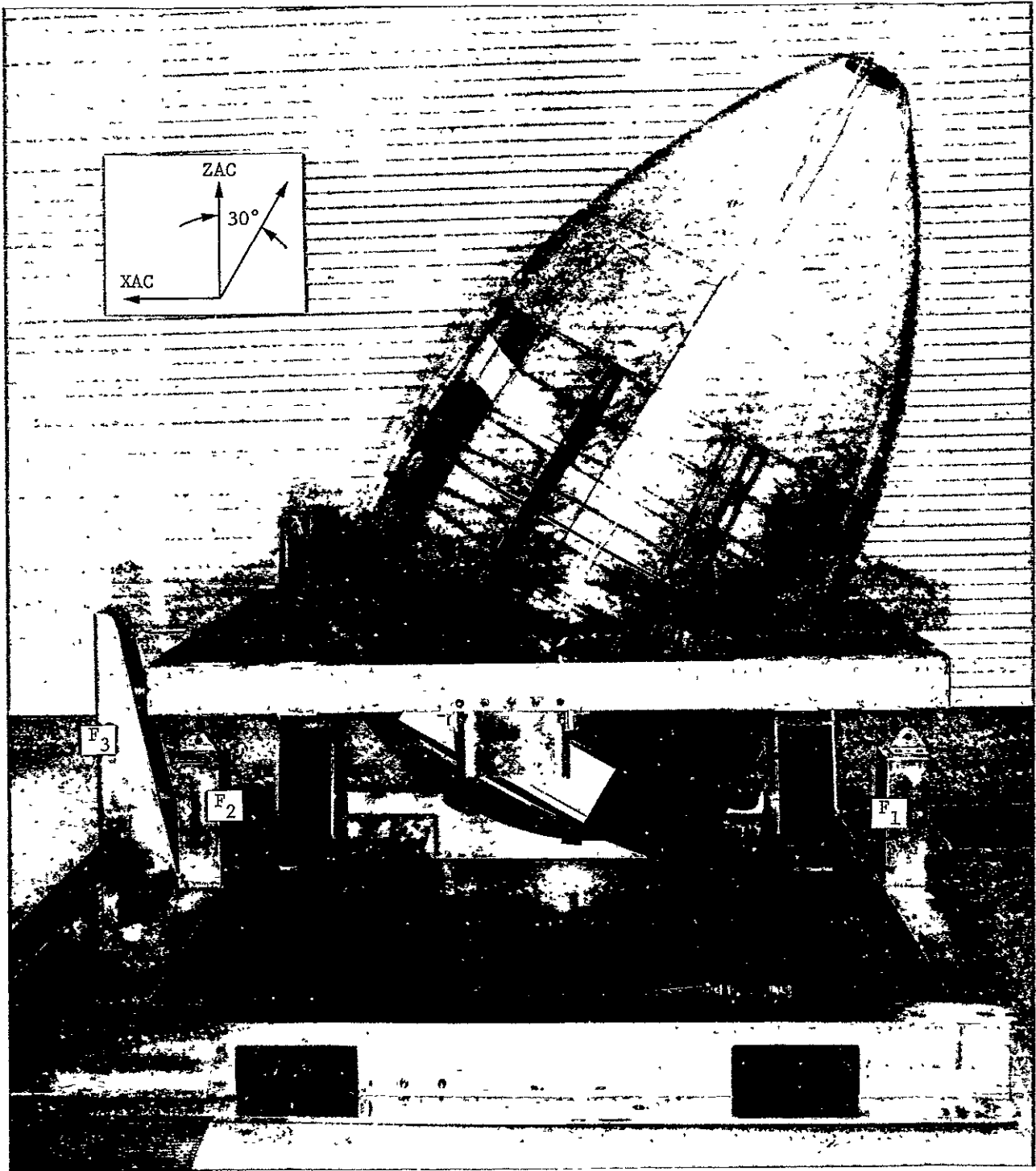


Figure II-4 1/10 Scale Model 30° Orientation

Transfer of the test liquid between the model tank and supply tank was performed with an electric motor-driven pump. The transfer system is shown schematically in Figure II-5. Interchanging of the lines at the valves adjacent to the pump permitted the direction of flow to be reversed. The supply tank had a calibrated sight gage to determine the volume of liquid transferred to the model tank.

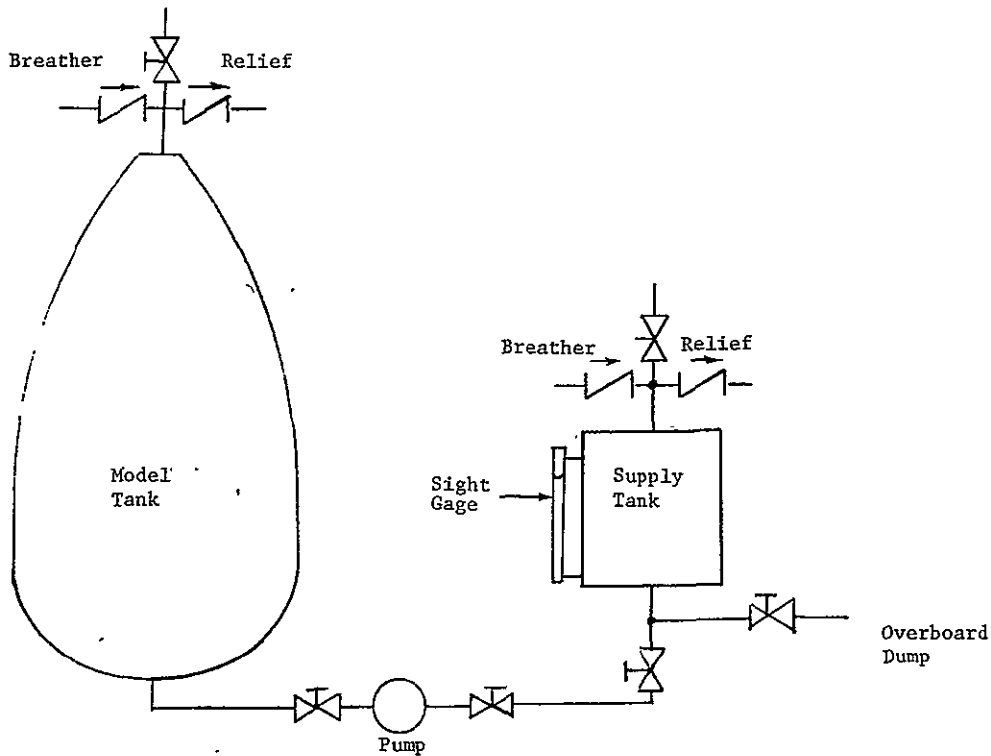


Figure II-5 Plumbing Schematic

The breather and relief valves are  $0.7\text{N/cm}^2$  (1 psi) cracking pressure-check valves, intended to prevent the pressure differential between the tank and the cabin from exceeding  $\pm 0.7\text{N/cm}^2$  (1 psi) as the cabin pressure varied. When using the Freon as the test liquid, rapid vaporization occurred when the cooler Freon contacted the warmer walls and baffles of the tank. With the liquid oriented at the relief valve inlet (top of tank), sufficient venting of the tank was not possible and failure of the tank

resulted. The tank was repaired and a large vent port was added in the side of the tank. A flexible rubber disk closed the port, but any increase in tank pressure caused it to open. This port permitted essentially unrestricted release of vapor and liquid was usually not located near the port. This relief port functioned satisfactorily to prevent any further problems with tank pressurization.

## 2. KC-135 zero-g Aircraft

The basic operating characteristics and requirements of the zero-g aircraft are defined in Reference 2. Aspects pertinent to this program are discussed here.

The aircraft flies a parabola to counteract gravity and obtain a period of low gravity relative to the aircraft. Depending upon the way throttles and the pitch rate of the aircraft are controlled during the parabola, various low-g acceleration vectors can be produced.

The aircraft dives and then climbs to achieve the necessary angle of attack and airspeed for the parabola. During the climb, the vertical acceleration perpendicular to the aircraft floor (ZAC) reaches between +1.8g and +2.0g. This acceleration acts to settle the liquid at the bottom of the tank, duplicating the propellant location in the ET prior to main engine shutdown. As the aircraft enters the parabolic arc, there is a rapid transition (about 2 s) from the positive high-g acceleration to the low-g acceleration. For this test program, the low-g acceleration was negative (acting to move the liquid to the top of the tank) and of -0.1g or -0.2g in magnitude. This gave the longitudinal acceleration component, ZAC in Figure II-1. To obtain the lateral component, XAC, the throttles were adjusted so that the aircraft continued to accelerate as it entered the parabola.

Some typical plots of ZAC and XAC, as measured during a test, are shown in Figures II-6 and II-7. The plot for ZAC begins as the acceleration decreases from the high-g during pull-out. For some tests, the time to reach the desired negative acceleration was as much as 3 or 4 s. There was always some variation in the acceleration, with a maximum variation of about  $\pm 0.05g$ . The value of XAC decreased from a value of about 0.1g toward zero. Note that the XAC component is acting on the liquid before the ZAC component becomes negative.

It was also possible to have accelerations acting perpendicular to the plane of the load cells (YAC). Due to the variability of the accelerations, three tests were performed for each test condition and tests with out-of-plane (YAC) liquid motion or similar defects were discarded.

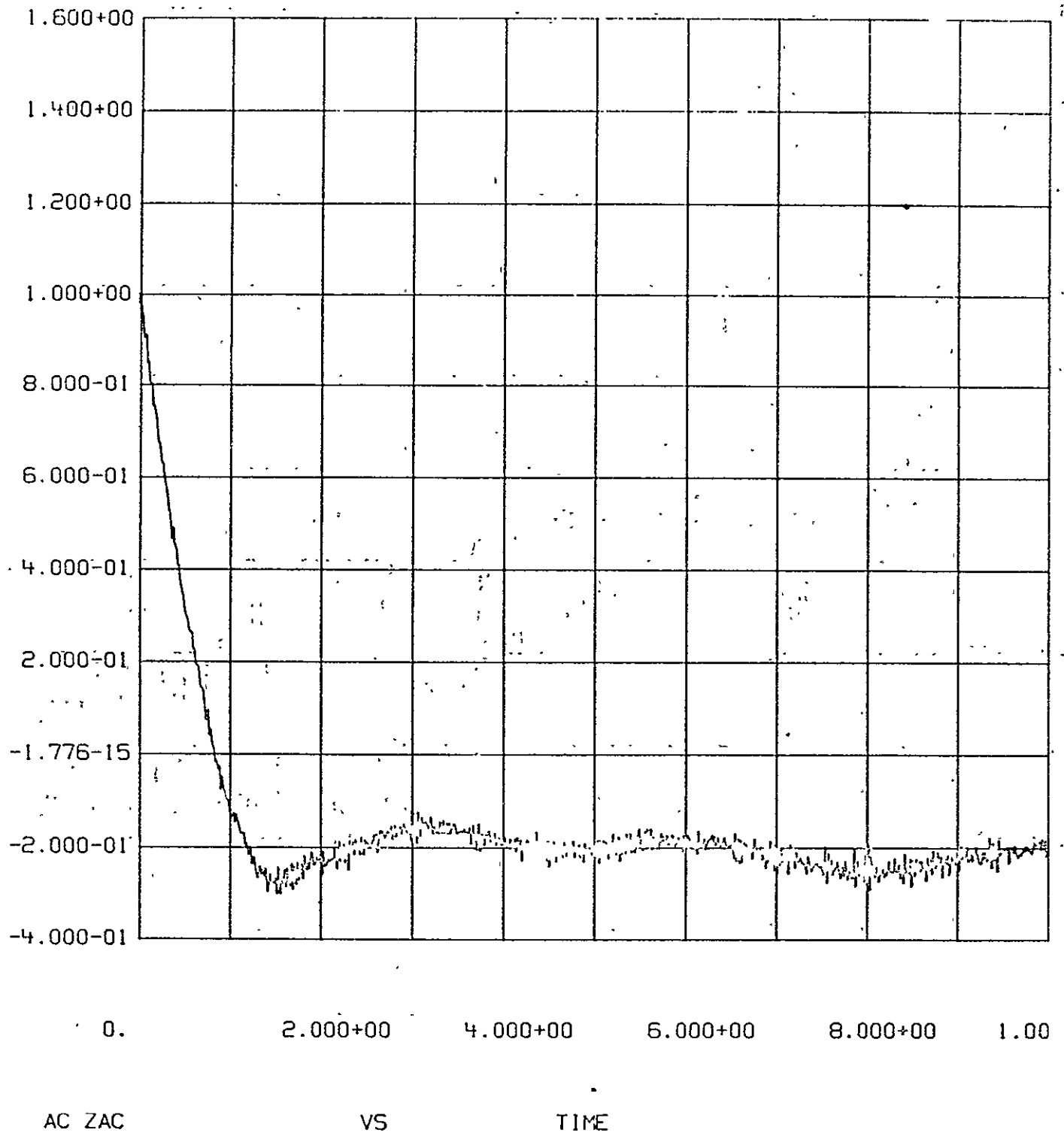
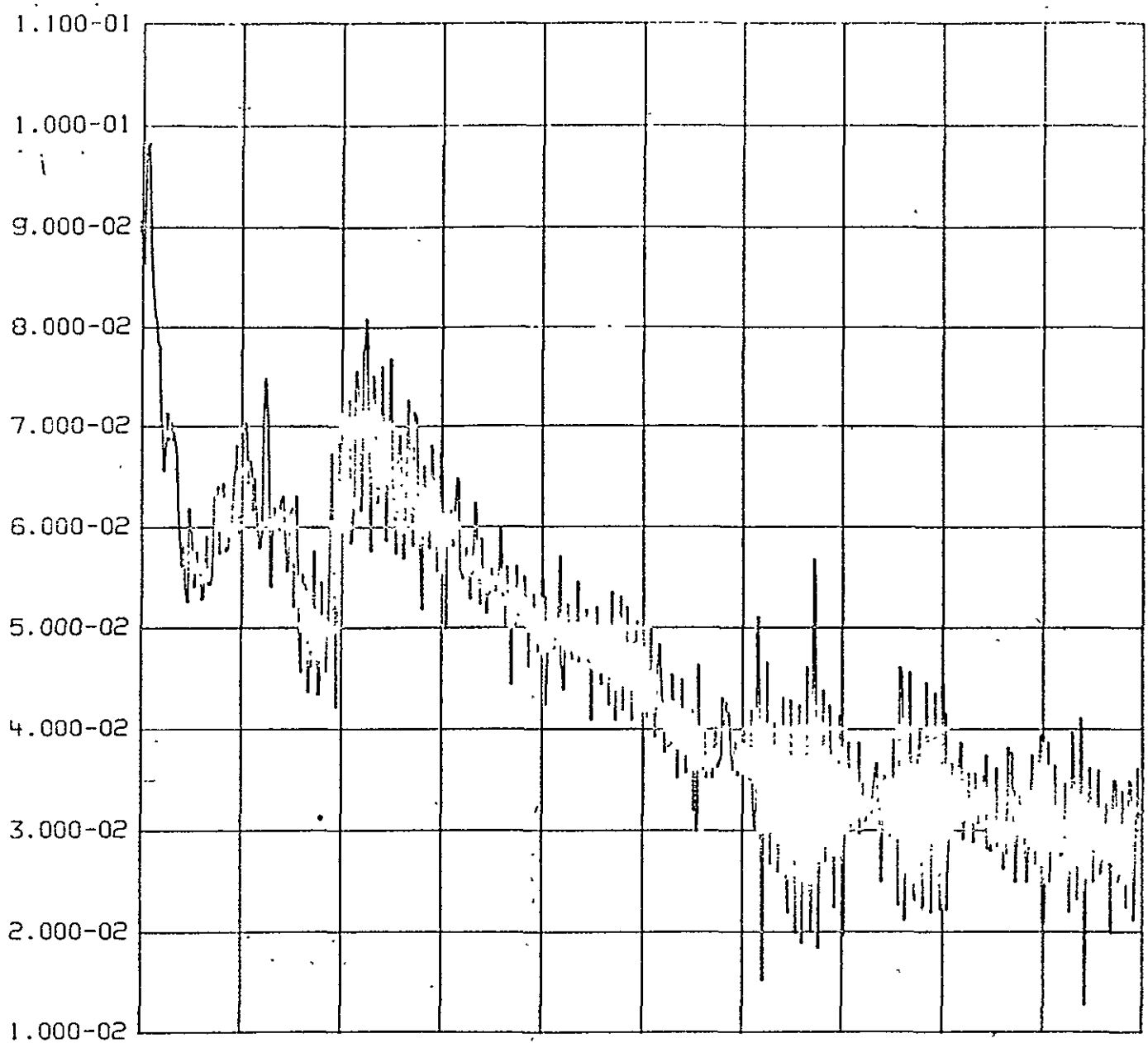


Figure II-6. Aircraft Z-Axis Acceleration from Time of 1g



0. 2.000+00 4.000+00 6.000+00 8.000+00 1.00

AC XAC VS TIME

Figure II-7 Aircraft X-Axis Acceleration from Time of 1g

The aircraft provided the electrical power to operate the pump and instrumentation, and provided lighting for photography.

### 3. Instrumentation

The motion of the liquid was recorded with 16-mm Milliken motion picture cameras, operating at 60 frames/s. One camera was mounted to view the tank from the side, the plane in which the accelerations act. Another camera was mounted forward of the tank, a view which detected any off-axis motion of the liquid. When the baffled tank was tested, a third camera viewed the tank from above and slightly aft, to record the initial motion of the liquid with respect to the antivortex and ring baffles. Figure II-8 shows the locations of the scale model, instrumentation rack, and the cameras in the KC-135 aircraft.

The load cells were of the strain gage type (super-mini model manufactured by Interface, Inc.). The two vertical load cells had a capacity of 2200N (500 lbf) and the lateral load cell had a capacity of 450 N (100 lbf). These load cells were highly linear (0.03% full-scale non-linearity) and had a relatively high sensitivity (45 mv/lbf full-scale when excited with 15 VDC). Their output was recorded on a chart recorder for quick-look data evaluation and was also tape recorded for subsequent data reduction.

The load cells were calibrated as part of the complete force measuring system. With the tank removed from the box frame, known weights were suspended from the fixture and the load cell output was recorded. A pulley arrangement was used to apply lateral forces. The system was also checked for zero-shift and coupling between axes.

A three-axis accelerometer, provided by NASA, measured the applied accelerations. Each axis had a normal and "times ten" output, which were tape recorded, to provide the necessary resolution of the low-g accelerations.

Synchronization between the film and tape recorded data was provided with a bi-level signal. When a push-button was depressed, lamps were illuminated in the field of view of the cameras and the change in level of a dc electrical signal was tape recorded.



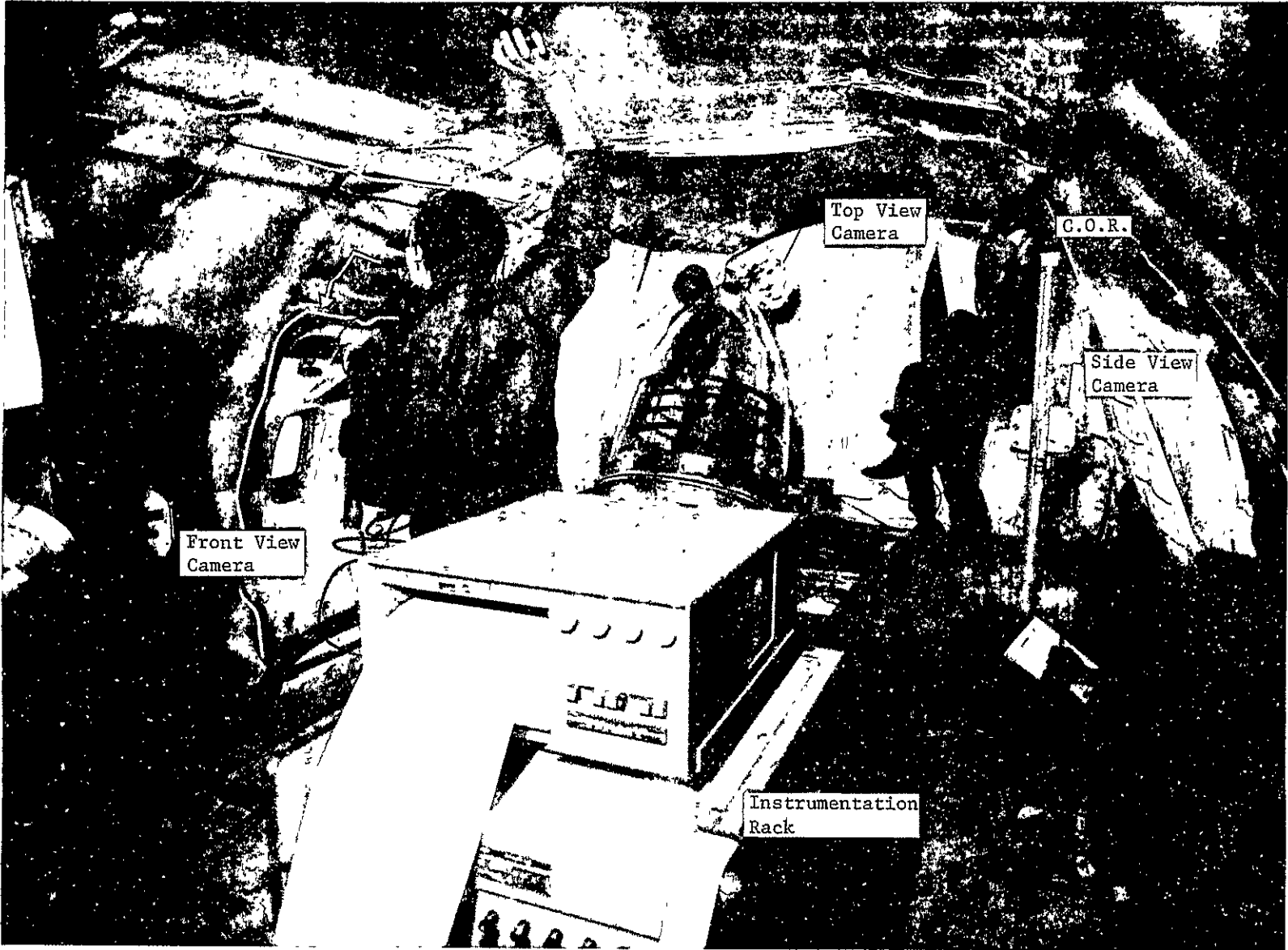


Figure II-8

II-16

ORIGINAL PAGE IS  
OF POOR QUALITY

Figure II-8 Location Scale Model, Instrumentation Rack and Cameras in KC-135

### C. TEST CONDITIONS

Test conditions were chosen to simulate the full-scale conditions encountered during RTLS abort. Listed in Table II-3 are the 30 different test conditions: The first digit of the test number indicates the flight on which the test was performed. Each of the tests was generally repeated three times, due to the variability of the low-g acceleration environment. Test condition 1.4 was repeated 4 times and one test was performed with a dry tank to verify operation of the force measuring system. This resulted in 89 low-g tests.

The actual acceleration environment has acceleration components  $A_x$  and  $A_z$  (see Fig. II-1) whose ratio ( $A_x/A_z$ ) can range from about 3 to 1. When these components are transformed into ZAC and XAC, which are rotated by the tank orientation angle, the ratio ZAC/XAC has a range of 1.64 to 0.62. Under certain conditions XAC was greater than ZAC.

The approach was to select values for ZAC which were to be produced and maintained during the parabola. This acceleration component was either -0.1g or -0.2g as identified in Table II-3 for each test. The pilot produced an XAC component by the manner in which the aircraft entered the parabola, but this component could not be sustained throughout the test period, as was described in the previous section.

Also listed in Table II-3 are the other parameters that were varied during the testing. For the first flight, baffles were not installed in the tank to establish the basic liquid motion in a bare tank. During the third flight, tank orientations of 0° and 30° were evaluated, rather than the standard 13° orientation. Fill volumes of 1%, 5%, 10% and 15% were used, with one test performed at 25% fill. For the fourth flight, the test conditions were essentially the same as those for the second flight, except that the water-Methocel mixture was used as the test liquid instead of Freon 113.

Table II-3 Test Matrix

Test Number	Liquid	Baffles	Acceleration (g)	Orientation, (degrees)	Fill Volume* (Percent)	
1.0	Empty	No	0.1	13	0	
1.1	Freon 113	No	0.2	13	5	
1.2			10			
1.3			15			
1.4			0.1		5	
1.5			10			
1.6			15			
2.1			Yes		0.1	1
2.2					5	
2.3					10	
2.4					15	
2.5			0.2	1		
2.6			3			
2.7			10			
2.8			15			
3.1				30	1	
3.2				5		
3.3				10		
3.4				15		
3.5				0	10	
3.6				0	5	
4.1	Water		0.1	13	2	
4.2					5.5	
4.3					10	
4.4					16	
4.5					25	
4.6			0.2		2	
4.7					5.5	
4.8					10	
4.9					16	

\*Actual Flight Values.

## D. DATA REDUCTION

The data reduction process is described in the following paragraphs and examples for one test condition are presented. Tables II-4 to II-7 delineate the time intervals selected for digitization from the analog flight tapes.

Figure II-9 delineates the data reduction process. The process consisted of two major parts: 1) digitization of the data and conversion to engineering units in CDC computer format, and 2) transformation of the load cell forces to the tank coordinate system for analytical comparison.

### 1. Digitization

The analog flight tape was digitized via a REDCOR system into a special digital format tape for specified time periods, including calibration times. The result was a digital tape in units of counts where 1000 counts was full scale for any channel of data.

Each time period corresponds to one test point and is considered one file on the digital tape. These files were made up of  $m$  records where one record is 0.2 seconds of real-time data. Each file is separated from every other on the tape by an end of file marker.

The calibrations were set up as follows:

zero values = file 1  
+ calibration = file 2  
- calibration = file 3

The digitized tape, therefore consists of  $N + 3$  files,  $N$  being the number of actual tests on the analog tape.

Digitization was accomplished at a rate of 5000 Hz over 8 channels, or 625 samples/s/channel.

The REDCOR digital tape was transformed to a CDC computer Scope Internal Binary (SIB) format via computer program HTCNVRT. This allowed processing of the data via standard FORTRAN programming

The SIB data files created by program HTCNVRT were then processed via program DIGIT. This program converted the digitized data to engineering units by using the calibration files and input calibration scale factors. Only every 10th data point was kept for an effective digitization rate of 62.5 samples/s/channel.

Table II-4 . NAS9-15302 Flight Data Digitization Times

FLIGHT 1/2 ABORT 1,2 AUG 1978  
 FREON, NO BAFFLES

MANEUVER #	TIME		DESCRIPTION
	START	END	
1	14:48:00	14:48:45	1.0-1
2	14:49:10	14:49:45	1.4-1
3	14:50:10	14:50:45	1.4-2
4	14:51:25	14:52:00	1.4-3
5	14:52:20	14:52:55	1.4-4
6	14:53:10	14:53:40	1.5-1
7	14:54:40	14:55:10	1.5-2
8	14:56:20	14:56:55	1.5-3
9	DATA LOST		1.6-1
10	NOT ON		1.6-2
11	TAPE		1.6-3
12	15:02:05	15:02:35	1.3-1
13	15:04:30	15:05:00	1.3-2
14	15:06:25	15:07:00	1.3-3
15	15:09:35	15:10:05	1.2-1
16	15:11:15	15:11:45	1.2-2
17	15:12:35	15:13:15	1.2-3
18	15:13:20	15:14:00	1.1-1
19	15:15:15	15:15:50	1.1-2
20	15:17:00	15:17:33	1.1-3

Table II-5 NAS9-15302 Flight Data Digitization Times

FLIGHT #2 29 AUGUST 1978  
FREON, BAFFLES

MANEUVER #	TIME		DESCRIPTION
	START	END	
1	20:36:40	20:37:10	2.1-1
2	20:37:30	20:38:50	2.1-2
3	20:38:24	20:38:47	2.1-3
4	20:39:08	20:39:36	2.2-1
5	20:39:53	20:40:20	2.2-2
6	20:40:40	20:41:07	2.2-3
7	20:41:23	20:41:50	2.3-1
8	20:42:04	20:42:30	2.3-2
9	20:43:04	20:43:30	2.3-3
10	20:43:50	20:44:18	2.4-1
11	20:44:44	20:45:10	2.4-2
12	20:45:28	20:45:54	2.4-3
13	20:46:13	20:46:38	2.8-1
14	20:46:48	20:47:14	2.8-2
15	20:47:28	20:47:55	2.8-3
16	20:48:20	20:48:47	2.7-1
17	20:49:08	20:49:34	2.7-2
18	20:49:55	20:50:20	2.7-3
19	20:50:42	20:51:09	2.6-1
20	20:51:28	20:51:57	2.6-2
21	20:52:10	20:52:36	2.6-3
22	20:53:14	20:53:40	2.5-1
23	20:54:00	20:54:25	2.5-2
24	20:54:48	20:55:14	2.5-3

Table II-6 NAS9-15302 Flight Data Digitization Times

FLIGHT 3

30 AUGUST 1978

FREON, BAFFLES

MANEUVER #	TIME		DESCRIPTION
	START	END	
1	17:56:30	17:57:10	3.1-1
2	17:57:40	17:58:10	3.1-2
3	17:58:30	17:59:00	3.1-3
4	17:59:20	17:59:50	3.2-1
5	18:00:00	18:00:50	3.2-2
6	18:01:10	18:01:40	3.2-3
7	18:02:10	18:02:40	3.3-1
8	18:03:00	18:03:30	3.3-2
9	18:03:50	18:04:20	3.3-3
10	18:04:30	18:05:00	3.4-1
11	18:05:20	18:05:50	3.4-2
12	18:06:20	18:06:50	3.4-3
13	18:07:20	18:07:50	3.5-1
14	18:08:10	18:08:50	3.5-2
15	18:09:00	18:09:30	3.5-3
16	18:09:50	18:10:20	3.6-1
17	18:11:00	18:11:20	3.6-2
18	18:11:20	18:11:50	3.6-3

Table II-7 NAS9-15302 Flight Data Digitization Times

FLIGHT #4

1 SEPT 1978

WATER, BAFFLES

MANEUVER #	TIME		DESCRIPTION
	START	END	
1	19:14:00	19:14:40	4.1-1
2	19:14:50	19:15:30	4.1-2
3	19:15:50	19:16:30	4.1-3
4	19:16:40	19:17:10	4.6-1
5	19:17:30	19:18:00	4.6-2
6	19:18:20	19:18:50	4.6-3
7	19:19:10	19:19:40	4.2-1
8	19:20:00	19:20:30	4.2-2
9	19:20:50	19:21:20	4.2-3
10	19:21:30	19:22:00	4.7-1
11	19:22:20	19:22:50	4.7-2
12	19:23:10	19:23:40	4.7-3
13	19:24:00	19:24:30	4.3-1
14	19:24:50	19:25:30	4.3-2
15	19:25:40	19:26:20	4.3-3
16	19:26:30	19:27:00	4.8-1
17	19:27:20	19:27:50	4.8-2
18	19:28:20	19:28:40	4.8-3
19	19:29:00	19:29:30	4.4-1
20	19:29:50	19:30:20	4.4-2
21	19:30:50	19:31:20	4.4-3
22	19:31:40	19:32:00	4.9-1
23	19:32:30	19:32:50	4.9-2
24	19:33:20	19:33:50	4.9-3
25	19:34:30	19:35:00	4.5-1
26	19:35:30	19:36:00	4.5-2
27	19:36:50	19:37:10	4.5-3
28	19:37:50	19:38:10	zero G
29	19:38:40	19:39:00	zero G



Figure II-9

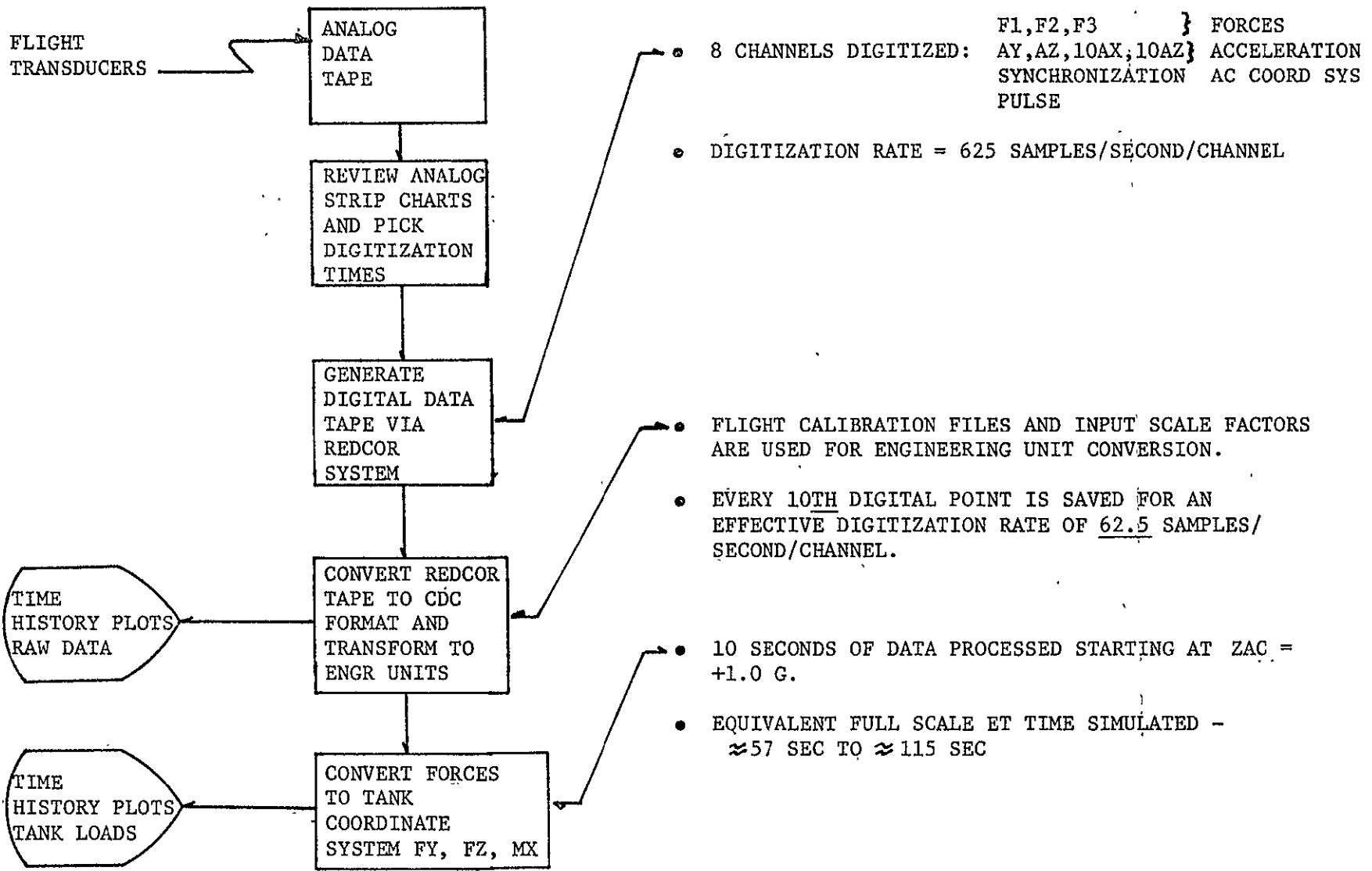


Figure II-9 Data Reduction Process

The result of program DIGIT is a set of digital time histories in engineering units. Figure II-10 through II-17 are examples of the 8 digitized channels of data for test 2.3-2. Shown in Figures II-10, II-11, and II-12 are the time histories of vertical load cell 1, vertical load cell 2 and the horizontal load cell. The aircraft Y acceleration; the aircraft fine resolution X acceleration the the aircraft fine and coarse resolution Z acceleration are shown in Figures II-13 through II-16. A manually operated timing pulse appears in Figure II-17. This timing signal is normally at a positive voltage, depression of the timing switch turned on an indicator light visible in the film data, and resulted in a negative voltage spike in the test data.

2. Transformation of Forces to Tank Coordinates

Once the data had been digitized and converted to engineering units the raw load cell data was converted to forces in the tank coordinate system: FY, FZ, MX (Fig. II-18). Only a portion of the test data was converted to tank coordinates. It was felt that 10 seconds of data starting when ZAC  $\approx$  +1g was sufficient to define the region of interest. The tank coordinate system is located such that the origin lies at the center of the tank barrel section. Figure II-17 presents the methodology employed. Figures II-19 through II-21 show the task forces and moments, FY, FZ, and MX for test 2.3-2. The aircraft accelerations AC XAC, AC YAC and AC ZAC, for 10 s from AC ZAC  $\approx$  1 g, are shown in Figures II-22 through II-24.

Upon completion of the data reduction process twenty-nine liquid motion tests were selected which best met the test conditions specified in Table II-3. Planor fluid reorientation in the aircraft X-Z plane was desired. This type of motion could best be correlated with the planor motions observed in the drop tower testing. There were an average of three tests for each test condition. The front view film data and time histories of the aircraft Y acceleration were used to select the tests with minimum out-of-plane motion. These selected tests are listed in Table II-8. The digitized and transformed time histories of these selected tests are presented in Appendix A (Volume II of this report). The empty tank test condition, 1.0-1, is included with these data.

*Table II-8 Tests Selected for Analytical Comparisons*

Flight 1	Flight 2	Flight 3	Flight 4
1.0-1	2.1-3	3.1-1	4.1-3
1.1-3	2.2-3	3.2-2	4.2-3
1.2-2	2.3-3	3.3-2	4.3-2
1.3-3	2.4-2	3.4-3	4.4-2
1.4-1	2.5-3	3.5-3	4.5-1
1.5-3	2.6-3	3.6-2	4.6-1
1.6-3	2.7-2		4.7-2
	2.8-2		4.8-1
			4.9-3

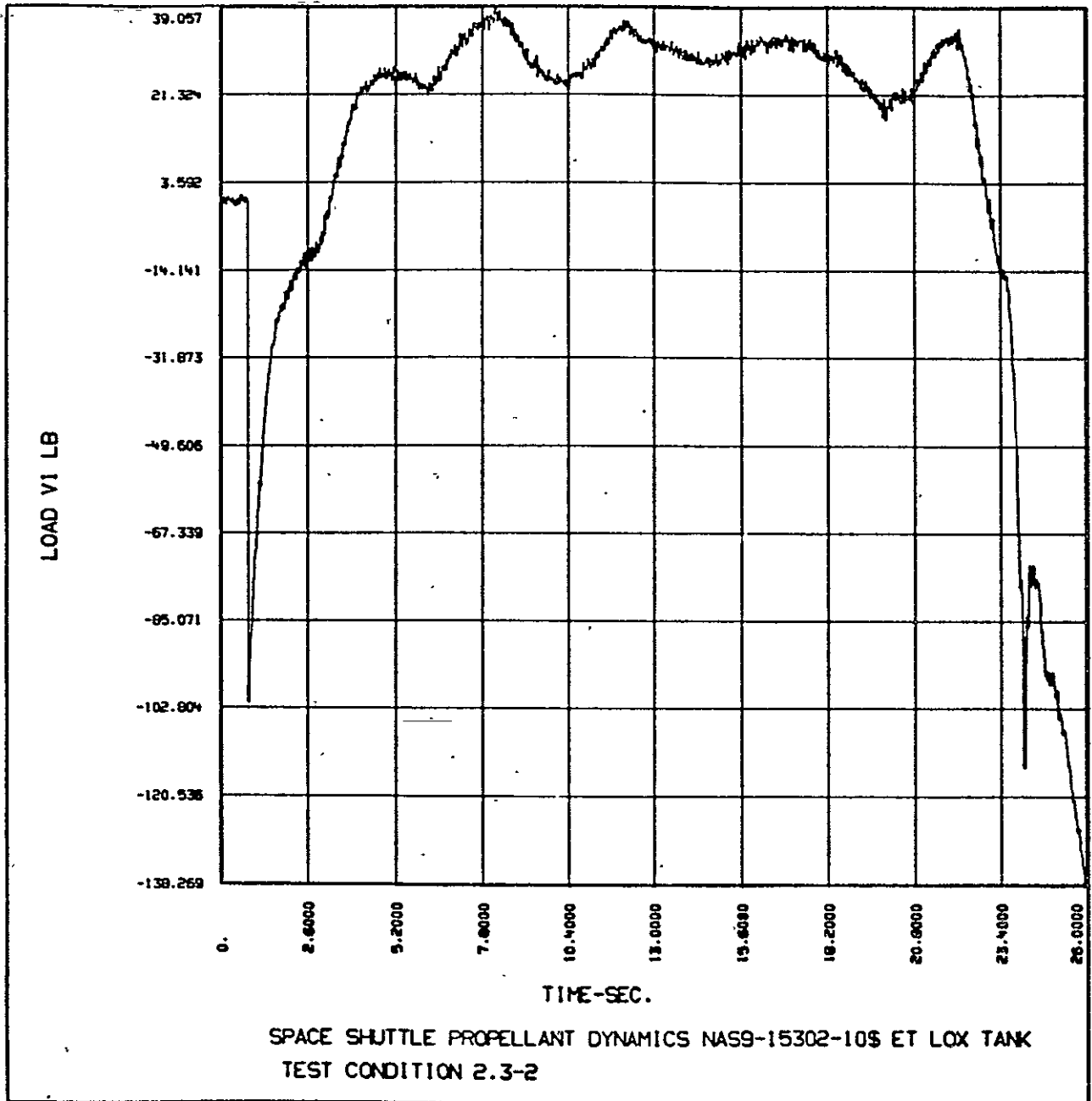


Figure II-10 Vertical Load Cell No. 1

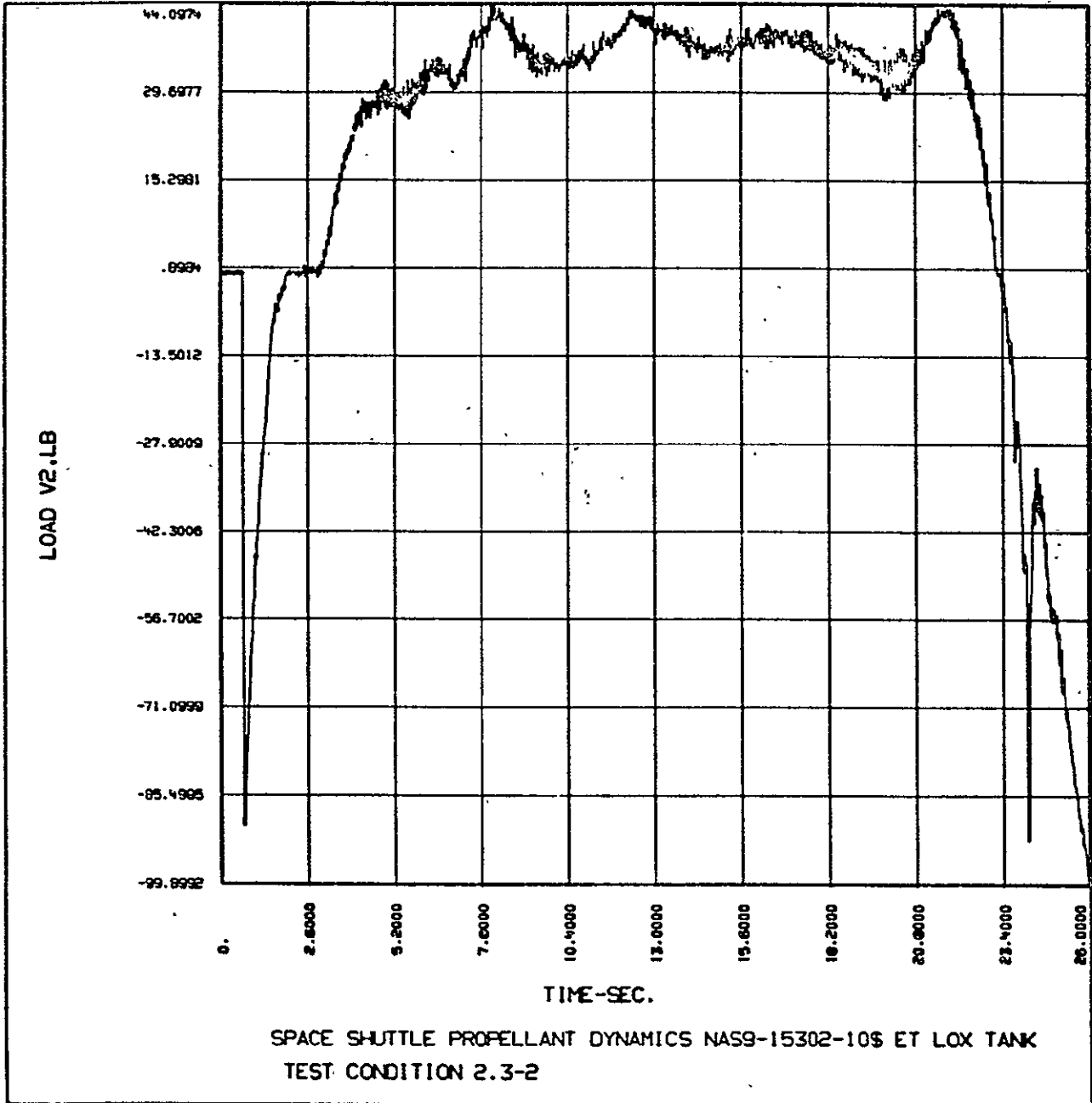


Figure II-11 Vertical Load Cell No. 2

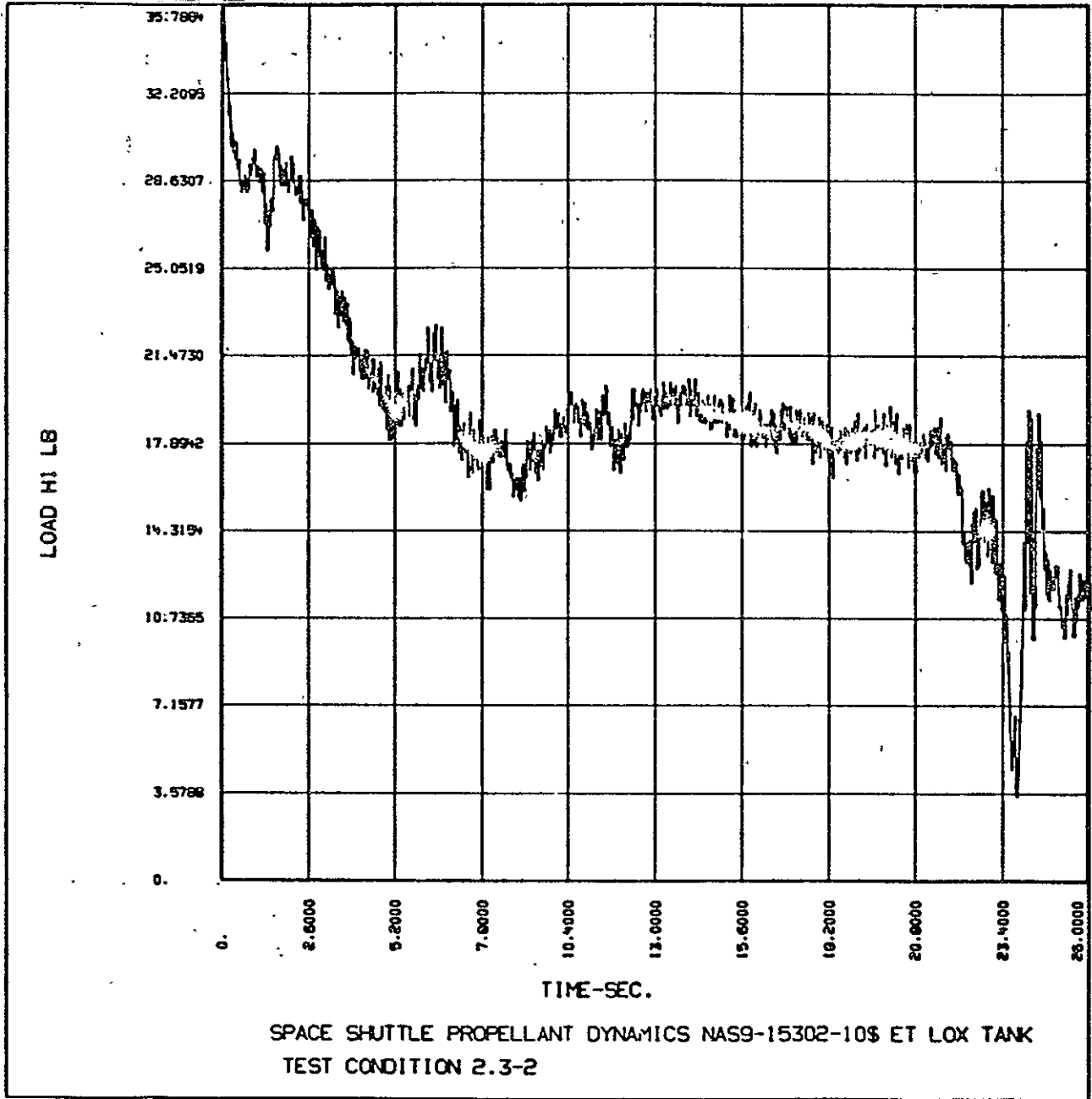


Figure II-12 Horizontal Load Cell

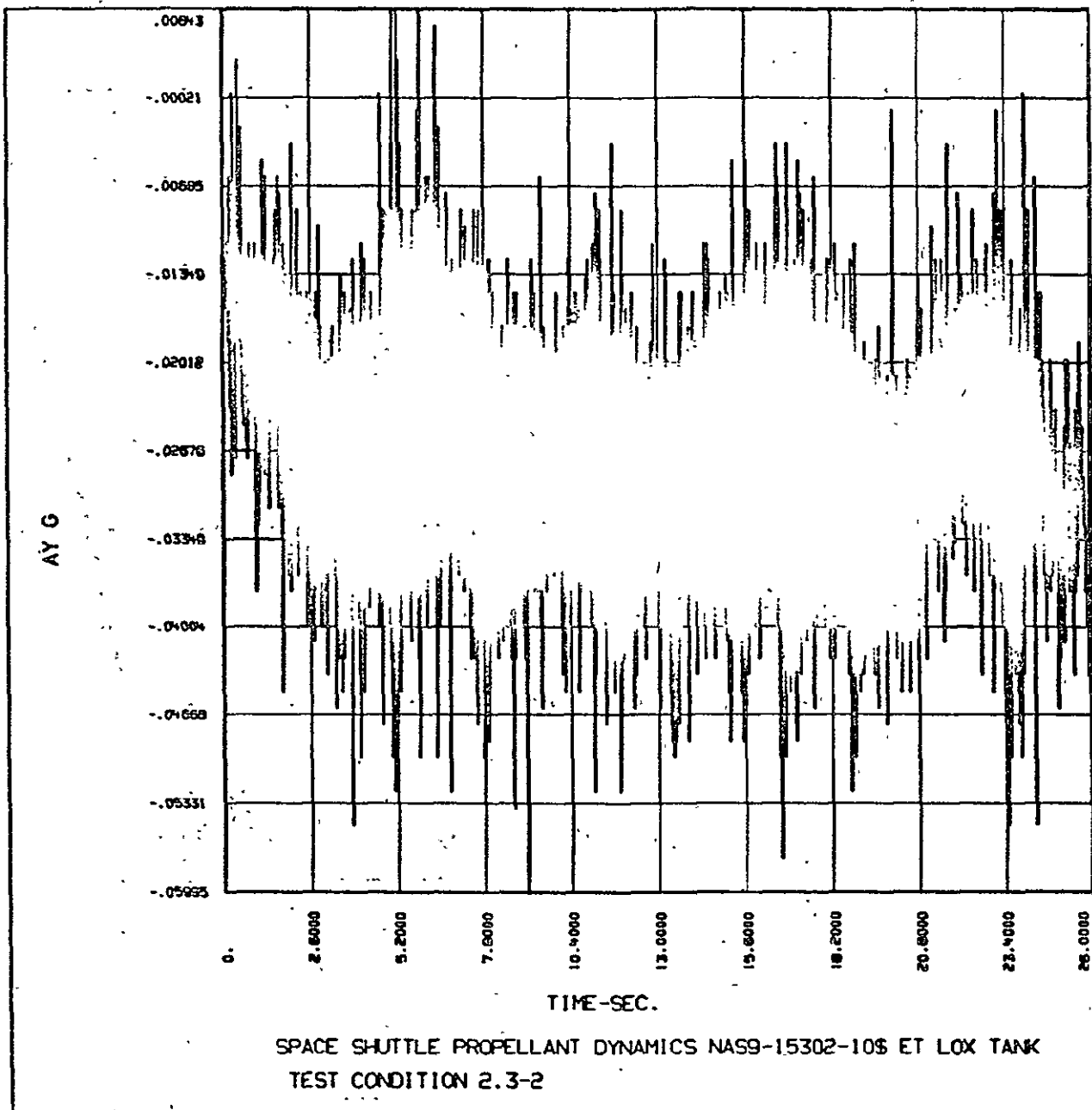


Figure II-13 Aircraft Y Acceleration

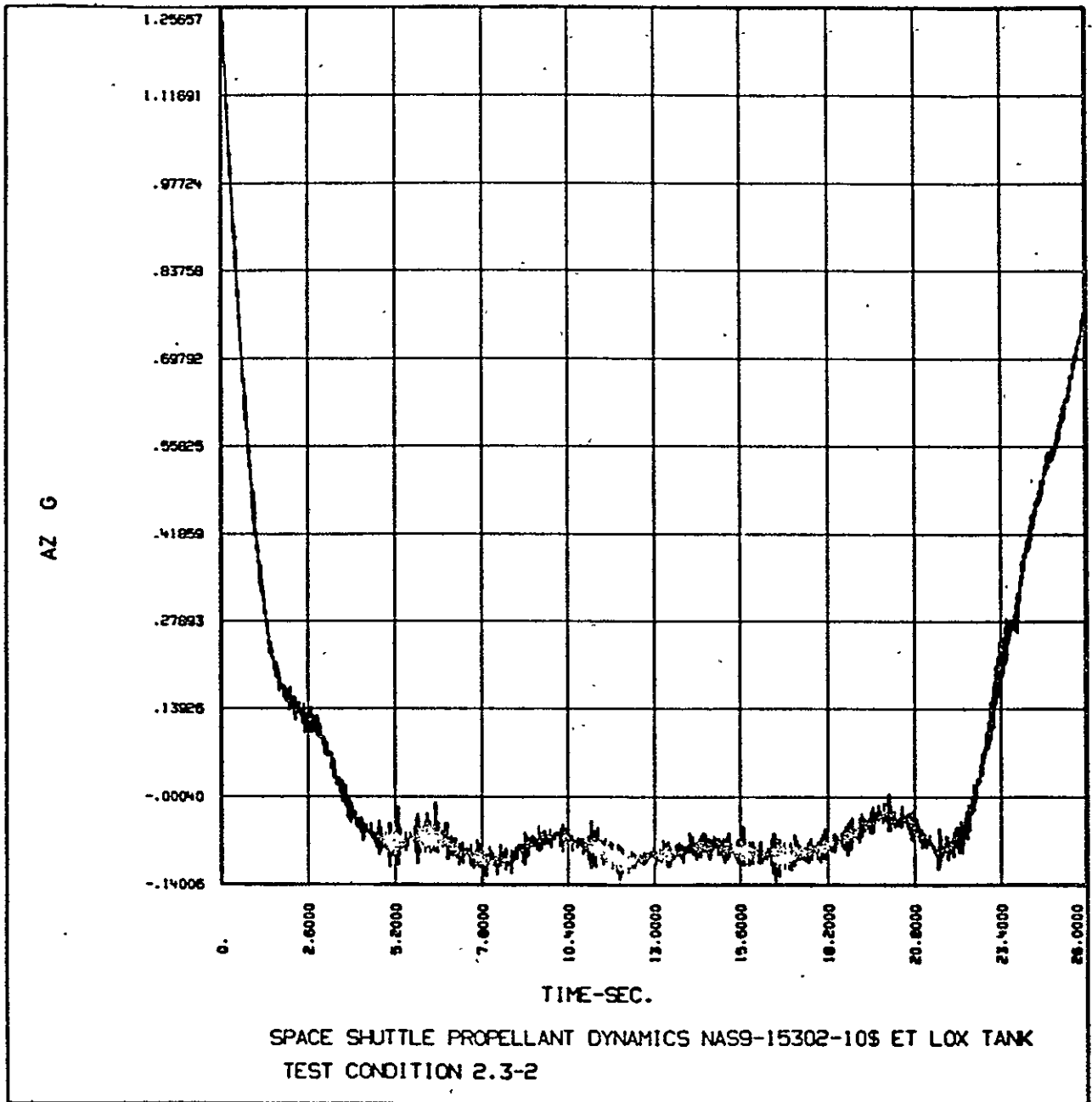


Figure II-14 Aircraft Z Acceleration

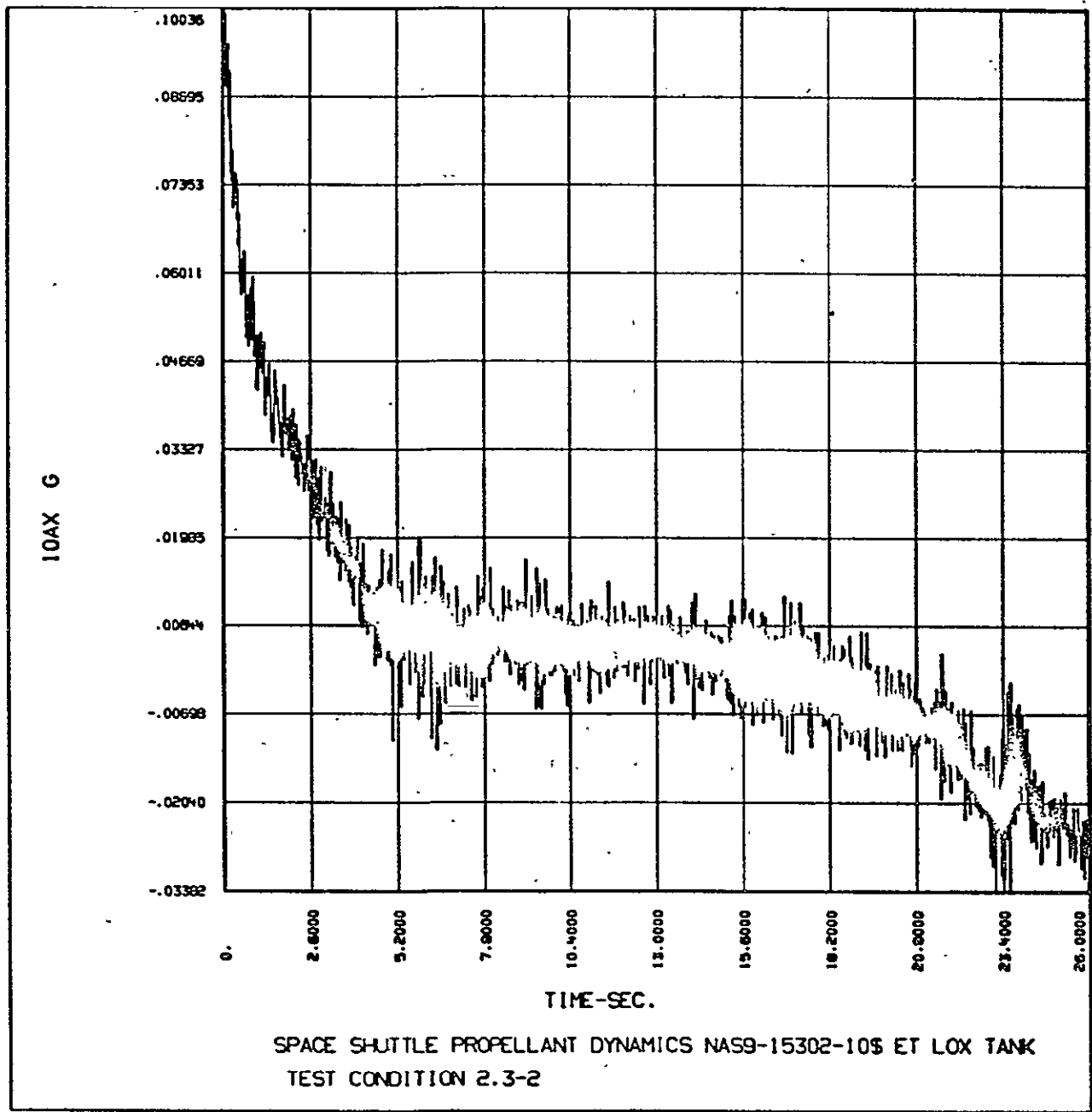


Figure II-15 Aircraft X Acceleration (Fine)



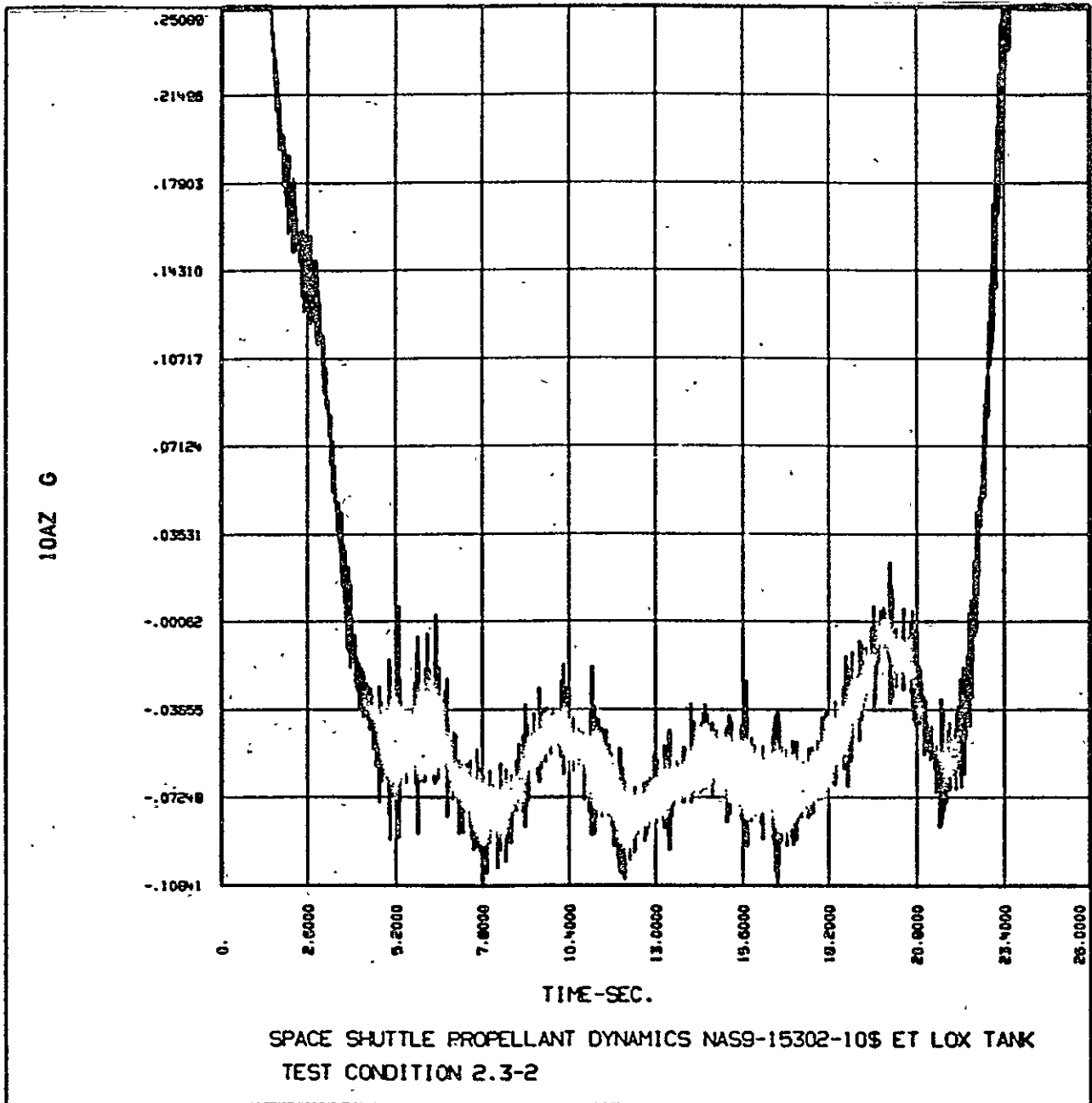


Figure II-16 Aircraft Z Acceleration (Fine)

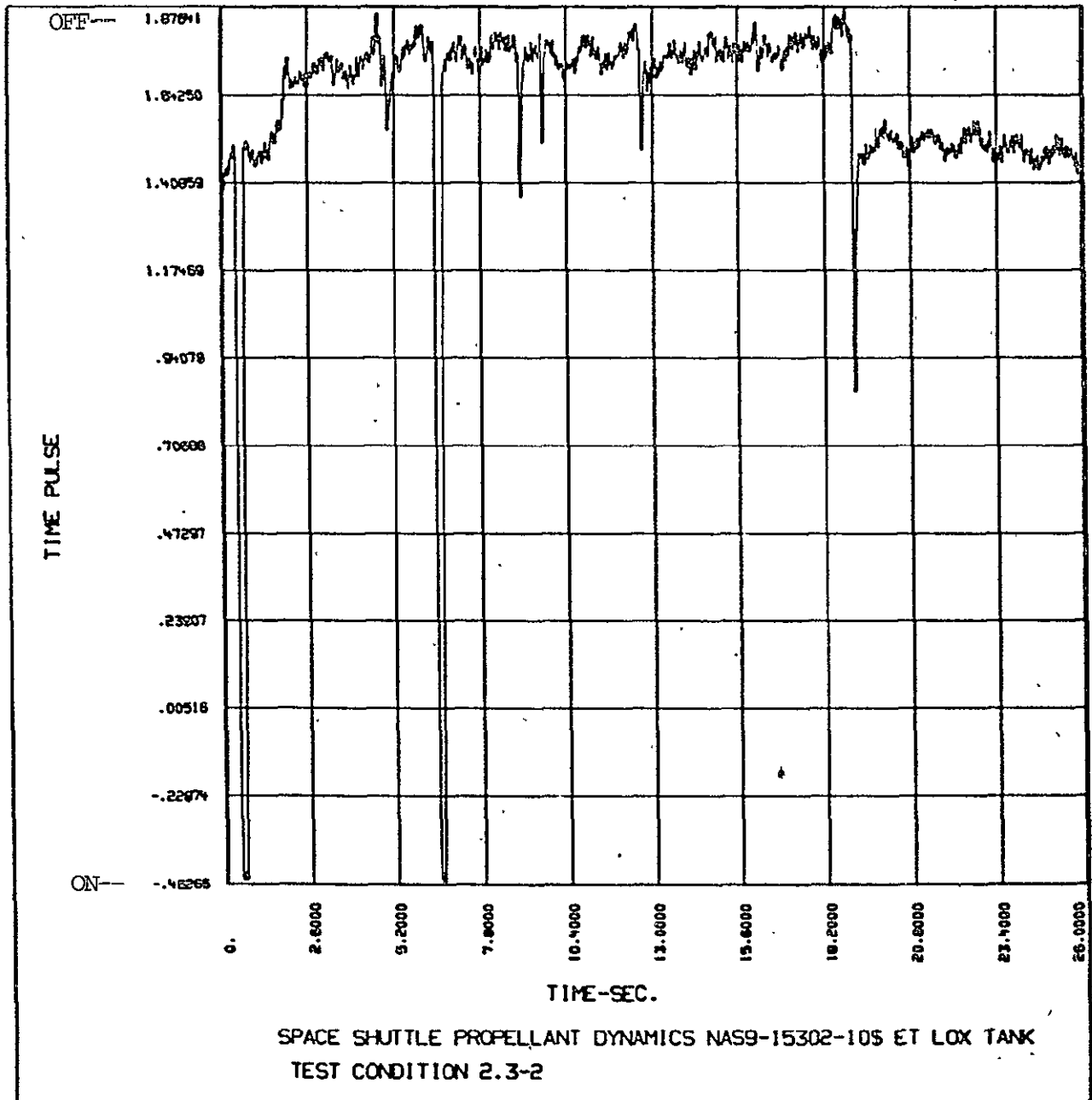
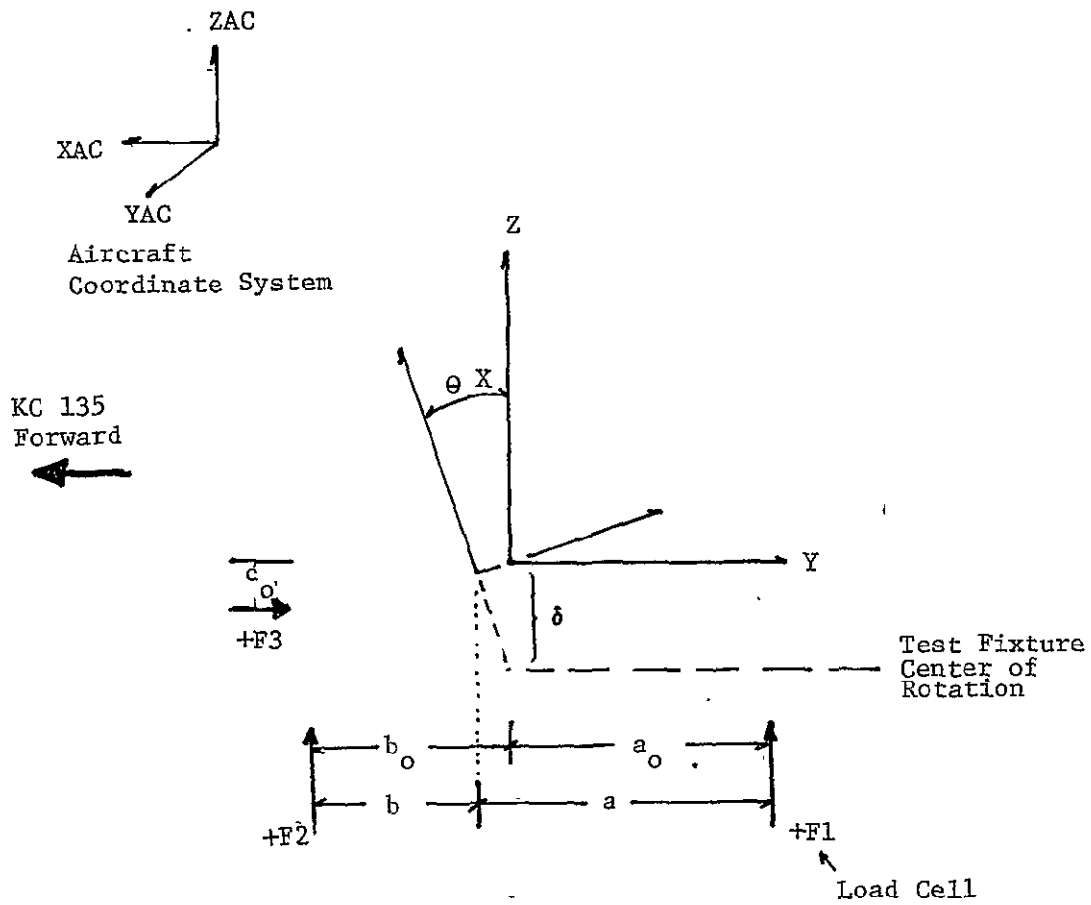


Figure II-17 Camera Synchronization Pulse



$$a = a_0 + \delta \sin \theta X$$

$$b = b_0 - \delta \sin \theta X$$

$$c = c_0 - \delta (1 - \cos \theta X)$$

$$FZI = F1 + F2$$

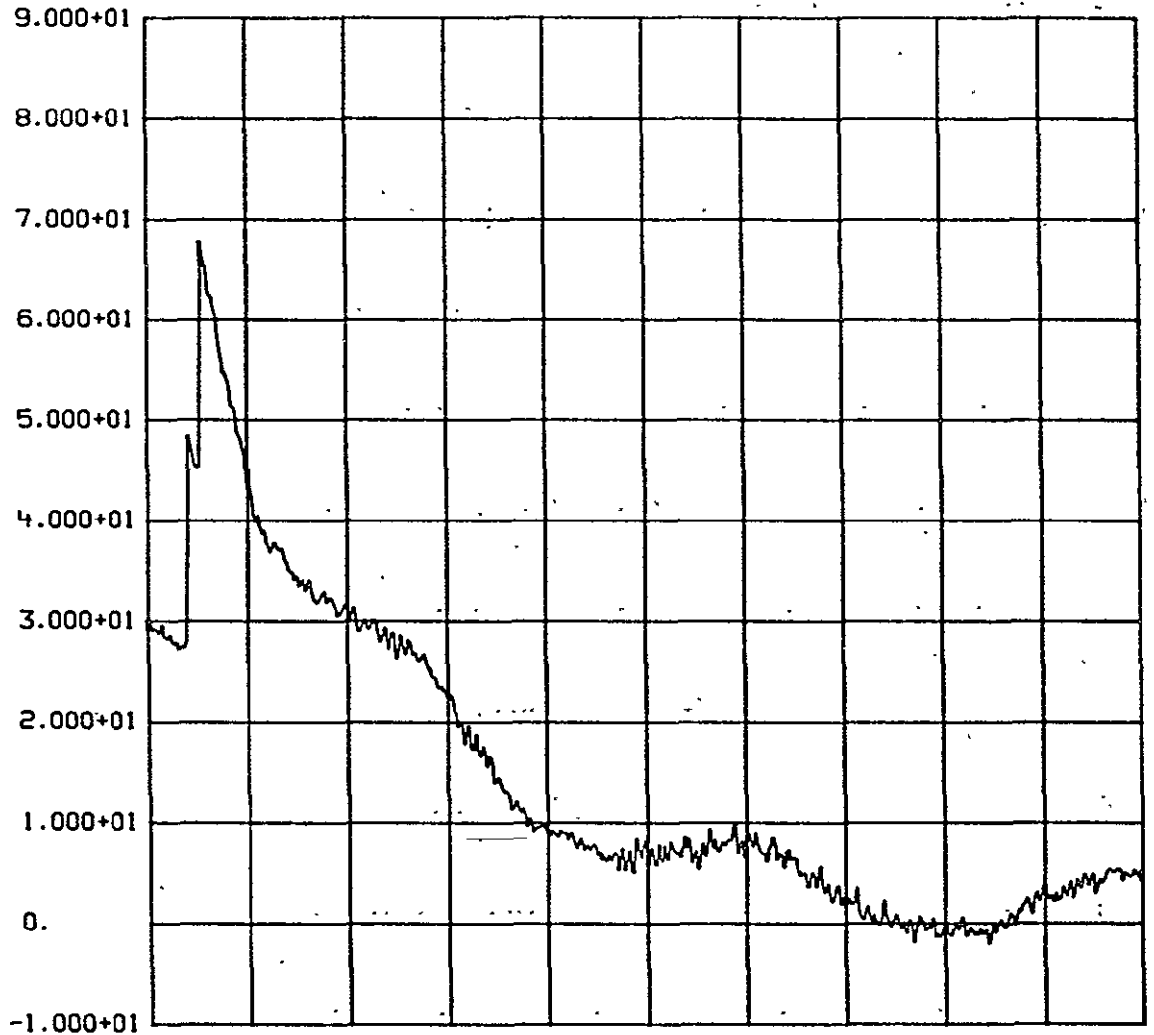
$$FYI = F3$$

$$FYT = FYI \cos \theta X + FZI \sin \theta X$$

$$FZT = FZI \cos \theta X - FYI \sin \theta X$$

$$MXT = F1(a) - F2(b) + F3(c)$$

Figure II-18 Force Transformation to Tank Coordinate System

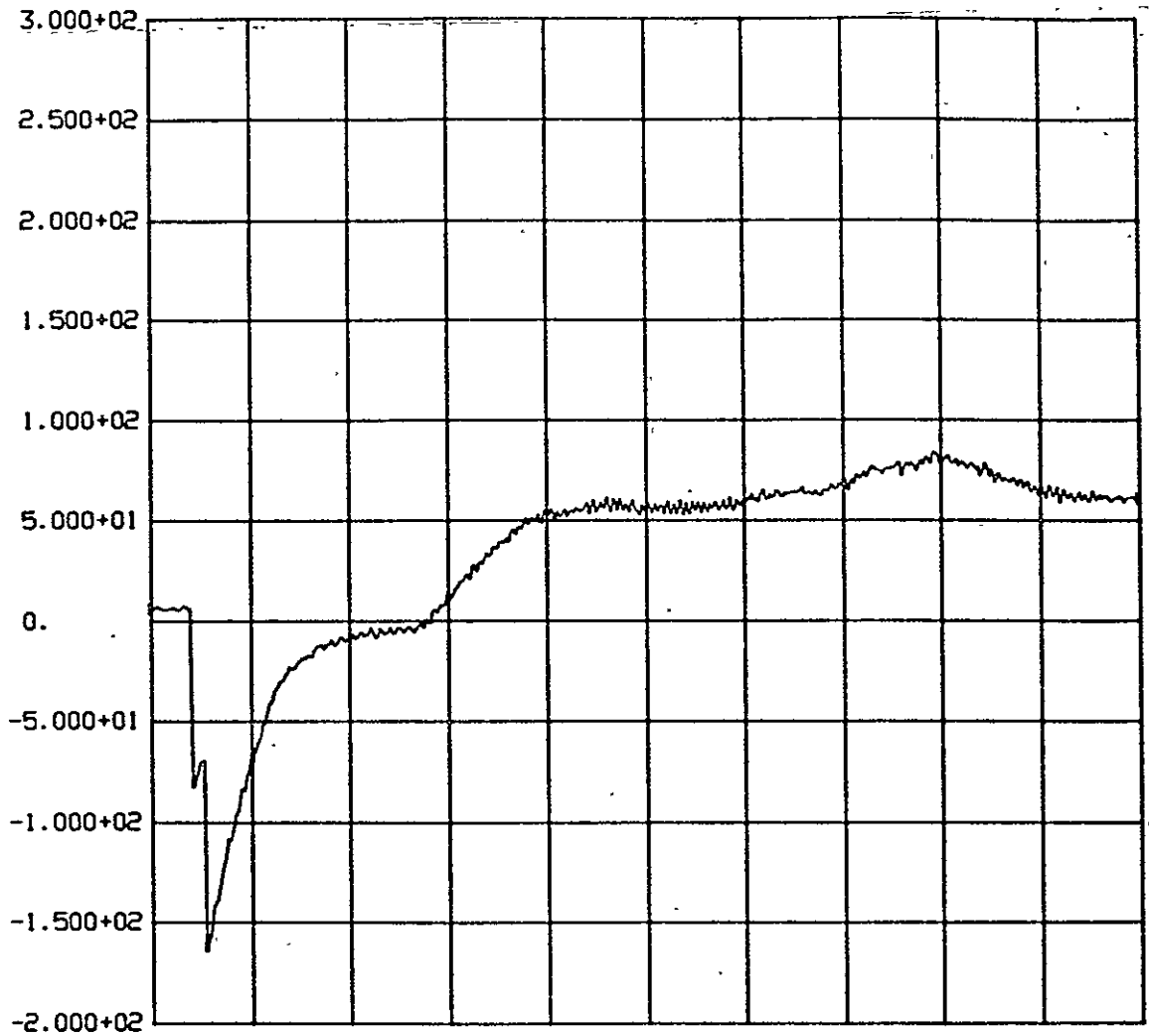


0. 2.000+00 4.000+00 6.000+00 8.000+00 1.00

Y-LOAD VS TIME

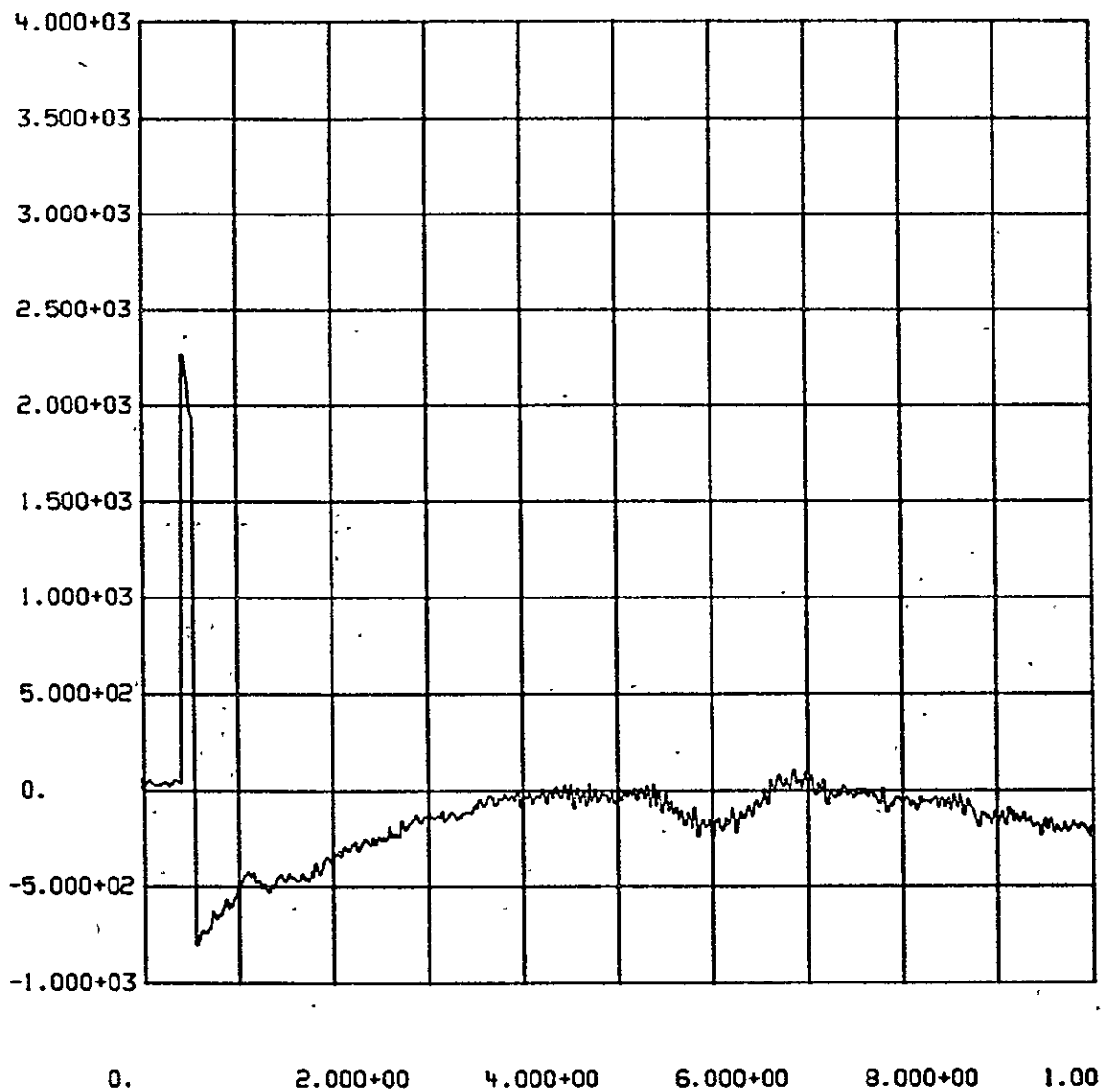
1 FLT 2 03N078 FLIGHT 2 TEST CONDITION 2.3-2 \* UNFILT \*

Figure II-19 Tank Y Load (lb)



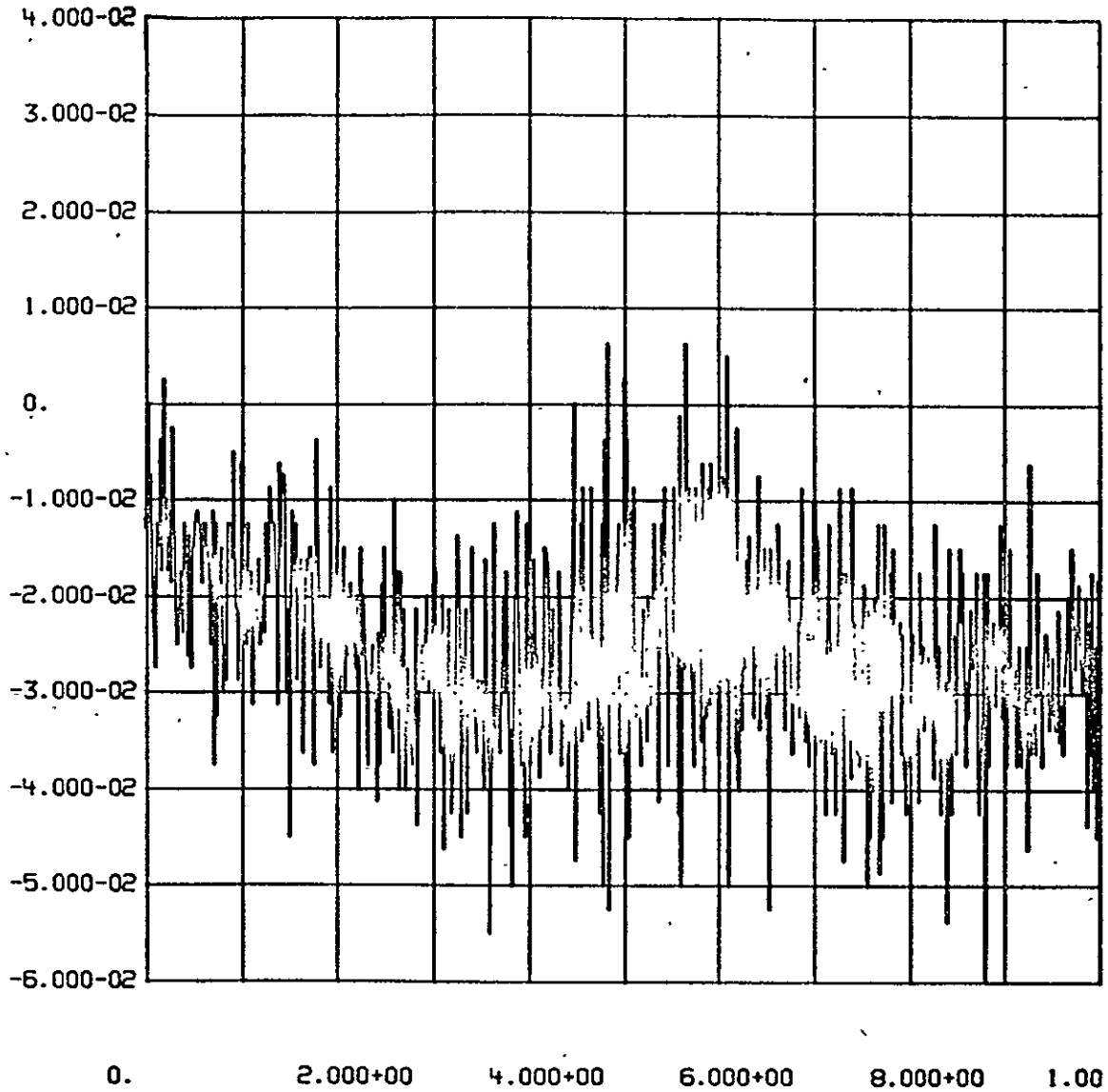
0.                    2.000+00                    4.000+00                    6.000+00                    8.000+00                    10.000+00  
 Z-LOAD                    VS                    TIME  
 1                    FLT 2                    03N078                    FLIGHT 2 TEST CONDITION 2.3-2 \* UNFILT \*

Figure II-20 Tank Z Load (lb)



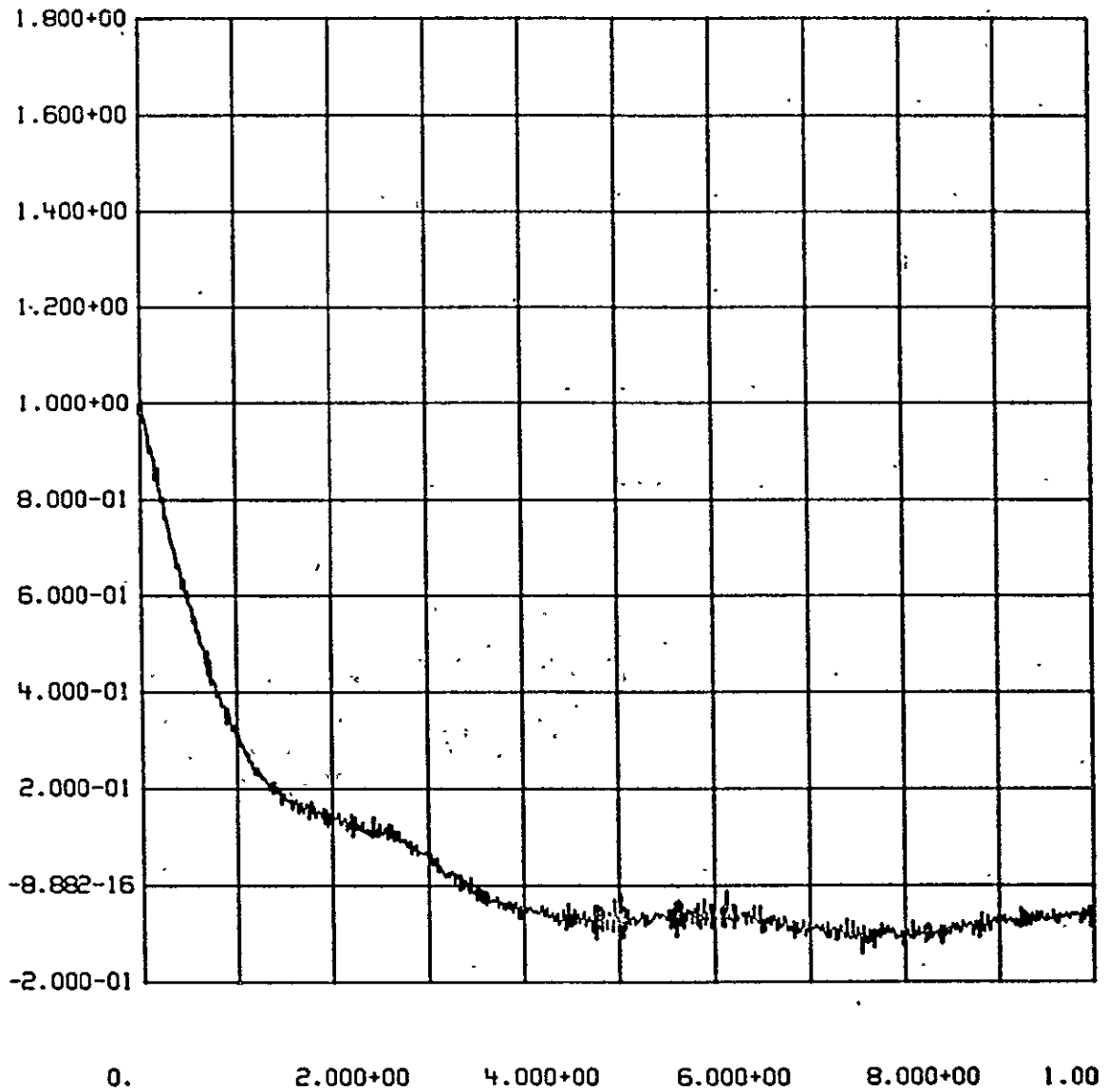
MOMENT VS TIME  
 1 FLT 2 03N078 FLIGHT 2 TEST CONDITION 2.3-2 \* UNFILT \*

Figure II-21 Tank X Moment (in-lb)



AC YAC VS TIME  
 1 FLT 2 03N078 FLIGHT 2 TEST CONDITION 2.3-2 \* UNFILT \*

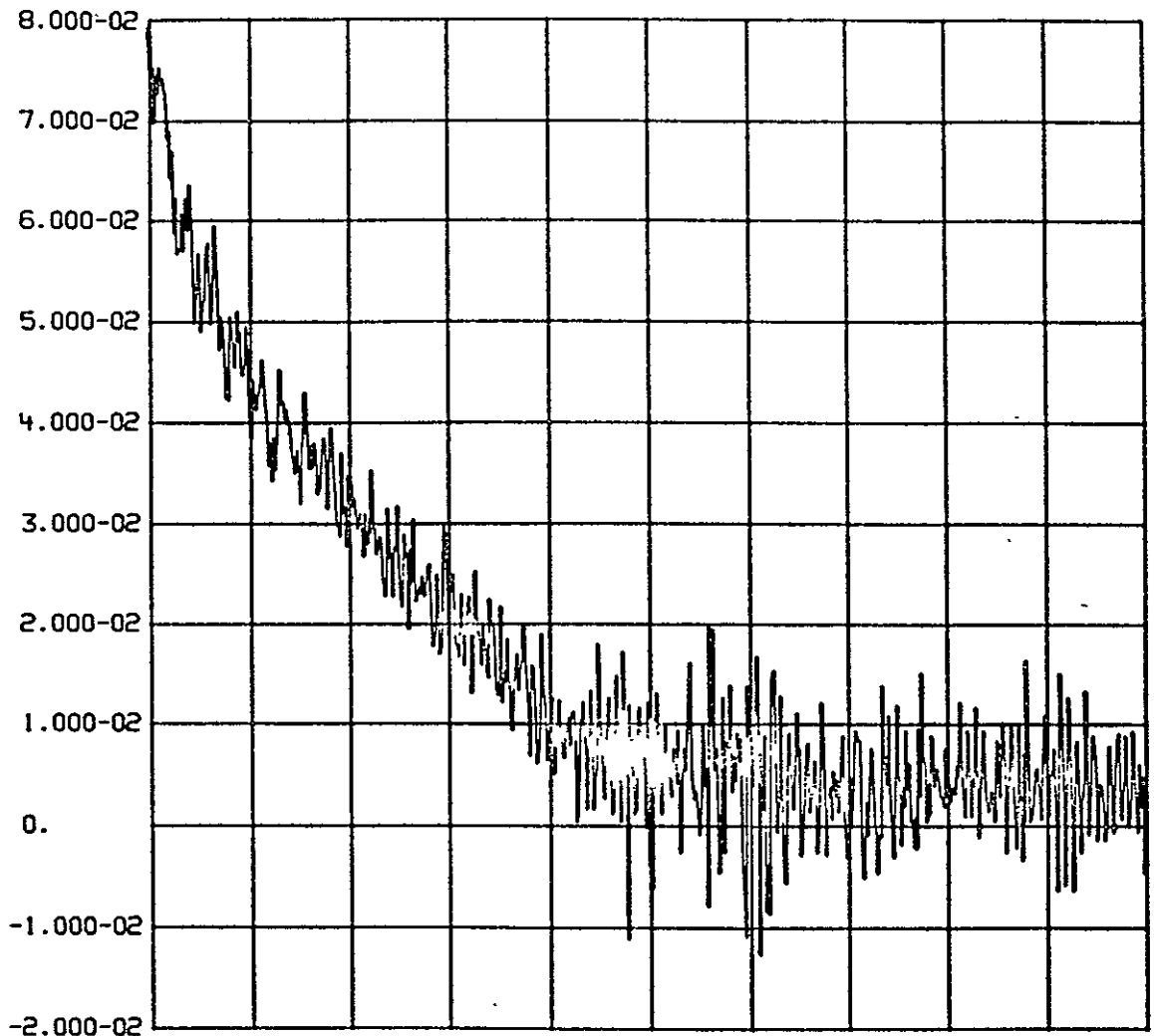
Figure II-22 Aircraft Y Acceleration (gs)



AC ZAC VS TIME  
 1 FLT 2 03NO78 FLIGHT 2 TEST CONDITION 2.3-2 \* UNFILT \*

Figure II-23 Aircraft Z Acceleration (gs)





0. 2.000+00 4.000+00 6.000+00 8.000+00 1.00

AC XAC

VS

TIME

1

FLT 2

03N078

FLIGHT 2 TEST CONDITION 2.3-2 \* UNFILT \*

Figure II-24 Aircraft X Acceleration (gs)

## E. TANK GEOMETRY AND TEST CONSTANTS

The mechanical drawings of the 1/10 scale tank model along with important test constants are presented in this section. Figure II-25 shows the assembled tank with slosh baffles and antivortex baffles. The test fixture pivot point is included as a reference point on this drawing. Figure II-26 shows the overall dimensions of the antivortex baffles and slosh baffles. Table II-9 delineates test constants which facilitate test-analytical correlations.

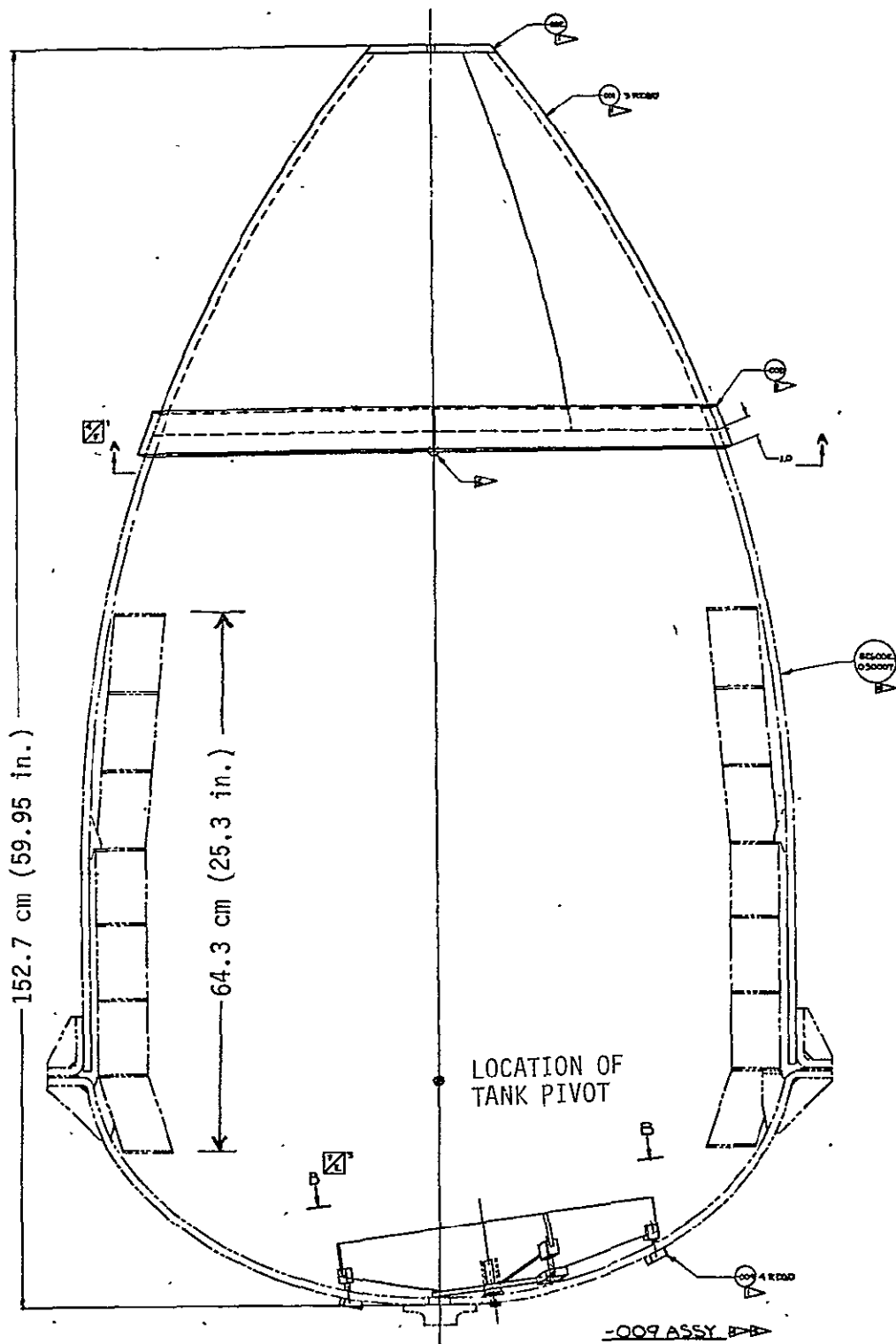
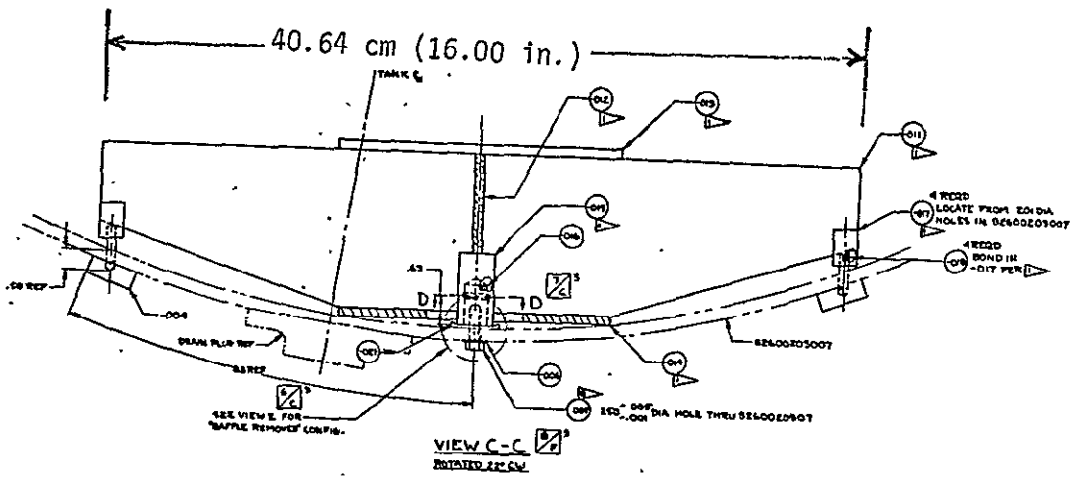
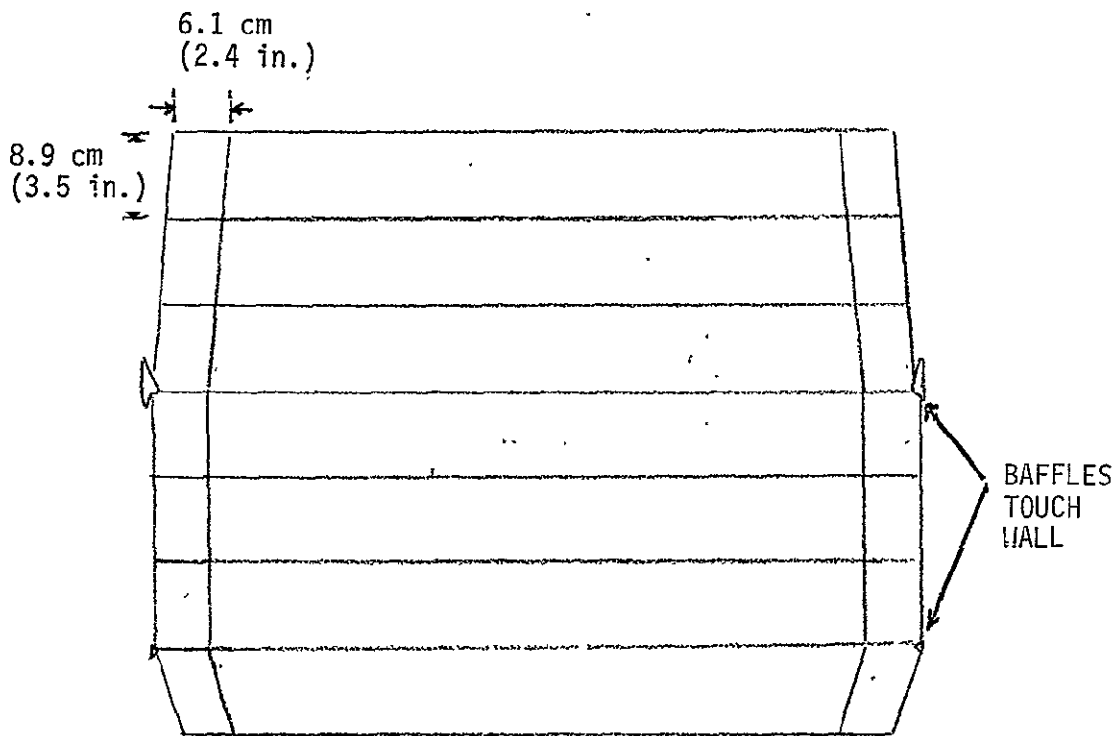


Figure II-25 1/10 Scale Model Tank Geometry



### ANTIVORTEX BAFFLES



### SLOSH BAFFLES

Figure II-26 Antivortex and Slosh Baffle Geometry

Table II-9 Test Constants

Weights	Original Tank		Repaired Tank	
	(lb)	kg	(lb)	kg
Unbaffled Tank	(128.85)	58.45	(130.8)	59.33
Baffled Tank	(146.05)	66.25	(148.0)	67.13
Slosh Baffles	(16.25)	7.37	(16.25)	7.37
Antivortex Baffles	(0.95)	0.43	(0.95)	0.43
Box Ring	(64.1)	29.08	(64.1)	29.08
Total Structural Weight Without Baffles	(192.95)	87.52	(194.9)	88.40
Total Structural Weight With Baffles	(210.15)	95.32	(212.1)	96.21
C.G. Location from Bottom of Tank	(24.78 in.)	62.94 cm.	(22.0 in.)	55.88 cm

Test Fixture Geometric Constants (See Figure II-18)

	(in.)	cm
$a_o$	(27.47)	69.77
$b_o$	(23.40)	59.44
$c_o$	(1.56)	3.96
$\delta$	(5.95)	15.10

Tank Fill Volumes

	(gal)	liters
100%	(146.05)	552.8
25%	(36.51)	138.2
15%	(21.91)	82.9
10%	(14.61)	55.3
5%	(7.30)	27.6
2%	(2.92)	11.1
1%	(1.46)	5.5

### III. OBSERVATIONS ON LIQUID MOTION

---

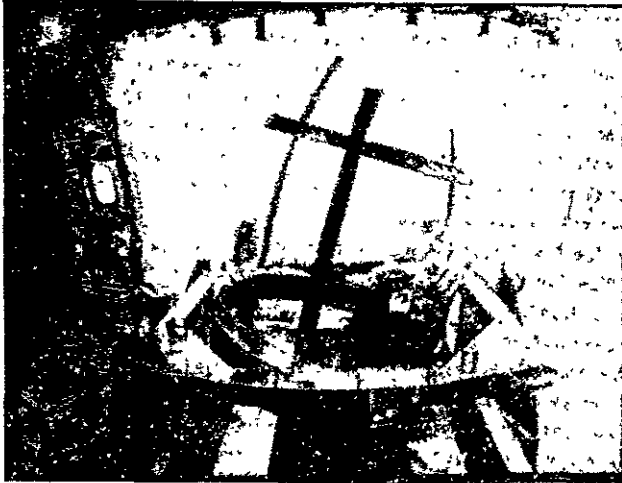
The film data collected during the test program showed how the liquid moved under conditions simulating the ET separation maneuver. The relationship between the observed liquid motion and the measured forces is the key to the analytical prediction of the forces. The film data permitted an evaluation of the manner in which the liquid moved as it reoriented within the tank. The film was used to evaluate the influence of factors such as the baffles, acceleration magnitude, tank orientation and liquid viscosity. Finally, a comparison between the film data from the zero-g aircraft tests and the drop tower tests was performed to evaluate the test scaling. The results of the film data evaluation are presented in this chapter.

In general, the liquid motion simulated by the tests was the reorientation of the liquid from its initial position at the bottom of the tank to the top of the ogive dome. The time scaling of the test and the test period were such that complete reorientation of the liquid could take place. At the end of the test the liquid was nearly quiescent, with some residual motion due to the variation in the aircraft acceleration and attitude.

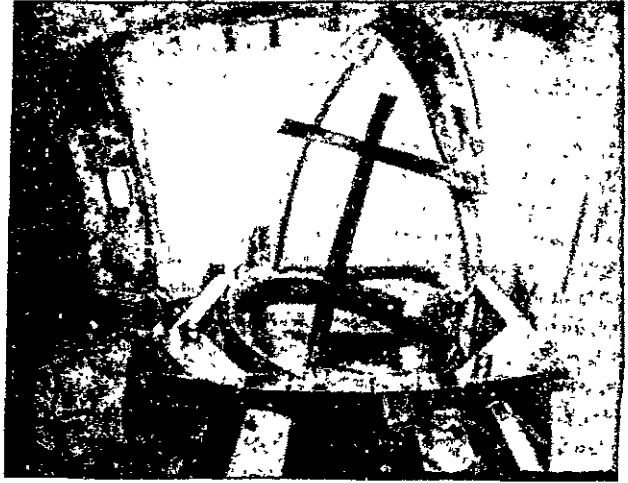
Figures III-1 through III-4 are photos made from single frames of four of the twenty-nine selected tests. These frames were taken from the side view films of the tank. In this view one acceleration component (ZAC) acted downward and the other component (XAC) acted toward the left. The time indicated is referenced to the point at which the ZAC acceleration passed through positive one-g. A photo of the time zero initial conditions was not possible because the liquid was obscured by the test fixture. Figures III-5 and III-6 are reproduced from the drop tower test report (Reference 1) for the purpose of comparing the aircraft and drop tower tests.

#### A. LIQUID MOTION IN BARE TANK

The sequence of pictures from test 1.2 in Figure III-1 shows the general nature of the liquid motion in the bare tank. Due to the XAC component, the liquid reoriented along the right side of the tank. Upon reaching the top of the tank the liquid returned toward the bottom of the tank on the left side. Some collection of the liquid in the tip of the ogive dome occurred as it passed through. The liquid that collected in the ogive had very little entrained gas. This liquid did not remain collected out flowed down the left side of the tank. Most of the liquid then came to rest along the left side of the tank, with a small portion continuing to the



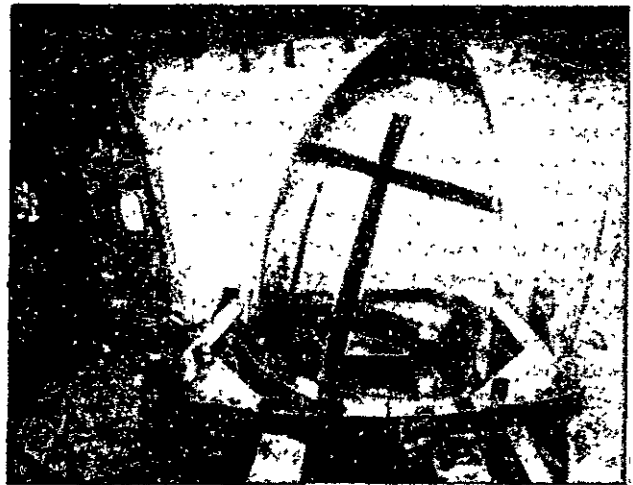
$t = 2.7 \text{ s}$



$t = 3.8 \text{ s}$



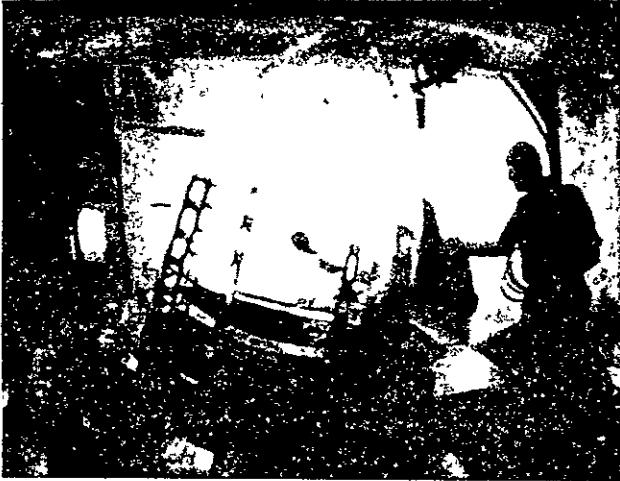
$t = 4.4 \text{ s}$



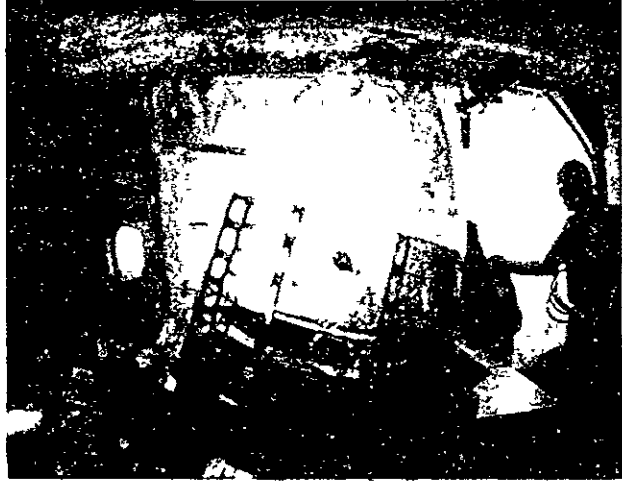
$t = 5.1 \text{ s}$

*Figure III-1 Aircraft Test 1.2-2, Freon 113,  $\gamma = 13^\circ$ , 10% Fill, 0.2g., No Baffles*

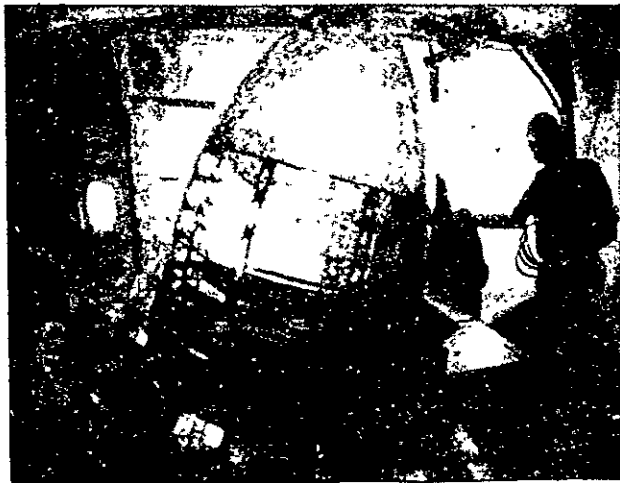
ORIGINAL PAGE IS  
OF POOR QUALITY



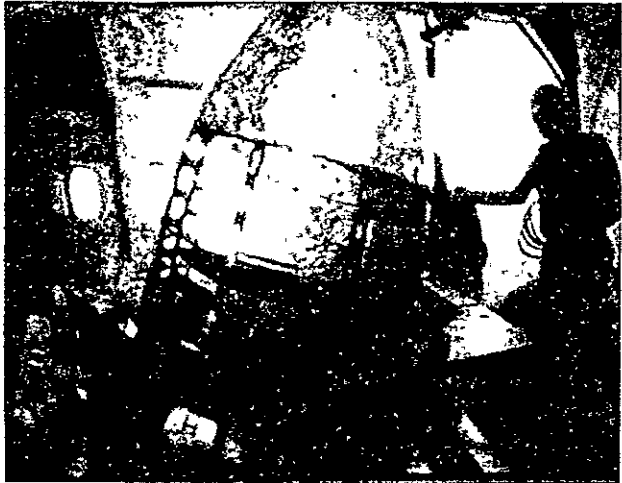
$t = 4.8 \text{ s}$



$t = 6.0 \text{ s}$



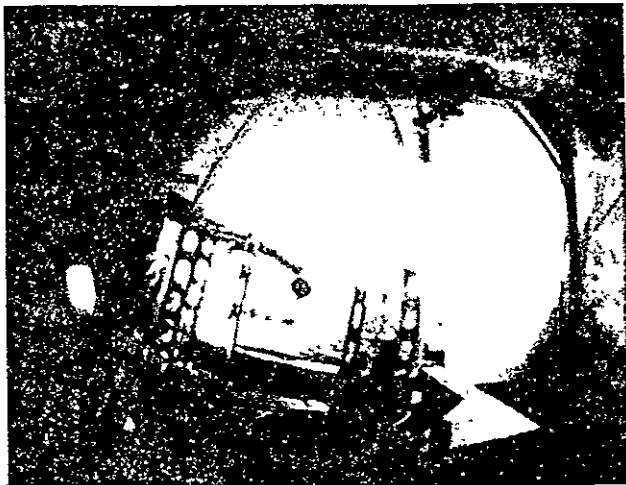
$t = 7.2 \text{ s}$



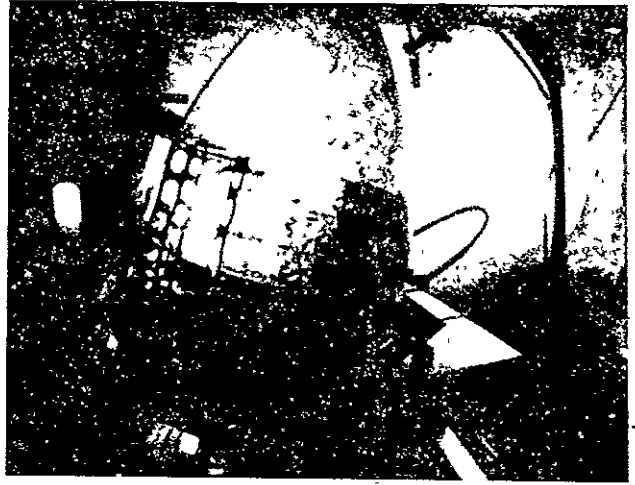
$t = 8.5 \text{ s}$

Figure III-2 Aircraft Test 2.3-3, Freon 113,  $\gamma = 13^\circ$  10% Fill, 0.1g, Baffles

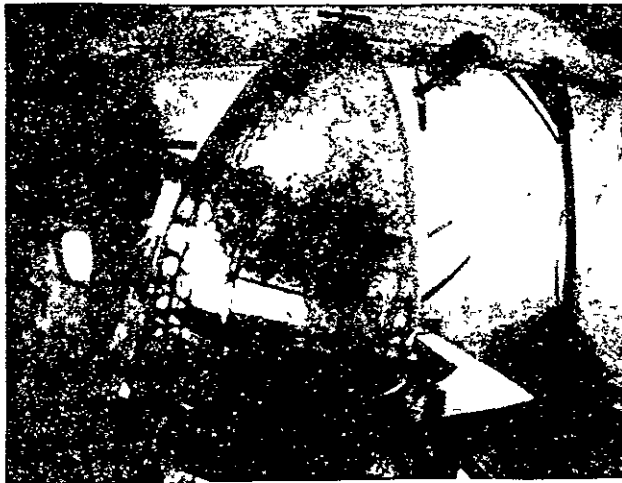




t = 3.9 s



t = 4.8 s

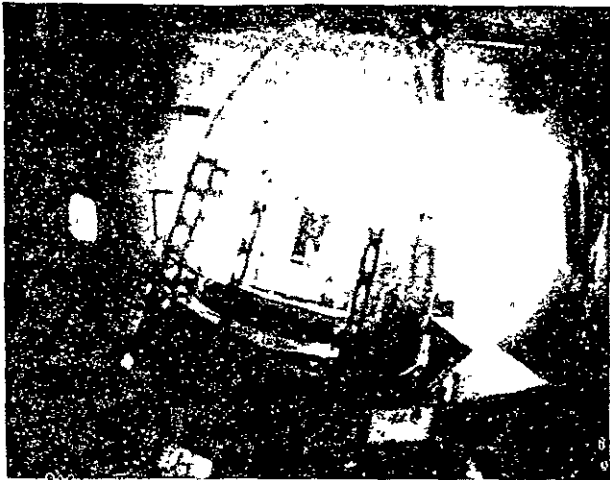


t = 5.6 s

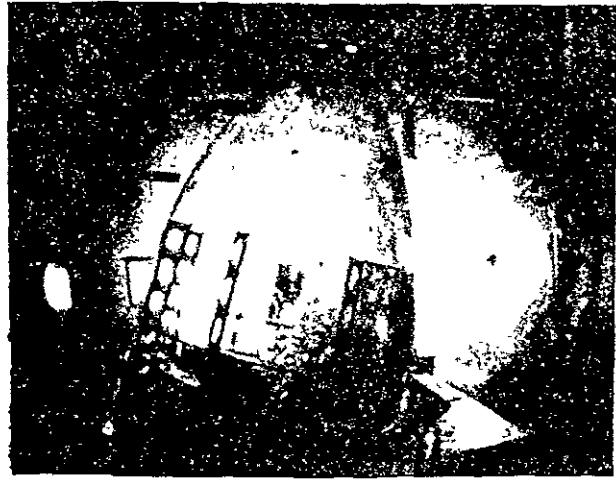


t = 6.4 s

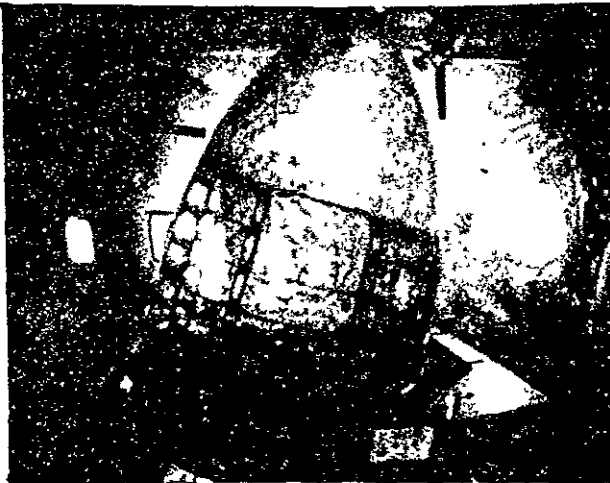
Figure III-3 Aircraft Test 2.7-2 , Freon 113,  $\gamma = 13^\circ$ , 10% Fill, 0.2g, Baffles



$t = 1.4 \text{ s}$



$t = 1.9 \text{ s}$

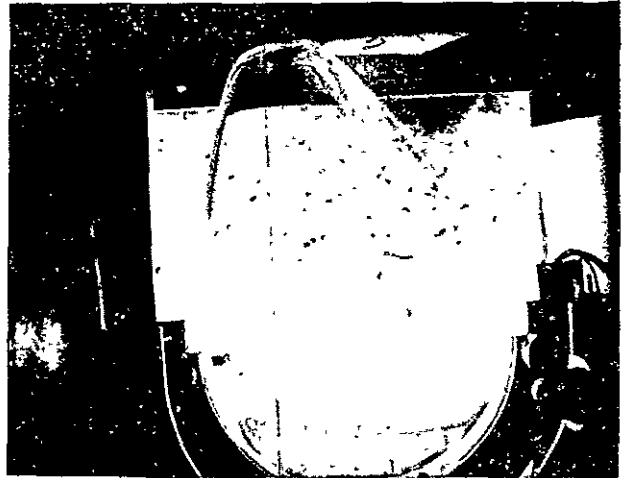


$t = 2.7 \text{ s}$



$t = 3.4 \text{ s}$

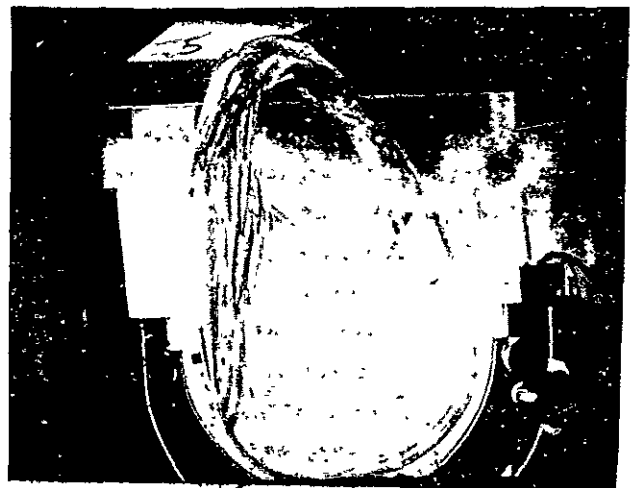
*Figure III-4 Aircraft Test 4.8-1, Water,  $\gamma = 13^\circ$ , 10% Fill, 0.2g, Baffles*



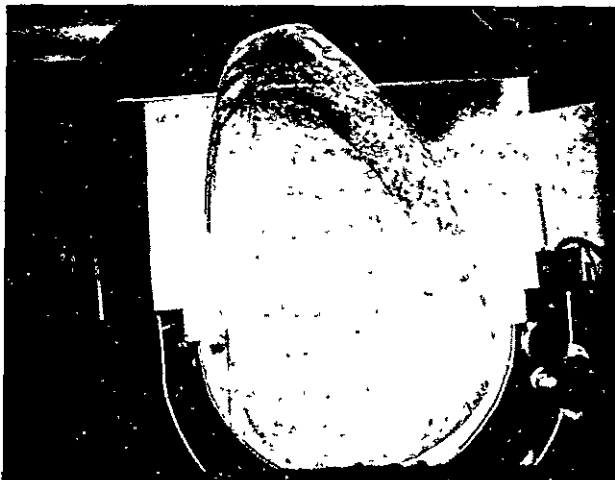
t = 0.0 s



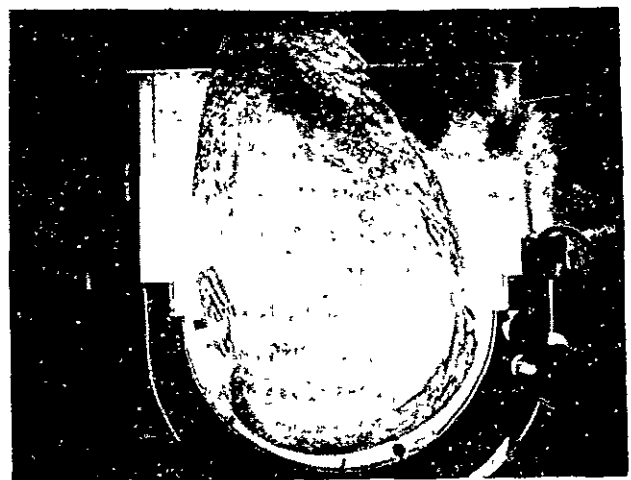
t = 0.4 s



t = 0.8 s



t = 1.2 s



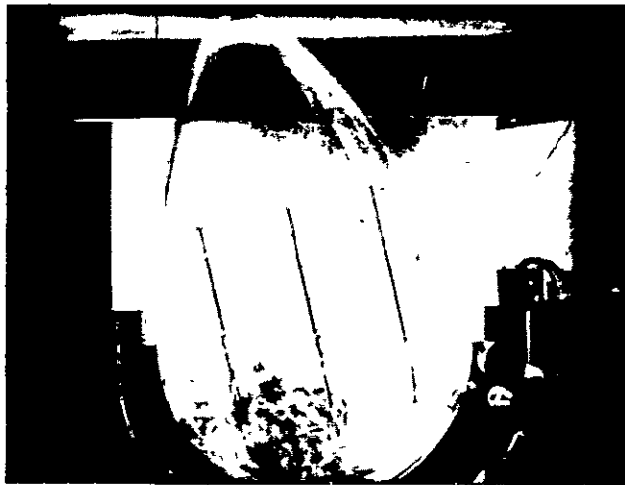
t = 1.6 s

Figure III-5 Drop Tower Test 5, EC-114B2,  $\gamma = 13^\circ$ , 10% Fill, No Baffles

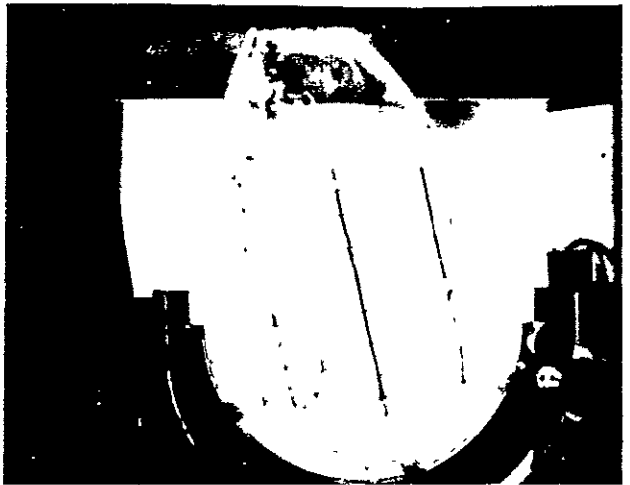
ORIGINAL PAGE IS  
OF POOR QUALITY



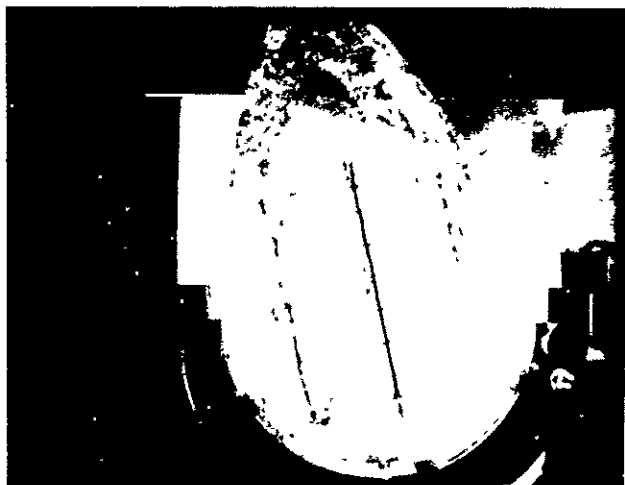
$t = 0.0$  s



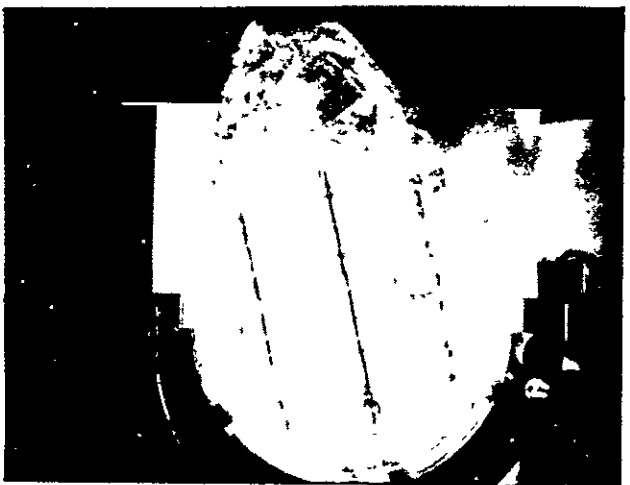
$t = 0.4$  s



$t = 0.8$  s



$t = 1.2$  s



$t = 1.6$  s

Figure III-6 Drop Tower Test 7, FC-114B2,  $\gamma = 13^\circ$ , 10% Fill, Baffles

bottom of the tank. The liquid that continued to the bottom, re-circulated up the right side of the tank and the liquid on the left side flowed up that side to the top. The liquid continued to collect in this manner, with the turbulence and entrained gas gradually disappearing. A sketch of this motion appears in the top sequence of tank drawings shown in Figure III-7.

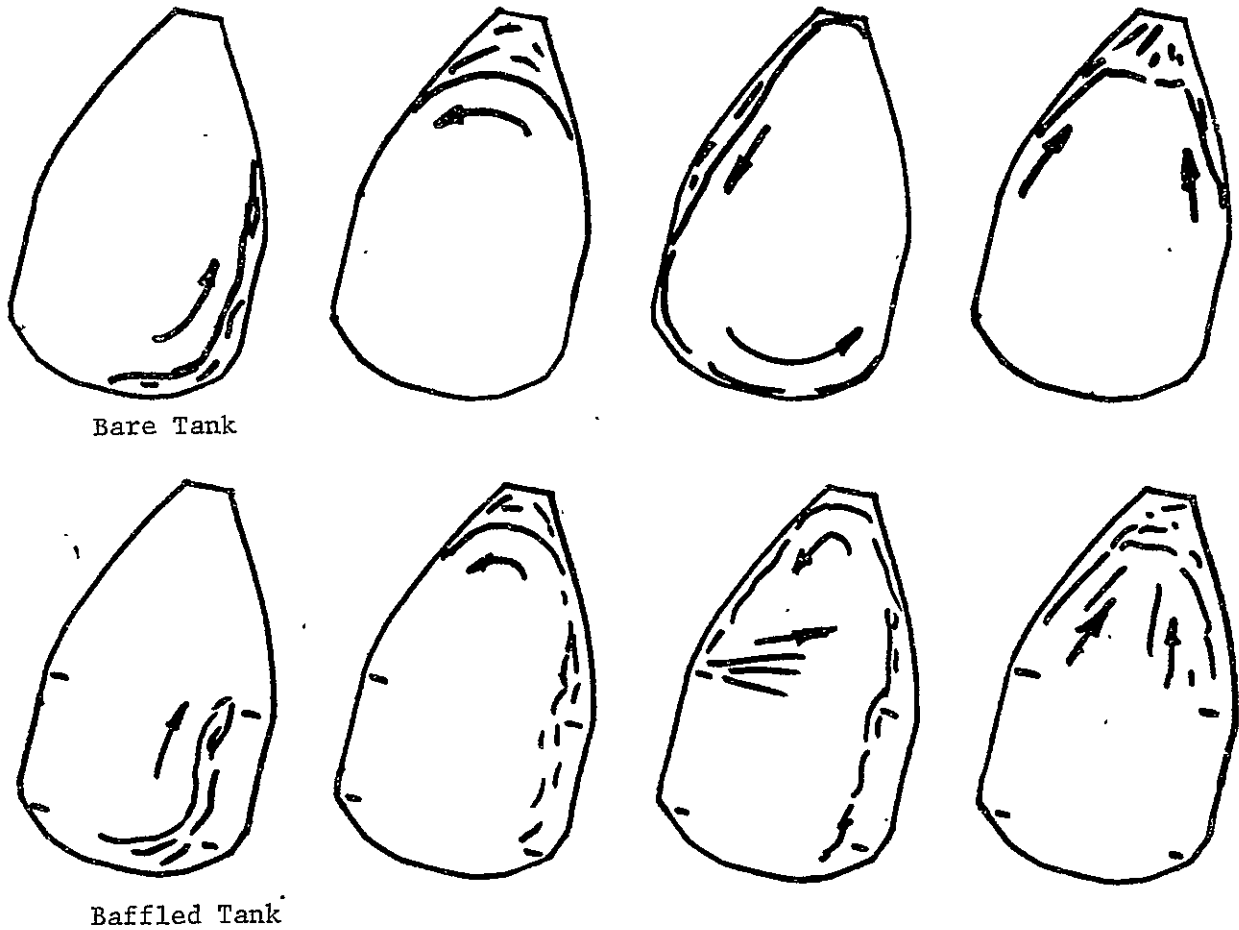


*Figure III-7 Liquid Motion Description*

## B. LIQUID MOTION IN THE BAFFLED TANK

Figures III-2, III-3 and III-4 show the liquid motion for three selected baffled tank tests. All three tests were performed with the same fill volume (10%) and tank inclination ( $13^\circ$ ). For figures III-2 and III-3 the aircraft ZAC acceleration was  $-0.1g$  and  $-0.2g$ , respectively; the test liquid being Freon 113. For Figure III-4 the ZAC acceleration was  $-0.2g$  and the test liquid was water.

The motion of the liquid in the baffled tank began with the liquid rising past the baffles on the right side of the tank. Considerable turbulence and break-up of the liquid surface was introduced by the flow over the baffles. The second ring baffle from the bottom extends to the tank wall (as it does in the full-size tank) so no liquid could flow behind the baffles. The liquid recontacted the tank wall in the lower portion of the ogive dome. It then flowed through the tip of the dome and returned down the left side of the tank. Some of the liquid accumulated in the top of the tank in a fashion similar to that which was observed in the bare tank tests. There was more turbulence and entrained gas in the accumulated liquid for the baffled tank.

After flowing down the left side of the tank, the liquid hit the top ring baffle. It was deflected off this baffle, through the center of the tank, toward the right side of the tank. The fourth ring baffle from the top extended to the tank wall, while the first three were spaced away from the wall (there are 8 ring baffles, two of which extended all the way to the tank wall). Essentially all the liquid deflected off the upper ring baffle, and there was very little flow behind the upper three rings.

The liquid that deflected to the right side of the tank joined the liquid that was still rising along the right side of the tank. This resulted in a recirculation of the liquid in the region of the ogive dome above the baffles. This manner of liquid motion left a large region on the left side of the tank, below the upper baffle, within which there was no liquid flow. The recirculation gradually slowed and the remainder of the liquid continued to rise along the right side of the tank. The liquid then collected at the top of the tank, the entrained gas was eliminated and a near-quiet condition was achieved. The lower sequence of tank sketches in Figure III-7 depict this liquid motion for the baffled tank.

### C. TEST COMPARISONS

Comparisons were made between the various aircraft tests and between the aircraft tests and the Phase I drop tower tests. A qualitative comparison was performed by simultaneously viewing the two sets of film data with two projectors.

A quantitative comparison of the tests required some analysis of the aircraft acceleration data. One of the advantages of the drop tower tests was that the applied accelerations were constant, repeatable and began acting at their full value almost instantly. In contrast, the acceleration environment for each aircraft test was different. It took a period of one to four seconds to achieve the desired ZAC acceleration component. The other component (XAC) began at a value of about  $0.1g$  and decreased toward zero during the test. The pilot flying the aircraft for each set of tests introduced variations in the acceleration environment due to his own particular technique.

A basis for comparing the aircraft tests between themselves and with the drop tower tests was provided by constructing a simple one-dimensional analog. Based on the scaling analysis in Chapter II the motion of the liquid is a function only of the geometric scaling and the acceleration forces, with the viscous and surface tension forces being negligible. Therefore the motion of a particle, acted upon by the same accelerations applied to the liquid motion. The particle was constrained to move only along the tank z-axis, taking into consideration the tank inclination. The distance the particle moves as a function of time was calculated by finding the double integral of the acceleration component parallel to the tank z-axis, the values of XAC and ZAC measured during the test were used to calculate the acceleration at any point in time. The distance the particle moves was made dimensionless by dividing by the tank length.

Since the motion of the liquid is only a function of the acceleration, its displacement should be proportional to the displacement of the particle. Therefore, for any two tests, the point in time at which the dimensionless particle displacements are the same, determines the equivalent elapsed time for each test. This scaling process is best applied to tests with the same fill volume and tank inclination, so that these geometric influences on the liquid motion are minimized.

An example of the scaling process is shown in Figure III-8. Drop tower test 7 and aircraft test 4.8 were selected for this comparison, both being baffled tank tests with 10% fill volume and  $13^\circ$  inclination. The dimensionless distance that was calculated by integrating the applied acceleration is plotted as a function of the test time. Consider the point where the distance is 1.0, this

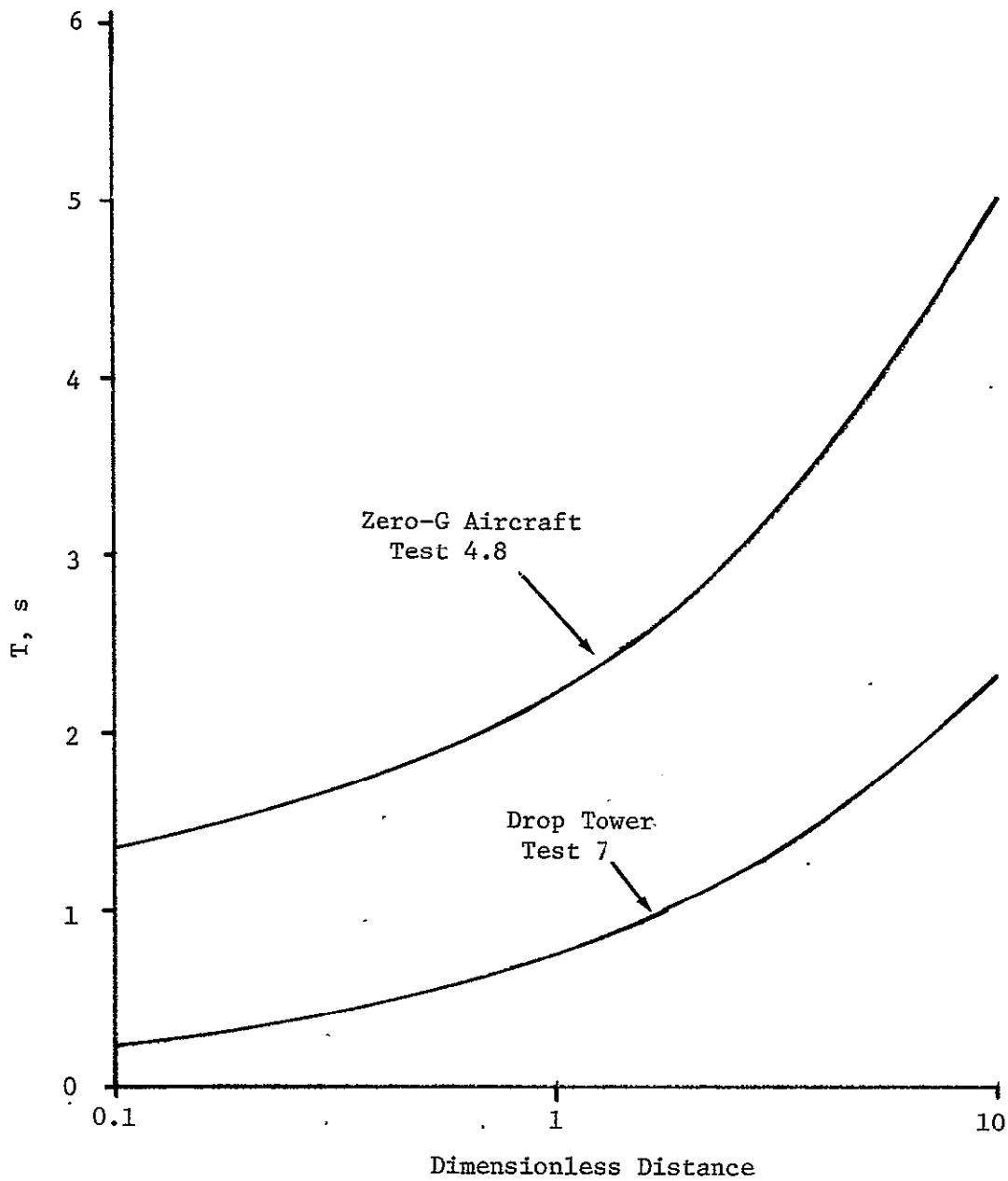


Figure III-8 Time Scaling for Test Comparison



corresponds to a time of 0.75 or the drop tower test and 2.2 in the aircraft test. If this scaling approach is valid, the liquid position should be the same for both tests at that point in time. The application of this scaling is discussed in the following paragraphs.

1. Comparison of Aircraft and Drop Tower Tests. . . . . . When the bare tank tests in the aircraft and drop tower were compared the same general liquid motion was observed. During the drop tower tests the recirculation of the liquid was observed, but the test terminated as the leading edge of the recirculating liquid returned to the top of the tank. Therefore, the final collection of the liquid could not be observed.

Due to the much larger Bond number obtained in the aircraft tests (see Chapter II, discussion of scaling) there were some differences in the behavior of the liquid surface in the bare tank when compared to the drop tower tests. At the start of the drop tower tests, the surface had an instability in the shape of a hump that formed in the center of the liquid surface. With a larger Bond number, the instability had a shorter wavelength, giving it the form of globules and drops leaving the liquid surface. Since the liquid reoriented along the side of the tank, this surface instability was not as evident as it would be if a purely axial reorientation was performed. More breakup of the surface was observed and no central hump formed during the aircraft tests.

Another difference that was observed in the bare tank involved the wetting of the tank wall. For the drop tower tests, a thin liquid film preceded the liquid motion at times and covered a portion of the tank. When the liquid recirculated, the rate of motion of this film as observed to be influenced by viscous effects. In contrast, there was no liquid film motion of that nature during the aircraft tests. Instead the entire tank wall became wetted by a fairly thick film of liquid as the liquid moved about the tank. After most of the liquid had collected, this liquid film continued to flow to the top of the tank throughout the remainder of the test period.

Some differences were also noted between the aircraft and drop tower baffled tank tests. As with the bare tank tests, these differences were primarily due to subtle differences in the influence of viscosity and surface tension on the behavior of the liquid surface. More breakup of the liquid surface into drops and globules was evident during the aircraft tests. These surface effects were most evident during the aircraft tests performed with a 30° tank inclination. The usual pattern of liquid motion was only slightly changed during the drop tower tests when the inclination was increased from 13° to 30°. However, in the aircraft tests there was much more breakup of the liquid surface at the 30° inclination. The spray of the liquid as it hit the baffles dispersed

the liquid throughout the tank giving the appearance that the tank was completely full of liquid at periods during the test.

During the drop tower tests the antivortex baffle caused small volumes of liquid (2% and less) to reorient through the center of the tank rather than along the wall. This occurred because the antivortex baffle delayed the lateral displacement of the liquid making its motion more strongly influenced by the longitudinal acceleration component (ZAC). This same manner of liquid motion was not observed during the aircraft tests. This result was due to the test technique and not the test scaling. Since the lateral component of the acceleration (XAC) began to act while the longitudinal component (ZAC) was still positive, some initial lateral displacement of the liquid occurred before it began to reorient. This reduced the influence of the antivortex baffle on the liquid motion, so the movement was along the wall of the tank at all liquid volumes.

A geometrical difference between the tank model for the drop tower test and the tank for the aircraft test also caused some differences in the liquid motion. Two of the baffles in the aircraft test tank extend to the tank wall (as they do in the actual ET tank) preventing any liquid from flowing behind the baffles. None of the baffles of the drop tower test tank extended to the tank wall in that manner. Therefore it was possible for a small quantity of liquid to flow behind the baffles during the drop tower test. While this difference was obvious when the tests were compared, it did not significantly alter the general motion of the liquid.

Other than these above mentioned differences, the motion of the liquid in the drop tower and aircraft tests was, in general, the same. This was most dramatically demonstrated when two projectors were used to view two tests at the same time. By running each film in small increments, the motion of the liquid was compared. Under similar test conditions, the manner of liquid motion was the same for both test methods, even though there is a factor of six difference in the tank model scale.

Figures III-1 through III-6 at the beginning of this Chapter show this test comparison. The frames for the drop tower tests were selected to give equal time intervals between frames. The selected frames for the aircraft test are those that best match the frames from the drop tower test. As mentioned the film of the aircraft test does not show the initial conditions at zero time.

A comparison of two of the baffled tank tests performed in the aircraft (Figures III-2 and III-3) with a baffled tank test performed in the drop tower (Figure III-6) shows the close correspondence between liquid motion. All of these tests were performed with a fill volume of 10% and a 13° inclination. Aircraft test

2.3 was performed at  $-0.1g$  and test 2.7 was performed at  $-0.2g$ . The scaling approach described at the beginning of this chapter was used to calculate which frames from the aircraft test should match the selected frames from the drop tower tests. This scaling analysis identified the corresponding frames of the aircraft tests well within the accuracy of the selection of the frames by visual comparison of the tests.

When the bare tank tests from the aircraft (test 1.2 in Figure III-1) and drop tower (test 5 in Figure III-5) are compared, similar liquid motion can be seen. However in this case, the frame identified by the scaling did not match the frame selected by visual comparison. Comparison of the selected frame with the frame calculated by the scaling showed that there was about a  $1/2s$  bias between the two. There was an offset in the timing of the aircraft test, such that the motion was occurring  $1/2s$  earlier than predicted by the scaling. Once the amount of the offset was established, the scaling could still establish the relative time of the tests.

The same type of offset was detected when aircraft test 4.8 (water,  $-0.2g$ ) in Figure III-4 was compared with drop tower test 7 in Figure III-6. The time of the selected frames from the aircraft tests was  $1/3s$  earlier than the scaled time.

Since this offset, discovered during the test comparison, was constant throughout the test, it was concluded that the basic principles of the scaling between the aircraft and drop tower tests is valid. The offset was due to differences in the initial conditions of the tests that were not accounted for in the simple scaling analog. The drop tower tests began in a very controlled manner, with one-g disappearing and the two accelerations components being applied instantly and in a repeatable manner. As has been discussed, there was considerable variation of the accelerations during the aircraft tests. The variation of the lateral component (XAC) was the most likely cause of offset in the scaling. That component caused an early lateral displacement of the liquid, while the other component (ZAC) was still acting to hold the liquid at the bottom of the tank. This conclusion was further confirmed by the evaluations discussed in the following paragraphs.

2. Comparison Between Aircraft Tests. In order to compare one aircraft test to another, the scaling approach discussed at the beginning of this section was applied to all the tests. In this case the scaling was applied by determining the time required for a particle to travel the length of the tank based upon the applied accelerations. Then, using the film data, the time it took for the leading edge of the liquid to reach the top of the tank was determined. The ratio of these two times (time for liquid to reach top of tank divided by time for particle to travel tank length)

was then used as the basis for comparing the tests. The times and their ratio are listed in Table III-1. This scaling is most appropriate when tests with the same fill volume and inclination are compared, but it can also indicate the influence of those two variables.

The time scaling of flights 1 and 2 shows some scatter of the time ratios, with the variation not being consistent with the change in fill volume. The average value of the ratios for flight 1 is about 10% less than the average for flight 2, indicating that the baffles slowed the liquid motion.

Tilting the tank to 30° caused the ratio to be somewhat less than it was for flight 2, with a 13° inclination. This could be accounted for by the reduction in the distance between the initial liquid surface and the top of the tank. The ratio also consistently decreases with increasing fill volume at the 30° inclination.

The time ratios calculated for flight 4 are inconsistent with the ratios for the other flights. It was expected that the influence of viscosity could be determined by comparing the Freon tests of flight 2 with the water tests of flight 4. As discussed in Chapter II, additives in the water yielded a Reynolds number for the water tests that was an order of magnitude less than that of the Freon tests.

The calculated ratios for flight 4 average, 20% less than those for flight 2. If our scaling approach is accurate, this result indicates that the water reached the top of the tank sooner than Freon under the same conditions. The velocity of the particle in our analog when it had traveled the tank length was also compared between the two tests. It was found to be the same in some cases and, on the average, the flight 4 velocities were 25% greater than the flight 2 velocities. Therefore the difference in Reynolds numbers, due to the test liquid viscosity, was not strongly influenced by differences in the velocity. The results of a similar evaluation of viscous effects based on the drop tower tests, indicated that there was no effect on the bulk liquid motion.

Flight 4 was different from the other tests with regard to how the accelerations varied due to pilot technique. Comparison of the values of  $t_1$  (the time required for the liquid to reach the top of the tank) listed in Table III-1 shows that they were about 2 less than the other flights. This difference in pilot technique must have caused the differences detected in the time scaling, both in the comparison with the drop tower tests and between aircraft tests. While the simple analog of an accelerated particle was adequate to make some general comparisons, it is not detailed enough to account for all the variables influencing the dynamic motion of the liquid during an aircraft test. Improvement of the analog was not considered worthwhile for this film data evaluation effort. The

Table III-1 Aircraft Test Time Scaling

Test No.	Fill Volume (Percent)	Inclination (Degrees)	t <sub>1</sub> , liquid at tank top (s)	t <sub>2</sub> , particle travel tank length (s)	$\frac{t_1}{t_2}$
1.1	5	13	3.1	4.1	.76
1.2	10		3.6	4.1	.88
1.3	15		2.8	3.2	.88
1.4	5		4.9	5.3	.92
1.5	10		5.1	5.6	.91
1.6	15		No data		
2.1	1		No timing		
2.2	5		5.4	5.5	.98
2.3	10		5.8	5.8	1.00
2.4	15		6.1	6.5	.94
2.5	1		3.8	4.0	.95
2.6	3		2.8	2.6	1.08
2.7	10		4.7	4.7	1.00
2.8	15	13	No timing		
3.1	1	30	4.1	4.3	.95
3.2	5		3.8	4.2	.90
3.3	10		3.3	4.0	.83
3.4	15	30	3.2	3.9	.82
3.5	10	0	3.5	3.7	.95
3.6	5	0	4.3	4.5	.96
4.1	2	13	2.5	3.2	.78
4.2	5.5		2.6	3.1	.84
4.3	10		No timing		
4.4	16		2.1	2.8	.75
4.5	25		2.2	3.1	.79
4.6	2		2.0	2.4	.83
4.7	5.5		1.5	1.9	.79
4.8	10		1.9	2.2	.86
4.9	16	13	1.7	2.1	.81

analytical model being developed for the next phase of this program will be capable of accounting for the actual acceleration environment in predicting the force of the liquid on the tank. Successful correlation of the predictions of that model with the measured forces will permit a complete evaluation of the influence of the variables.

D. SUMMARY

The conclusions drawn from the film data are summarized as follows.

The motion of the liquid in the bare and baffled tank observed in the aircraft tests was the same as that observed in the drop tower tests, with the exceptions noted. The differences were minor, concerning only the details of the liquid motion. The bulk motion of the liquid was the same.

A simple analog was used to provide a more quantitative comparison of the tests. Scaling of the test time between aircraft tests and between the aircraft and drop tower tests was shown to be possible. In some cases, there was an offset in time due to the variability of the accelerations at the beginning of the aircraft tests. The consistency of the scaling indicated that the premise, that the time scaling is only a function of the geometric scale and the accelerations, is valid.

IV. OFT 1 EVALUATION

Orbiter-ET separation studies for the RTLS abort mission sequence have been performed by NASA JSC through the use of the Space Vehicle Dynamics Simulation (SVDS) computer program. These studies indicate the ET clearance is provided somewhat by the orbiter reaction control jets moving the orbiter away, but more significantly by the aerodynamic forces. The analysis has also shown that the ET motion can be significantly influenced by the liquid motion of the ETs residual propellants, mainly LOX. More specifically, the analysis indicates nominal separations, i.e., no recontact, for the OFT 1 initial conditions shown in Table IV-1, and a potential collision for some higher propellant fill volumes. The liquid motion is represented in the SVDS program as a point mass constrained to move on an ellipsoidal surface. This model has not been previously verified by test data. This chapter investigates the ability of the analytical model to accurately predict the liquid reorientation forces. This investigation was accomplished by comparing test data to the analytical model's prediction of the test.

*Table IV-1 ET Separation Initial Conditions, OFT 1*

Parameter	Target Value	+ Dispersion Value	- Dispersion Value
Pitch Rate	-0.25°/s	+0.25°/s	-0.75°/s
Angle of Attack	-4.0°	-2.0°	-6.0°
LOX Fill Volume	1%	2%	0%

The Phase I, 1/60 scale model drop tower test data were selected to compare with the analytical model. The accelerations applied in these tests were constant, repeatable and acted in the X-Z (orbiter coordinate system) plane of the tank. Additionally, both acceleration components acted at the same time.

The Martin Marietta LAMPS (Reference 3) two-dimensional liquid motion analytical model was used in place of the SVDS three dimensional model. This is reasonable in that the LAMPS liquid motion results can be compared directly to the planar liquid motion observed in the SVDS studies.

The test analytical comparisons were performed in two phases. In the first phase, direct comparisons of the test force and moment time histories were made with those generated by the LAMPS analytical model. The LAMPS force time histories were calculated by applying the test accelerations to the analytical model. The structural mass of the test fixture was included in the model to permit more accurate comparisons. Figures IV-1 through IV-3 show

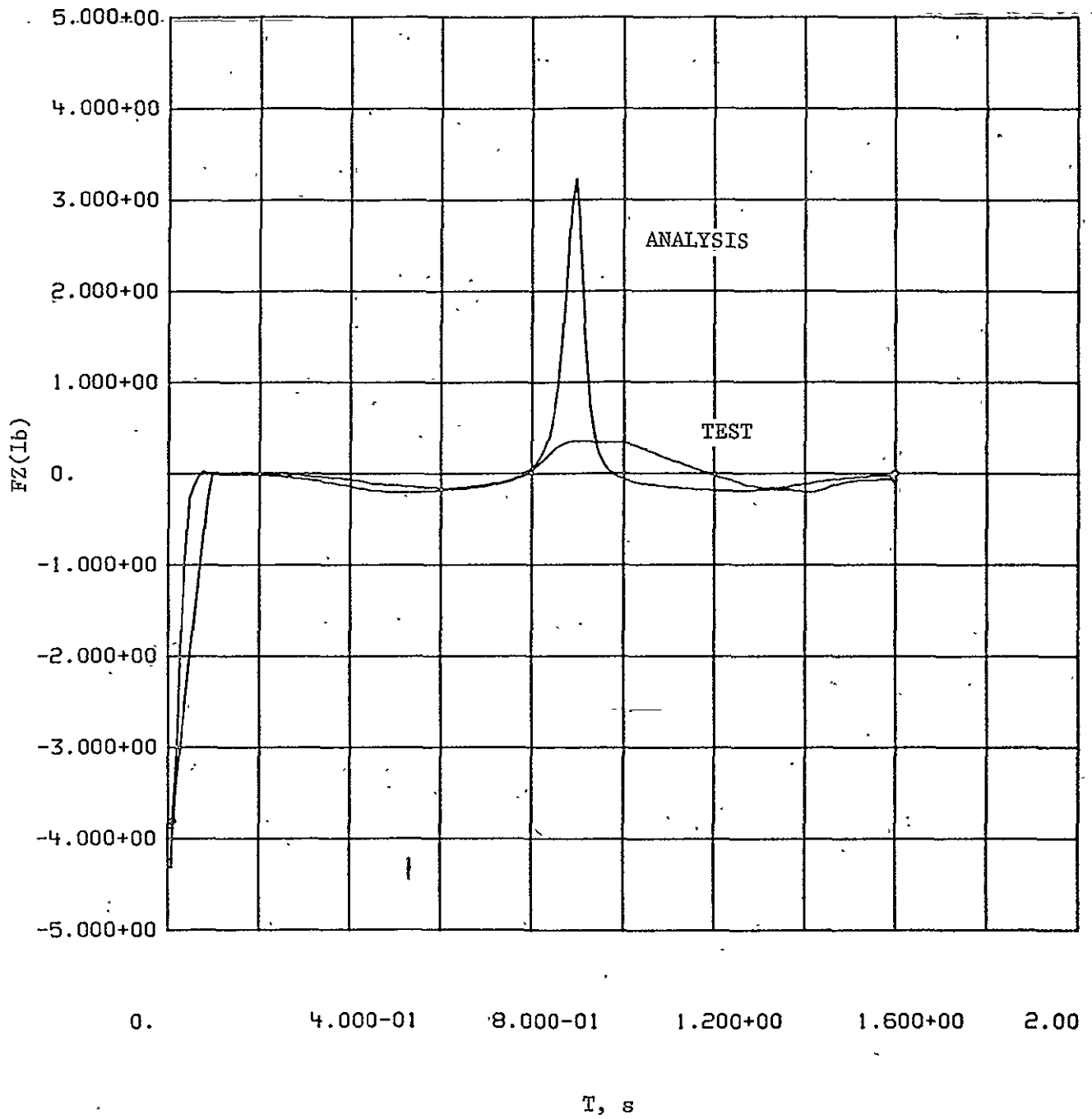


Figure IV-1  
 Test/Analytical Comparison of Tank Z-Axis Forces for Test 22,  
 15% Fill Volume, Unbaffled Tank



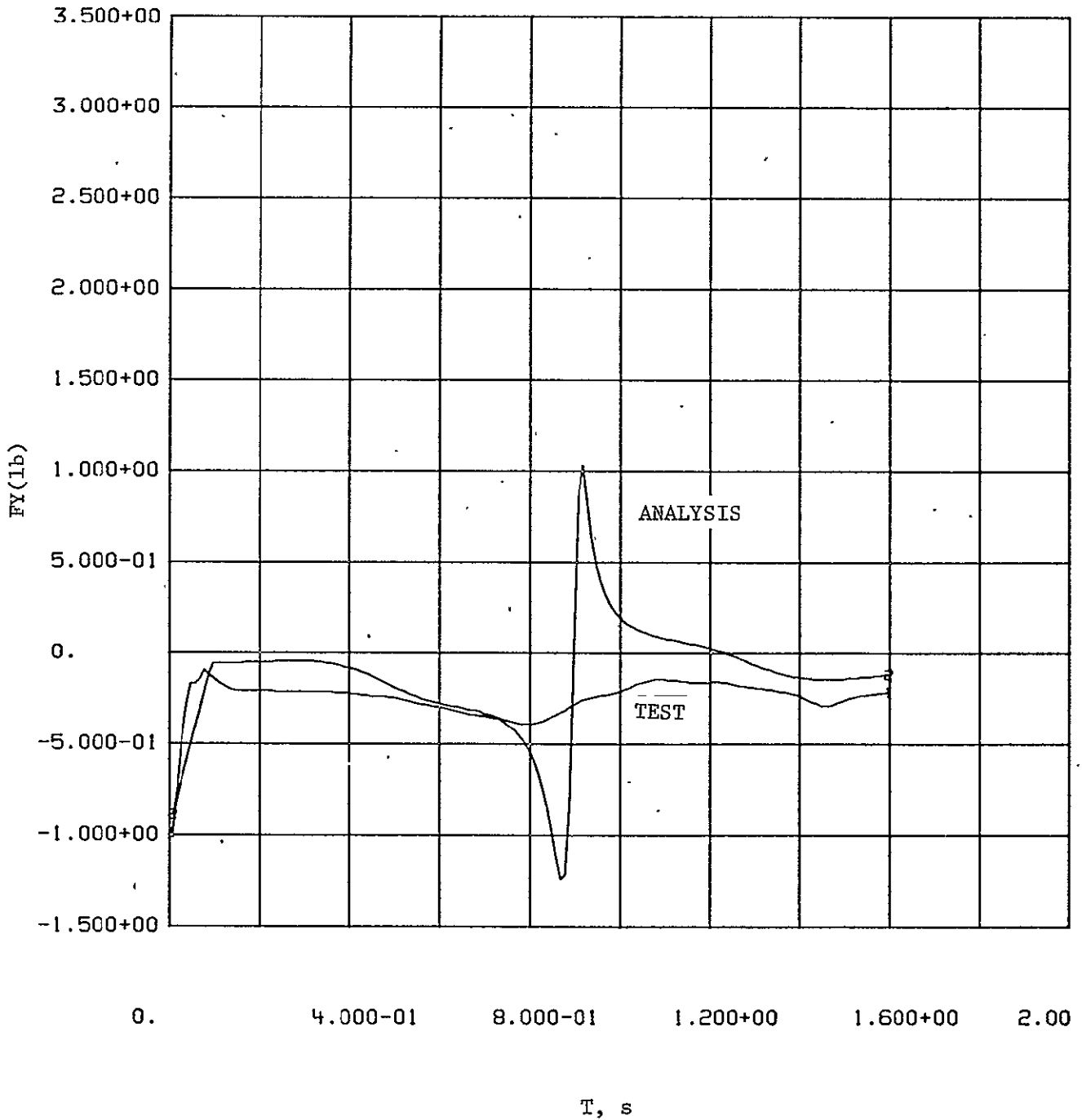


Figure IV-2  
 Test/Analytical Comparison of Tank Y-Axis Forces for Test 22,  
 15% Fill Volume, Unbaffled Tank

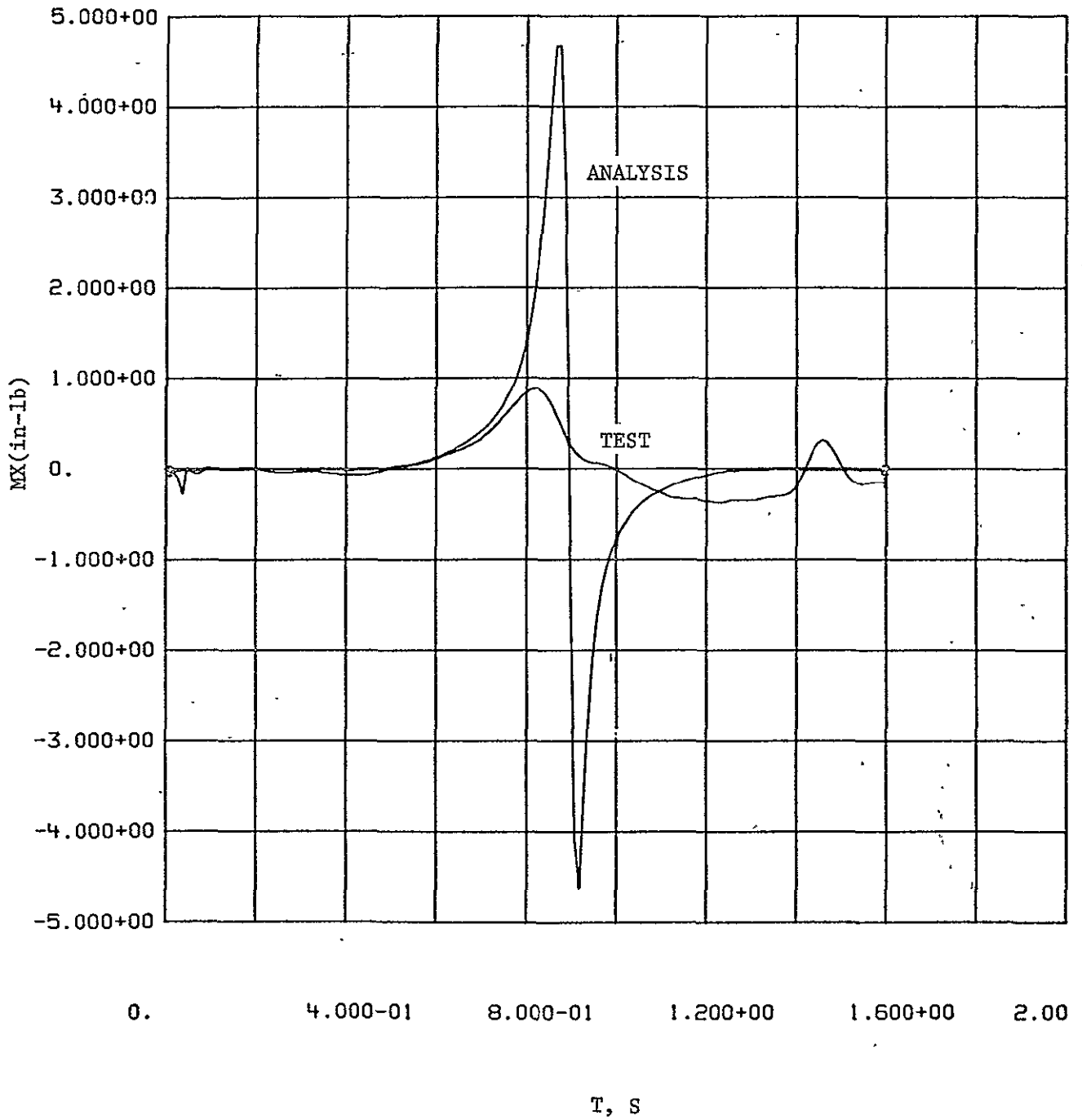


Figure IV-3  
 Test/Analytical Comparisons of Moment About Tank X-Axis for  
 Test 22, 15% Fill Volume, Unbaffled Tank

comparison time history plots for test 22 force data and the analytical simulation of that test data. The forces and moments shown in these plots are in the tank axis systems. Test 22 was performed with an un baffled tank, inclined at 13°, using FC114B2 as the test liquid. The magnitude of the analytical forces and moments exceed those of the test data. This result was typical of all the analytical-test comparisons performed on the drop tower data and indicates the analytical model over predicts the magnitude of the liquid forces.

The influence of the liquid forces on the ET motions are a function of the magnitude, phase and duration of each force component. Therefore, a second comparison effort was performed to include the effects of force phasing and duration. A generalized ET pitch rate and rotation was calculated for the test liquid forces and those generated by the analytical model. The resulting pitch rates and rotations calculated from test data and the analytical model were compared to assess the conservatism of the analyses. The following paragraph discusses the techniques employed to obtain this second comparison of the test/analytical data.

The angular impulse of the liquid forces and moments about the ET pitching axis can be obtained by referring to Figure IV-4. Thus,

$$M_{\alpha} dt = M_{xt} + (F_{yt})(L_x)(SF) - (F_{zt})(L_z)(SF)$$

where  $M_{\alpha}$  = Summation of moments about the ET pitch axis,

$dt$  = Duration of pitch moment,

$L_x, L_z$  = Components of the position vector,  $\vec{r}_E$ , (orbiter coordinate system)

$F_{yt}, F_{zt}$  = Liquid forces resolved to the origin of the tank axis system,

$M_{xt}$  = Moment of the liquid forces about the tank axis system,

SF = Scale factor from full scale to test scale, i.e., 1/60.

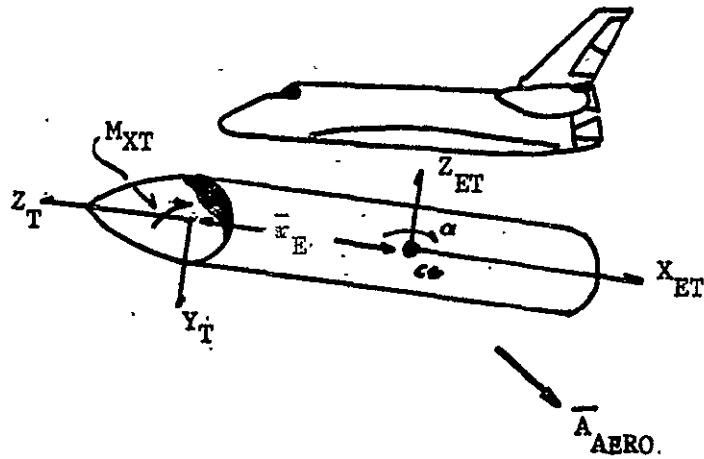
The position vector components were computed to be:

$$L_x = 583.5 \text{ in}$$

$$L_z = 6.05 \text{ in}$$

The  $L_z$  component is small and can be neglected. Thus the pitching angular impulse becomes:

$$M_{\alpha} dt = M_{xt} - (9.725)(F_{yt})$$



Relationship of  
Tank/Orbiter Coordinate Systems

$$Z_T = -X_E$$

$$X_T = Y_E$$

$$Y_T = -Z_E$$

$$M_\alpha = M_{XT} + \vec{r}_E \times \vec{F}_T$$

$$M_\alpha = M_{XT} + (F_{YT})(L_X)(SF) - (F_{ZT})(L_Z)(SF)$$

Figure IV-4  
Summation of Moments of Liquid Reorientation Forces about  
ET Pitch Axis

The angular impulse can be related to the change in angular momentum of the ET. Furthermore, if we assume planar motion rotating about the pitching axis we can write:

$$I_{et} \dot{\alpha} = M_{\alpha} dt$$

where  $\dot{\alpha}$  = angular velocity about the pitch axis,

$I_{et}$  = Moment of inertia about the ET pitch axis.

Now, if we assume a unit moment of inertia for the ET (remove the effects of variation in the moment of inertia) we can integrate the above expression once, to obtain the generalized pitch rate of the ET and a second time to obtain the generalized pitch rotation. Thus,

$$\dot{\alpha} = \int M_{\alpha} dt$$

and

$$\alpha = \iint M_{\alpha} dt$$

These integrations were performed on the test and analytical force time histories. Comparison plots of the test and analytical pitch rate and pitch rotation are shown in Figures IV-5 through IV-8. Figures IV-5 and IV-6 show the results for test 11, a 2% fill volume un baffled tank. The results for test 21, a 5% fill volume un baffled tank are shown in Figures IV-7 and IV-8.

The SVDS analysis has shown that positive pitch rates and positive pitch rotations increase the angle of attack of the ET and result in a higher probability of recontact. Thus, if the above integrations of the analytically generated liquid forces produce larger positive pitch rates and rotations than those computed by the test data, the analysis overpredicts the liquid/ET tank interaction forces. Both the pitch rate and pitch rotation of the liquid forces produced by the analysis exceed those observed in test. Therefore, the SVDS slosh model should predict conservative results for the effects of the liquid motion on the ET separation dynamics.

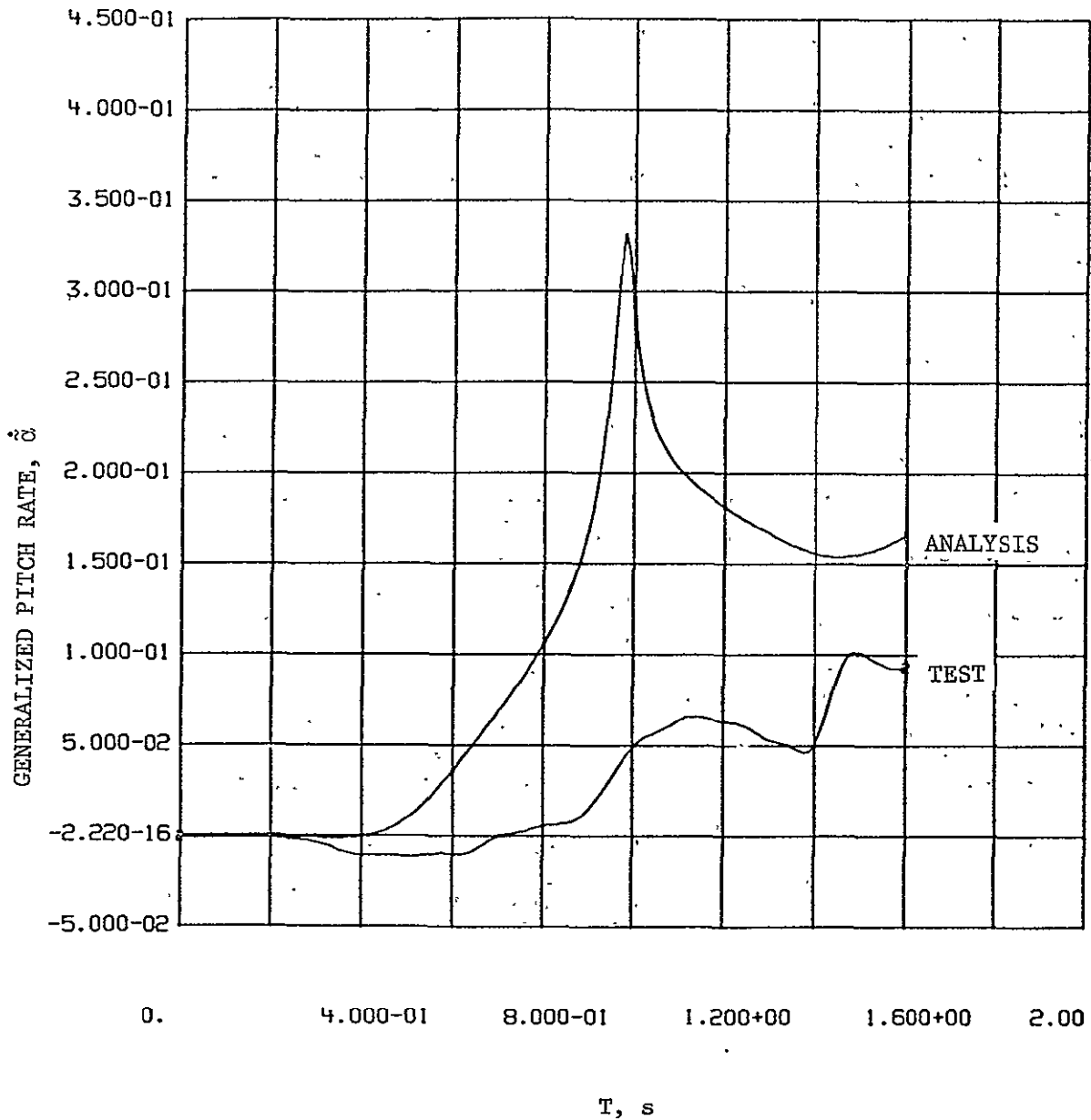


Figure IV-5  
 Test/Analytical Comparisons of Generalized Pitch Rate for  
 Test 22, 2% Fill Volume, Unbaffled Tank

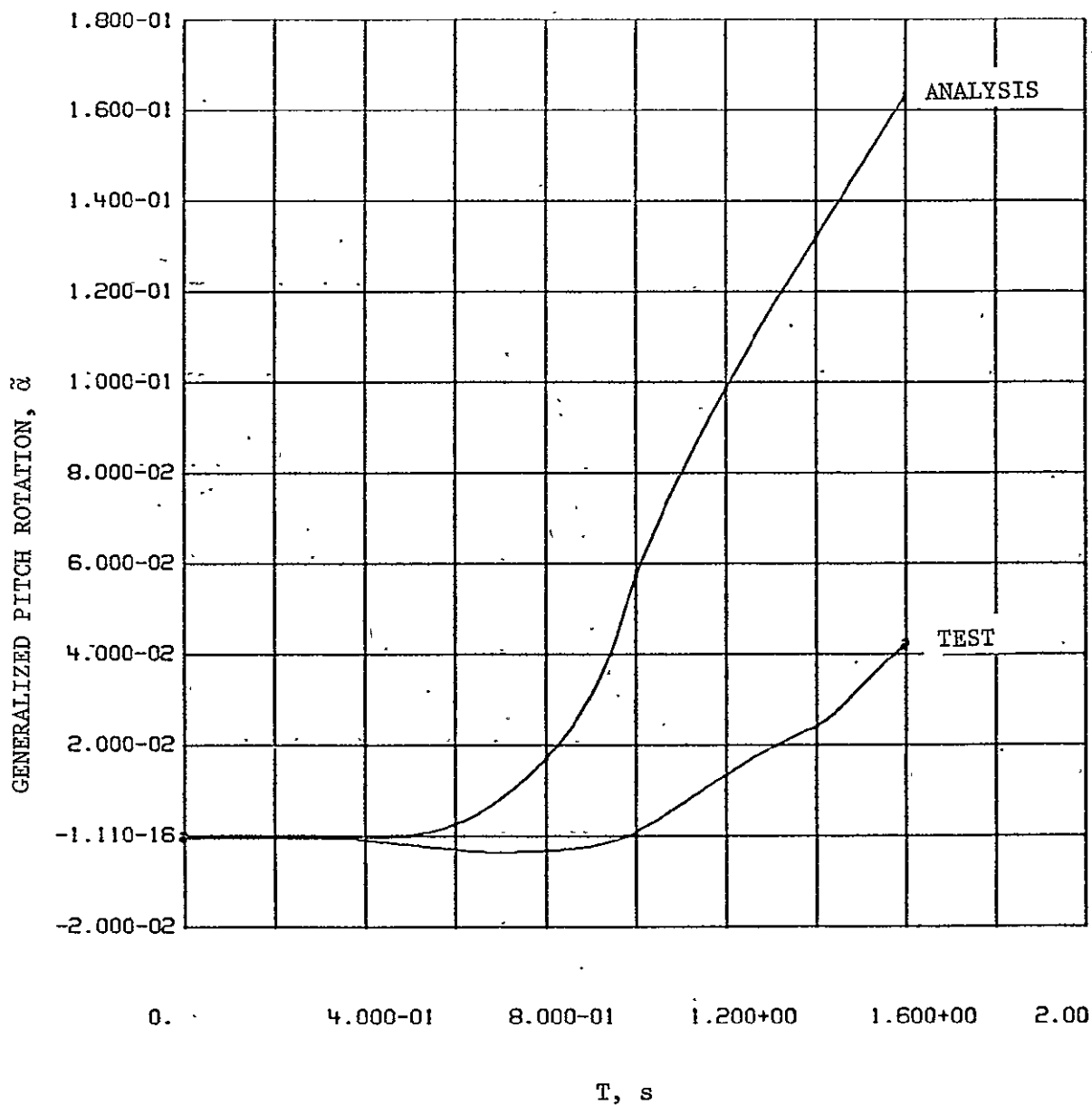


Figure IV-6  
 Test/Analytical Comparisons of Generalized Pitch Rotation for  
 Test 22, 2% Fill Volume, Unbaffled Tank

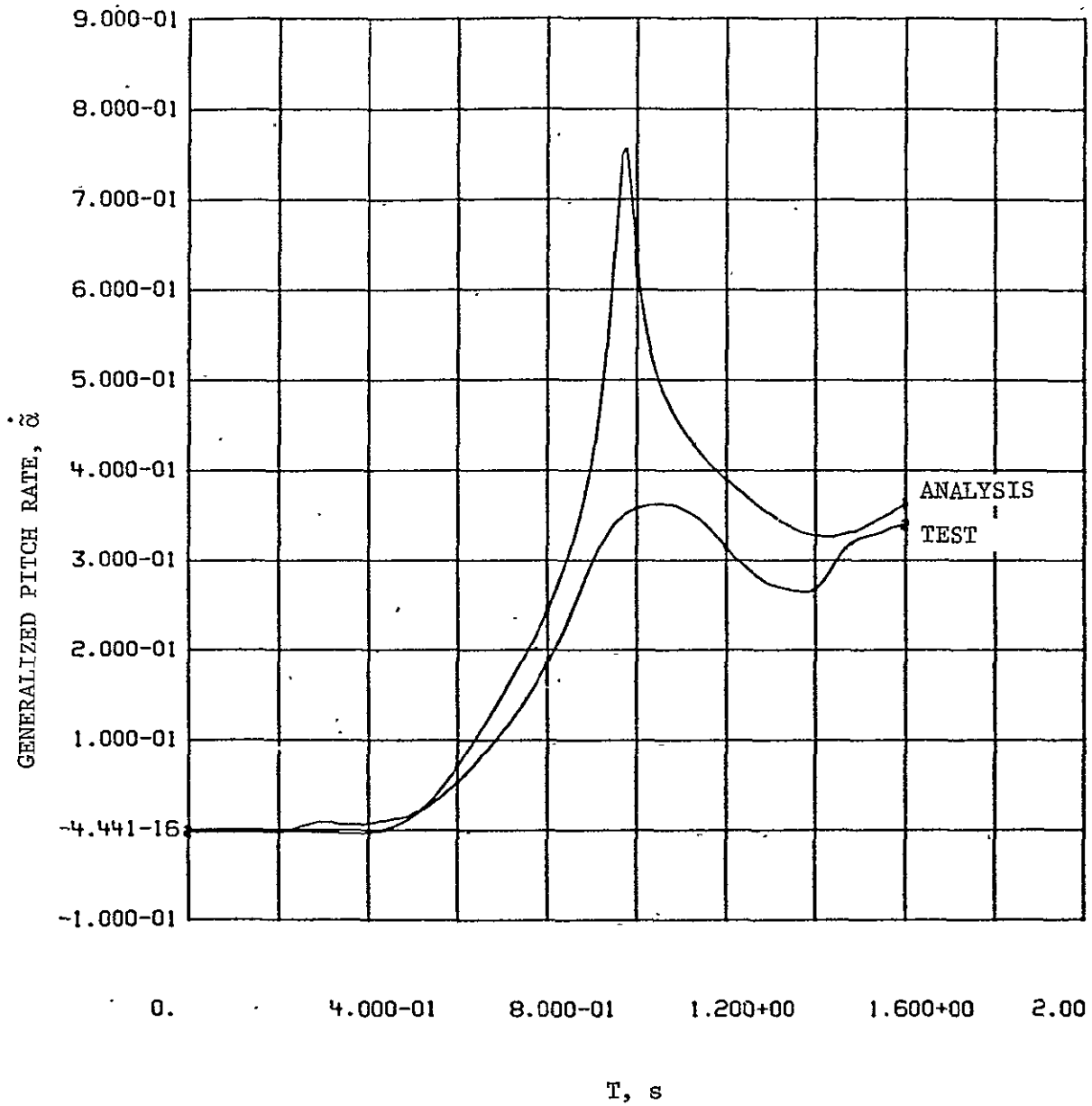


Figure IV-7  
 Test/Analytical Comparisons of Generalized Pitch Rate for  
 Test 21, 5% Fill Volume, Unbaffled Tank



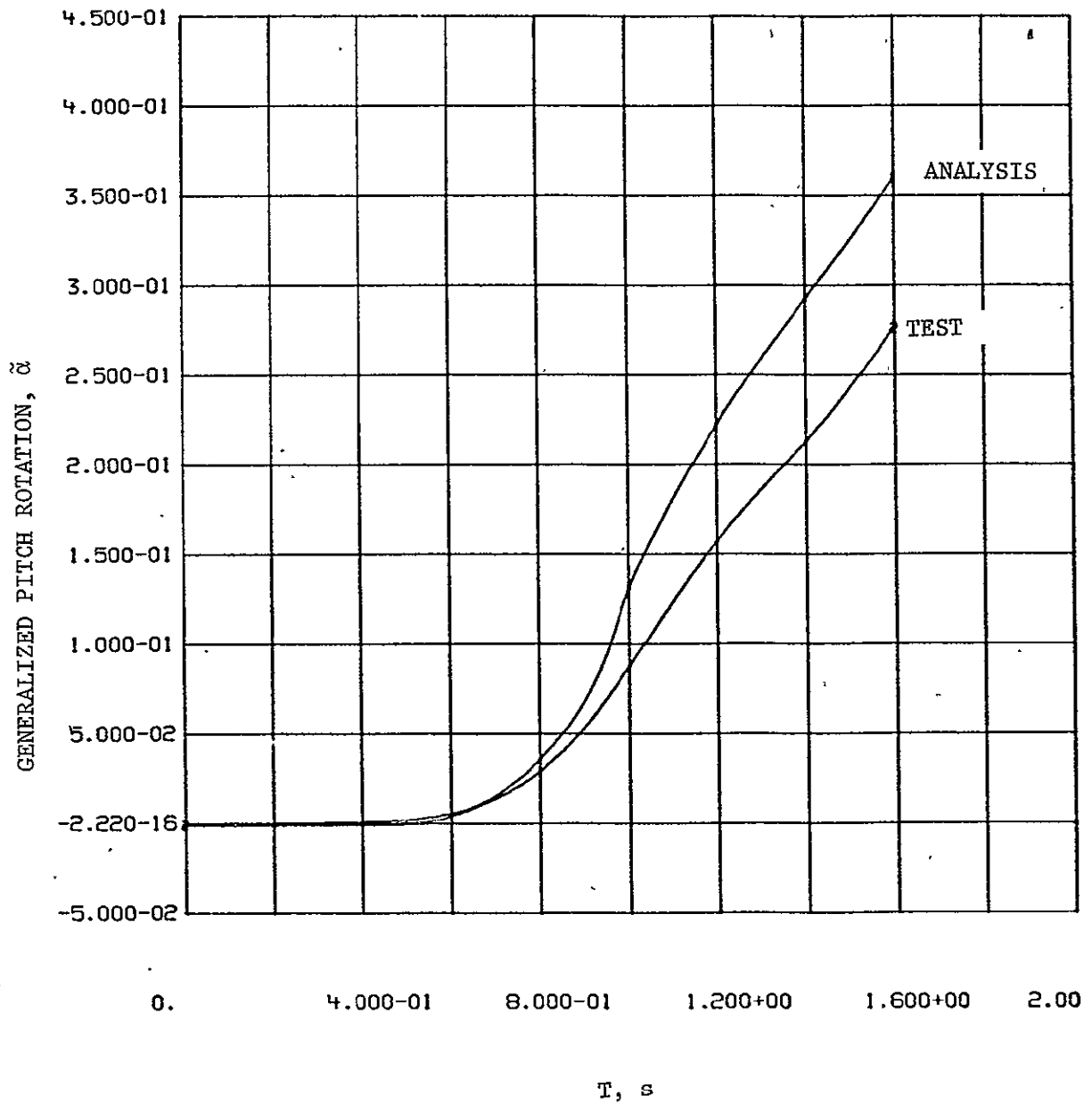


Figure IV-8  
 Test/Analytical Comparisons of Generalized Pitch Rotation for  
 Test 21, 5% Fill Volume, Unbaffled Tank

## V. CONCLUSIONS

---

The objectives of this study are to obtain a test derived data base of liquid motion representative of the ET LOX tank liquid motion for the space shuttle RTLS mission and to develop a mathematical simulation of this liquid motion. The phase II, 1/10-scale ET LOX tank test program expanded the test data bank accumulated in the phase I, 1/60-scale LOX tank drop tower test program. The 1/10 scale model tests, performed with the NASA KC-135 zero-g aircraft provided additional data to study the validity of Froude number, scaling and the effects of tank baffles and liquid viscosity for the scaled ET liquid motion.

The evaluation of the test film data established that the manner of the liquid motion was the same in both the aircraft and drop tower tests even though there was a factor of six difference in the geometric scaling. The differences noted between the test programs was primarily due to the reduced influence of surface tension forces (i.e., higher Bond number) in the aircraft test, leading to more break-up of the liquid surface.

A simple analog of a particle moving under the action of the test acceleration was used to make quantitative test comparisons. Scaling of the test time based upon the geometric scaling and the applied accelerations was shown to be valid. The test time for the liquid to move to the top of the tank in the drop tower test could be scaled to give the time required for the liquid to move to the top of the tank in the aircraft tests. This indicates that scaling between the drop tower and aircraft tests is valid and that both the liquid motion observed in both the drop tower test and aircraft tests can be scaled to the full-sized ET LOX tank.

A time bias was detected in some of the test comparisons. This bias was attributed to the variability of the applied accelerations during the aircraft tests. These effects could not be accounted for in the simple analog. The three-dimensional finite element model being developed in phase III of this study will be able to account for the actual acceleration environment and permit more accurate correlation studies to be performed.

The LAMPS two-dimensional point mass model was compared to the phase I drop tower test data for evaluation of the OFT 1 RTLS mission. This liquid motion model was found to be conservative in predicting the forces the liquid motion applied to the test tank. Both the magnitude and impulse of the liquid forces predicted by the analysis exceed those observed in test. Therefore the NASA SVDS slosh model, which is a three-dimensional point mass model, will overpredict the LOX liquid motion forces applied

to the ET. A multiple mass representation of the liquid motion is needed to more closely simulate the observed propellant dynamics and interaction forces. The feasibility of a finite element concept for the multiple mass model was demonstrated and presented in a Program Progress Review at JSC in February 1979. It is felt that development of this concept into a three-dimensional model will permit more realistic analysis of the effects of the liquid motion on the ET-orbiter separation dynamics.

VI. REFERENCES

---

1. R. L. Berry, J. R. Tegart: *Analysis and Test for Space Shuttle Dynamics, 1/60th Scale Model Test Results*, Interim Report, MCR-78-523. Martin Marietta Corporation, Denver, Colorado, March 1978.
2. *Zero Gravity Program for Using Organization*. Aircraft Operations Division, NASA Johnson Space Center, Houston, Texas, January 2, 1975.
3. R. L. Berry and J. R. Tegart: *Experimental Study of Transient Liquid Motion in Orbiting Spacecraft*, Interim Report, MCR-75-4, Martin Marietta Corporation, Denver, Colorado, February 1975.